# DELIVERY OF NUTRACEUTICALS USING NOVEL PROCESSING METHODS AND EMULSION-BASED FORMULATIONS WITH ENHANCED DISSOLUTION, BIOACCESSIBILITY AND BIOAVAILABILITY

By

MUWEN LU

A dissertation submitted to the

Graduate School-New Brunswick

Rutgers, The State university of New Jersey

In partial fulfillment of the requirements

For the Degree of

Doctor of Philosophy

Graduate Program in Food Science

Written under the direction of

Dr. Qingrong Huang and Dr. Chi-Tang Ho

And approved by

_____

_____

_____

_____

New Brunswick, New Jersey

October, 2017

# ABSTRACT OF THE DISSERTATION

# DELIVERY OF NUTRACEUTICALS USING NOVEL PROCESSING METHOD AND EMULSION-BASED FORMULATIONS WITH ENHANCED DISSOLUTION, BIOACCESSIBILITY AND BIOAVAILABILITY

By MUWEN LU

Dissertation Directors:

Dr. Qingrong Huang and Dr. Chi-Tang Ho

Encapsulation and controlled-release of active food ingredients, such as oil-soluble flavors, preservatives, vitamins, and nutraceuticals, are important applications in food and nutrition that can be attained with nanotechnologies. Functional foods refer to foods that have a potentially positive effect on health beyond basic nutrition; such as regulating blood glucose and cholesterol level, preventing inflammation and cancer, and

cardiovascular protection. Capsaicin (CAP, trans-8-methyl-N-vanillyl-6-nonenamide) and quercetin (QC, 3,3′,4′,5,7-pentahydroxyflavone) are food-grade nutraceuticals with many health-related beneficial functions, including anti-cancer, anti-inflammation, anti-oxidation, cardioprotection and anti-obesity activities. However, as hydrophobic compounds, their low water solubility greatly limits the *in-vivo* bioavailability. To overcome these problems, novel processing methods and emulsion-based delivery systems were used in my research to enhance the bioavailability of nutraceuticals.

In the first part of this work, the wet-milling technologies were used to increase the quercetin (QC) dissolution and bioaccessibility by reducing the particle sizes to around 340 nm with a saturation solubility of 28.78 ± 0.31 μg/mL, about eleven times higher than coarse quercetin. The addition of hydrophobically modified starch could help reduce the particle size by working as a stabilizer to prevent the agglomeration of QC nanosuspensions after wet milling. An *in-vitro* digestion model-TNO model, which was used to mimic the digestion process in the upper GI tract, had determined an increased bioaccessibility of quercetin for the formulated nanoparticles.

In the second part of this study, a lipid-based nanoemulsion system was developed towards the encapsulation of capsaicin (CAP) in order to increase CAP stability, dissolution, bioaccessibility, and reduce the gastric mucosa irritations caused by free unformulated CAP crystals. Oil samples (medium-chain triacylglycerol (MCT), corn oil and canola oil) were used to dissolve the CAP and evaluated by *in-vitro* lipid digestion test. Lipolysis results showed that MCT system had both the highest bioaccessibility of

CAP and the largest extent of lipolysis. Sucrose stearate S-370 was chosen as the gelator to form the CAP-loaded organogel. After the addition of Tween 80 as the emulsifier and processing of ultrasonication, the organogel-derived nanoemulsion was formed with CAP's loading of 80 mg/ml and emulsion droplet sizes of 168 nm. Animal studies using male rats showed that the acute gastric mucosa irritation caused by CAP was alleviated effectively.

Moreover, the CAP-loaded nanoemulsion (C-NE) was further proved to have an enhanced anti-obesity effect compared with free unformulated CAP water suspensions. . C-NE demonstrated an enhanced effect in controlling the HFD-induced weight gain compared to free unformulated CAP water suspensions. MCT, which was contained in the wall material of C-NE, might work synergistically with CAP as a weight-loss agent due to its ability to increase fat oxidation and energy expenditure. Serum biochemical evaluations showed that C-NE had an anti-hyperlipidemic potential with low toxicity for rats. Histological sections of liver and adipose tissues proved the inhibitory activity of C-NE on HFD-induced hepatic steatosis and HFD-induced adipocytes hypertrophy, which was effective in a dose-dependent manner. Gastric mucosa irritation test showed that chronic applications of C-NE alleviated the inflammations in rat stomach tissues caused by CAP.

# ACKNOWLEDGEMENTS

First of all, I want to give my sincere gratitude to my advisors, Dr. Chi-Tang Ho and Dr. Qingrong Huang, for their guidance and support throughout the course of my research studies in Food Science Department, Rutgers University. With their help, I was able to increase my scientific and logical thinking ability and discover the research topics that were really interesting to me. Dr. Ho's patience and enthusiasm in science has relieved my frustration during work and taught me to remain calm when being questioned by other scholars. During my research studies in the past few years, Dr. Huang provided me lots of support in understanding and conducting physiochemical experiments. I truly feel very fortunate to have Dr. Ho and Dr. Huang both as my advisors and faithful friends.

I would like to thank Dr. Yong Cao, who offered me great help in conducting animal test and allowed me to use his research resources in Food Science Department, South China Agricultural University. Every time when I was faced with some difficulties in my experiment, he spared no effort in helping me by consulting those who were expert in solving my problems in relevant fields of study. Without his help, I wouldn't finish my graduate research work so smoothly.

I'm also grateful for Dr. Shiming Li and Dr. Qingli Wu, who kindly agreed to be my committee members. They were very instructive and helpful to share with me their novel ideas in my research work. Every time when I get stuck with my experiment, they always give me a hand by offering me valuable suggestions and instructing me on how to carry out the measurements.

I would like to express my gratitude for my beloved parents, Yuhua Lu and Run Xu, who are both mathematics professors in Qufu Normal University. Ever since I was a child, they were role models to me. From them I started to know how to be a qualified scholar and get motivated every once in a while. Without their love and support, I would never complete my graduate study. I am also indebted to my husband Chengyu Chen, who provides lots of caring and encouragement in my Ph.D. studies. Every time I was feeling depressed, he could always mitigate my anxiety and cheer me up. It was really nice to have someone who can both understand my research work and share same interests in life. Now we are both working hard towards our Ph.D. degree and taking care of our baby comes to the world on 12:07 pm of May 9, 2017.

Finally, I am thankful for all my labmates and friends for their kind help and collaborations to my work. Five years here as a graduate student give me a great opportunity to experience the American culture, meeting with many wonderful people, and have such a precious memory in my life.

# CONTENTS

# LIST OF TABLES

# LIST OF ILLUSTRATIONS

# CHAPTER I. INTRODUCTION

Nanotechnologies in recent years have been applied to the encapsulation and processing of active food ingredients, such as oil-soluble flavors, preservatives, vitamins, and nutraceuticals. Functional foods refer to foods that have a potentially positive effect on health beyond basic nutrition; such as regulating blood glucose and cholesterol level, preventing inflammation and cancer, and cardiovascular protection. Moreover, certain nanotechnology-based consumer products have already been introduced on the market. As the development of food science and technology, novel functional foods are in need to meet the requirement from consumers all over the world.

Generally speaking, oral administration and dermal/transdermal penetration are most common and convenient methods for food and drug administration. However, the bioavailability for most hydrophobic compounds is very low due to their limited water solubility, which results in insufficient concentration of bioactive compounds to produce effective therapeutic functionalities. Therefore, various delivery systems for nutraceuticals are designed and applied to carry higher amounts of active ingredients into our circulation system than pure compound to better perform their beneficial bio-functions.

In the past decade, technologies that are designed to increase the solubility of nutraceuticals have been strongly desired, because more than 40% of the promising compounds are reported to be categorized as poorly soluble (*1*). To address this issue,

many “solubilization tools” have been developed and evaluated. Among them, the high-shear beads milling technique in aqueous medium has been adopted in many researches to disintegrate micro-sizes drug into nano-sized particles since its preparation process is simple and the suspension to be orally administered to animals could be directly prepared (*2, 3*).

## FUNCTIONAL FOODS AND NUTRACEUTICALS

Nowadays, with the development of modern science and technology, consumers are more willing to spend money on functional foods due to the beneficial effects of their effective component. According to the Institute of Food Technologists (IFT), functional foods are defined as “foods and food components that provide a health benefit beyond basic nutrition” such as conventional foods; fortified, enriched or enhanced foods; and dietary supplements (*4*). And FDA gives the definition as “the rate and the extent to which the therapeutic moiety is absorbed and becomes available to the site of drug action”. Those foods could provide essential nutrients beyond quantities necessary for normal maintenance, growth and development.

The functional food market in the US has grown 31% from 2006 to 2011, with beverages leading the charge, according to a report from Leatherhead Food Research (*5*). Functional beverages mainly gained attention by health-conscious consumers, driving sales to an estimated 18.6 billion U.S. dollars by 2015 (**Figure 1**). And in 2018, it is forecast to reach the value of $41,292.6 million, an increase of 52.7% since 2013.

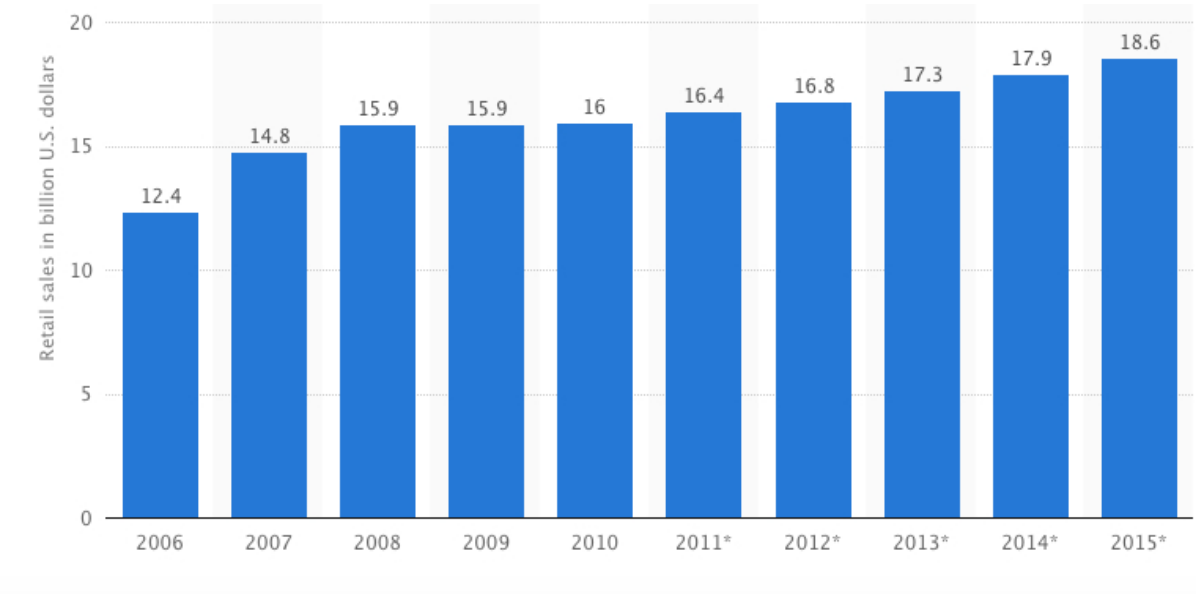


**Figure 1**. United States functional beverage market value: $ million, 2006-2015.

## NUTRACEUTICALS

Nutraceuticals, similar to functional foods, have no official definition according to US law. The word "nutraceutical" is composed of "nutrients" and "pharmaceutical". Nutrients are defined as "traditional vitamins, minerals, essential fatty acids for which recommended intakes have been established and other components that include phytonutrients or bioactives present in foods for which a physical or physiological effect has been scientifically documented or for which a substantial body of evidence exists for a plausible mechanism, but for which a recommended intake and function have not been definitively established" (*4*). And a pharmaceutical drug is a drug used to diagnose, cure, treat, or prevent disease (*6*). Taken together, the nutraceuticals are applied to products that range from isolated nutrients, dietary supplements and herbal products, specific diets and processed foods such as cereals, soups, and beverages, which have very potent

bioactivities, such as anti-oxidant, anti-obesity, anti-inflammation, and anti-cancer effects, etc.

## BIOAVAILABILITY OF NUTRACEUTICALS

According to the nutritional sciences, the term bioavailability is defined as the fraction of nutraceutical or bioactive compound ingested that is eventually available for use in physiological functions or storage (*7*). According to **Figure 2**, the overall bioavailability of nutraceuticals that are consumed with food is affected by three processes: bioaccessiblity, intestinal transport and metabolism (*8*).

For nutraceuticals that can be easily dissolved in water, they will be solubilized into the juices of the gastrointestinal tract. However, for those that has very low water solubility, certain emulsifiers and surfactants are in need so as to form micelles or mixed micelles in the small intestine lumen. The fraction of nutraceuticals that are released from the food matrix and get absorbed by the GI tract can be calculated as bioaccessibility.

After getting absorbed by small intestine, nutraceuticals will go through intestinal transport and enter systematic and general circulation through two routes: water-soluble compounds will diffuse through the epithelium into the portal vein, being transported into liver. In order for water-insoluble compound to be permeated through epithelium, they may be carried by micelles or mixed micelles. If the sizes of micelles are too large to enter the portal vein, they will go directly into lymphatic system and avoid the hepatic metabolism in liver (*9*).

The metabolism refers to the whole range of biochemical processes, which include the process of oxidation, reduction and so on. It is mainly composed of two parts: intestinal metabolism, which is occurring in the intestinal epithelium; and herpetic metabolism occurring in liver. After the metabolism, all nutraceuticals will reach the systematic and general circulation system (*10*).

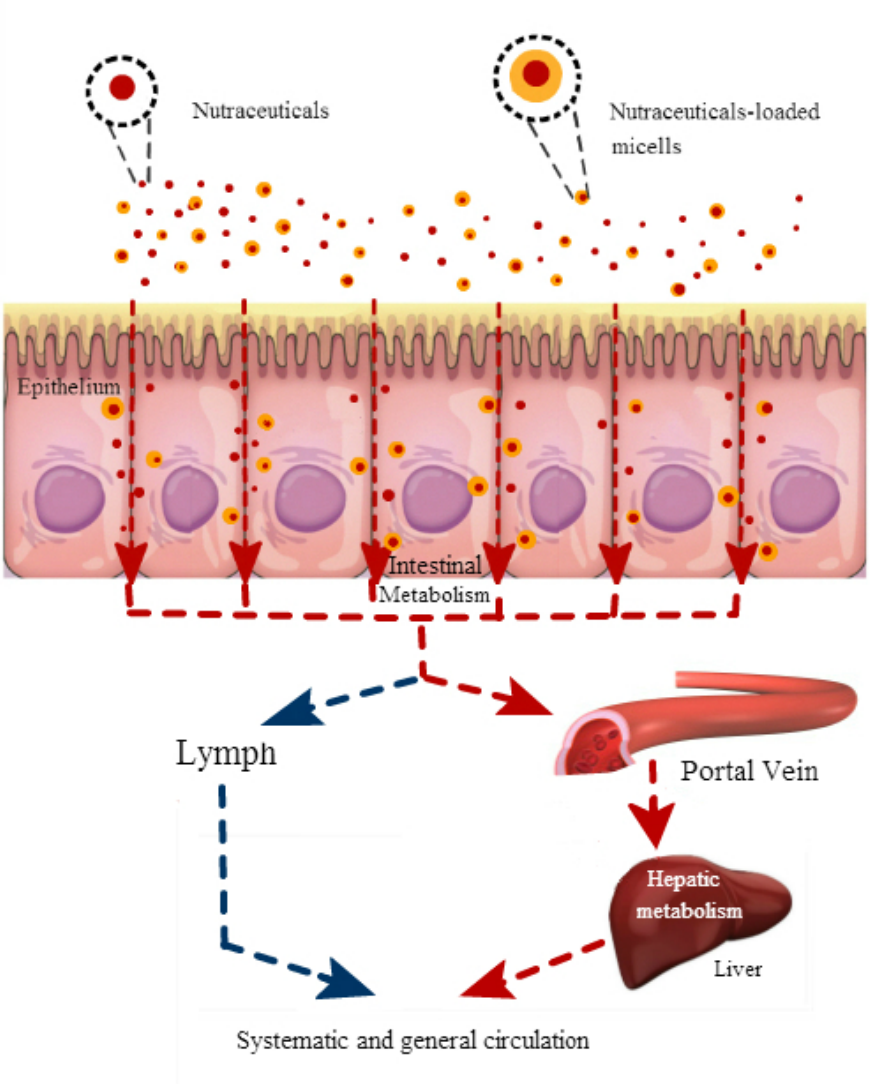


**Figure 2**. A schematic representation of the process in which nutraceuticals in foods become bioaccessible.

As the orally-ingested nutraceuticals are passing through the GI tract, their efficacy for the disease prevention can be limited by several factors, such as low water solubility, large particle sizes, short residence time in the GI tract, instability to changing physiological environments, low diffusion rate across the epithelial walls, and susceptibility to rapid metabolic transformation, etc. (*11*). To increase the bioavailability of nutraceuticals, various approaches have been used when designing delivery systems to overcome the limiting factors. According to Ting, the frequently-utilized approaches include protection of labile compounds, extension of gastric retention time, increase of the solubility and control/release properties of nutraceuticals, enhancing the intestinal permeability and modulation of metabolic activities (*10*). Most of them are designed to increase the concentration of effective component in the systematic circulation by enhancing the intestinal absorption. In the next section, the common delivery systems aiming to improve the bioavailability are summarized and evaluated.

## COMMON DELIVERY SYSTEMS TO ENHANCE THE ORAL BIOAVAILABILITY *IN VIVO.*

As foods are ingested through oral administration, the nutraceutical needs to go through mouth, stomach, small intestine before it enters the systematic circulation and gets excreted by colon. During this process, the physiochemical environment such as the change in pH, enzymatic activities and ionic strength (0.1 mol/L in stomach and 0.14 mol/L in small intestine) (*12*) will influence the solubility, dissolution, stability, bioavailability and efficacy of bio-active compounds based on their chemical structure. To avoid the negative effects from the physiochemical environment of the digestive

system and enhance the bioavailability of nutraceuticals, various delivery systems are developed to ensure a high concentration of active ingredients reaching the systematic circulation.

## LIPID-BASED DELIVERY SYSTEMS

Phospholipids are a class of lipids that are a major component of cell membranes, which is composed of a hydrophilic head containing a phosphate group and two hydrophobic fatty acid tails (*13*). As they are naturally occurring compounds, the lipid-based delivery systems for nutraceuticals can be more biocompatible and biodegradable when passing through the digestive system, ensuing a higher loading and enhanced bio-efficacy of bioactive compounds. Examples of lipid-based delivery systems are listed as follows.

Liposomes have been used as carriers of hydrophilic and hydrophobic drugs, which contain phospholipid bilayer structures (*10*). This chemical structure of liposome allows it to encapsulate the hydrophilic compounds in the center with polar phosphate groups and encapsulate lipophilic compounds in the phospholipid bilayers. It has been proved by researches that liposomes protect the nutraceuticals from the physiochemical degradation and enzymatic activities, and enhance the permeability through the intestinal epithelial cells (*14, 15*).

Phytosomes are phospholipid complexes that have a similar structure to liposomes. However, the active ingredients are bound to the phospholipid structure instead of being simply encapsulated in the core of the carrier. Compared with liposomes, phytosomes

have a higher loading capacity and stability against the physiochemical environment and metabolic activities. It has been used as carriers of many popular herbal extract including curcumin isolated from turmeric (*16*) and epigallocatechin-3-gallate (EGCG) extracted from green tea (*17*), etc.

## EMULSION-BASED DELIVERY SYSTEMS

Emulsions are composed of two originally immiscible aqueous solutions, usually oil and water, stabilized by the surface active molecules. Many researches have demonstrated the efficacy of emulsions in improving the aqueous solubility, enhancing the stability against bio-degradation and permeability across the small intestine of nutraceuticals. In most cases, the emulsion-based delivery system can increase the oral bioavailability of poorly-water-soluble compounds by increasing the dissolution, protection from the physiochemical environment, prolonging the residence time in the gastro-intestinal tract and controlling the metabolic process.

Among all emulsion-based delivery systems, the nanoemulsions and microemulsions are usually produced through nanotechnology with particles sizes lower than 100 nm. Due to the nano-scale particle sizes, the solubility in the body fluid has been increased effectively as well as the uptake of nutraceuticals in the GI tract. In an experiment conducted by Choi Ah-Young, et al.(*18*), they applied chitosan-/alginate-based nanoemulsions in the delivery of capsaicin, a lipophilic compound. The pharmacokinetic study proved that area under the curve (AUC) increased in a nano-size-dependent manner: as particle size reduces, the AUC will increase, showing that the nano-emulsions could

significantly enhance the bioavailabilty of capsaicin compound.

Solid-lipid nanoparticles (SLN), which were developed at the beginning of the 1990s, have also been used in food, cosmetic and pharmaceutical industries for encapsulation of hydrophobic compounds (*19*). A solid-lipid nanoparticle is typically consists of lipid droplets suspended in aqueous buffer stabilized by an emulsifier layer at the lipid/water interface with particle sizes between 10 to 1000 nm(*20*). Compared with liposomes or phytosomes, SLN has its advantages such as flexibility in modulating the control-release of the compound and protection against the chemical degradation of the active ingredient in the GI tract. Emulsions developed using the SLNs have a more sustained release profile and delayed peak time than the liquid-lipid emulsions during pharmacokinetic studies. In a study conducted by Hailong Yu, *et al.* (*21*), an organogel system was first developed by dissolving curcumin into medium chain tryglyceride oil with monostearin working as the gelator. Later, he added water and emulsifier into the semi-solid gel to produce an organogel-based nanoemulsion. Physiochemical characterization studies of this nanoemulsion demonstrated an improved loading capacity, stability and efficiency during lipid digestion process. Moreover, biological studies also revealed an enhanced permeation rate across Caco-2 cell monolayers and increased oral bioavailability by 9-fold compared with unformulated curcumin. To sum up, SLN is an alternative carrier system to lipid-based delivery systems and polymeric nanoparticles to enhance the oral bioavailability of nutraceuticals.

## OTHER DELIVERY SYSTEMS

Chemical modification methods have been utilized to form bio-reversible conjugates of active compounds and their carrier systems to enhance the bioavailability and bio-efficacy of nutraceuticals. Examples such as demethylation of tangeretin (*22*) and acetylation of EGCG (*23*) have proved the increased bioactivities of chemically-modified nutraceuticals compared with the original compound. According to Ting (*10*), the chemical modification method is effective in improve the aqueous solubility, gastric stability, cell permeabilities and oral bioavailability of active ingredients.

In addition, physical modification methods, mostly nanotechnology-based processing methods, are also useful in decreasing the particle sizes of nutraceuticals into nanoscale, thereby increasing the cellular uptake and transport through the epithelial cells and enhancing the oral bioavailability. Those nanotechnology-based processing mthods include solid dispersions prepared by spray-drying (*24*), freeze-drying (*25*), or hot melt extrusion; complex formation with water-soluble excipients, self-emulsifying drug-delivery systems (SEDDS), and so on. In a research conducted by Niwa, *et al.*(*3*), they used mechanical milling process in aqueous buffer solutions combined with spray freeze drying process for particle size reduction of compound phenytoin. By reducing the particle size of the compound, an increase in surface area of powdered phenytoin results in faster dissolution rates, effective redispersing properties and higher plasma concentration during pharmacokinetic study compared with coarse phenytoin compound. Through the nanotechnology-based processing method, nanodispersions can be produced with increased gastric lumen solubility and dissolution rate, higher membrane

concentration gradient and better oral bioavailability *in vivo*.

## QUERCETIN

## CHEMISTRY OF QUERCETIN

Flavonoids were polyphenolic compounds rich in fruits, vegetables and plant-derived beverages such as tea and red wine (*26*). They have a structure of 15-carbon skeleton, which consist of two benzene rings connected by a short three carbon chain. Flavonoids can be divided in to 6 major subtypes, including flavonols, flavones, flavanones, flavan-3-ols, etc, which are listed in Table 1.

**Table 1**. Major subtypes of flavonoids.

| Group | Examples |
|---|---|
| **Flavonol** | Isorhamnetin, Kaempferol, Myricetin, quercetin |
| **Flavone** | Apigenin, Luteolin |
| **Flavanone** | Eriodictyol, Hesperetin, Naringenin |
| **Flavan-3-ol** | Catechin, EGCG |
| **Theaflavin** | Theaflavin |
| **Anthocyanidins** | Cyanidin, Delphinidin, Malvidin, Pelargonidin, Peonidin, Petunidin |

Quercetin (QC, 3,3′,4′,5,7-pentahydroxyflavone) as one of abundantly consumed flavonoid has a chemical structure shown in **Figure 3**. According to recent researches,

quercetin has many biological activities, including antioxidative (*27*), anticarcinogenic (*28*), anti-arthritic (*29, 30*), anti-inflammatory, anti-proliferative and anti-atherosclerotic effects (*32*). The molecular formula for quercetin is $C_{15}H_{10}O_7$, which includes 2 phenyl groups and a heterocyclic ring. It has a molecular weight of 302.24 g/mol, and melting point of 316 °C. It is practically insoluble in water, which greatly limits the bioavailability in vivo.

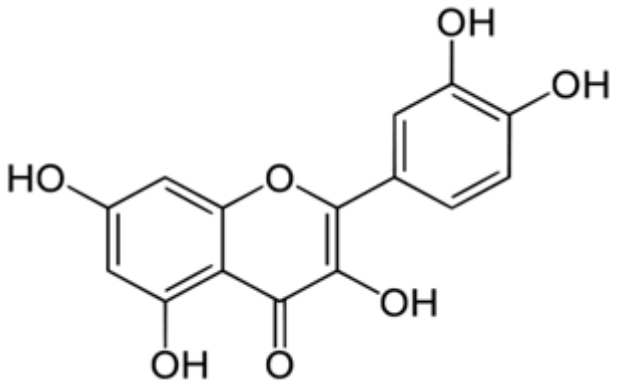


**Figure 3.** Chemical Structure of Quercetin.

In order to improve its bioavailability, researchers attempted various encapsulation methods to increase its dissolution rate. According to Kakran (*2*), QC nanocrystals have been fabricated by means of three methods, including high-pressure homogenization, wet bead milling, and cavi-precipitation. The smallest nanocrystals were fabricated by wet bead milling with a saturation solubility of 25.59 ± 1.11 μg/mL, about nine times higher than coarse QC. Niwa (*3*) also reported that the technique of wet-milling and spray & freeze-drying processes could enhance the dissolution for poorly water-soluble drugs.

## *IN VIVO* PHARMACOKINETICS

The *in vivo* pharmacokinetics studies of quercetin using animal models have been carried out by various researches. According to Bagad *et al*. (*31*), they used male Wistar albino rats to study the pharmacokinetics and biodistribution of quercetin. Before the test, the rats were fasted overnight at a temperature of 25°C ± 2°C and relative humidity of 50% - 60%, allowed free access of water ad libitum. During the test, the rats were fed with quercetin suspensions at a dose of 50 mg/kg body weight via oral gavage. Plasma and tissue samples were taken from those rats for pharmacokinetics analysis using HPLC. The mean quercetin concentration - time profiles in the plasma after oral administration are shown in **Figure 4**, and the corresponding pharmacokinetics parameters are summarized in **Table 2**.

After oral administration of free quercetin solution in rats, the maximum plasma concentration ($C_{max}$) was achieved at 6 hours with the concentration of 11.26 ± 0.09 μg/mL. Plasma concentration declined rapidly after 6 hours, demonstrating the quick distribution and metabolism of quercetin in the circulation system.

The result of *in vivo* tissue distribution study was shown in **Figure 5** (*31*). The maximum concentrations of quercetin in the heart, liver, kidney, and spleen were 18.88 ± 2.09, 21.44 ± 3.97, 43.67 ± 2.28, and 19.44 ± 1.35 μg/mL, respectively. And the values for pharmacokinetics constants are demonstrated in **Table 3**.

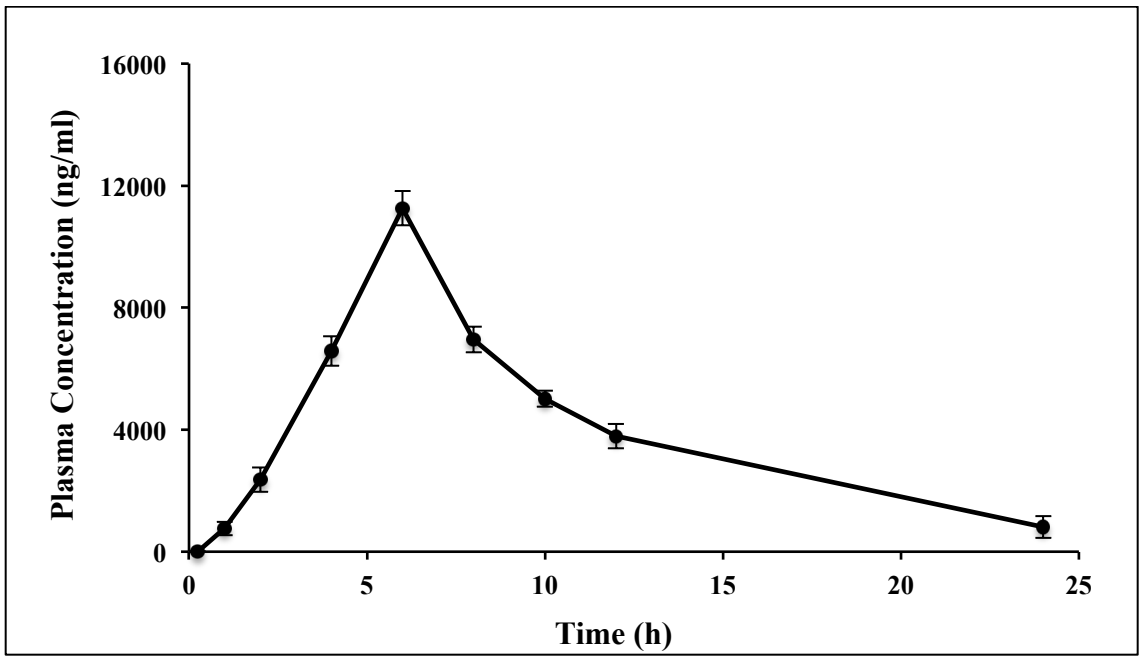


**Figure 4.** Mean (± SD) plasma concentration-time profile of quercetin after oral administration of free quercetin suspension at 50 mg/kg dose to rats.

**Table 2.** Pharmacokinetic parameters of oral administration of free quercetin in rats.

| Parameters | Free quercetin |
|---|---|
| **$C_{max}$ (µg/mL)** | 11.26 ± 0.09 |
| **$T_{max}$ (h)** | 6 |
| **$t_{1/2}$ (h)** | 6.09 ± 1.71 |
| **$AUC_{0–24\ h}$ (µg·h/mL)** | 3,786.4 ± 324.4 |

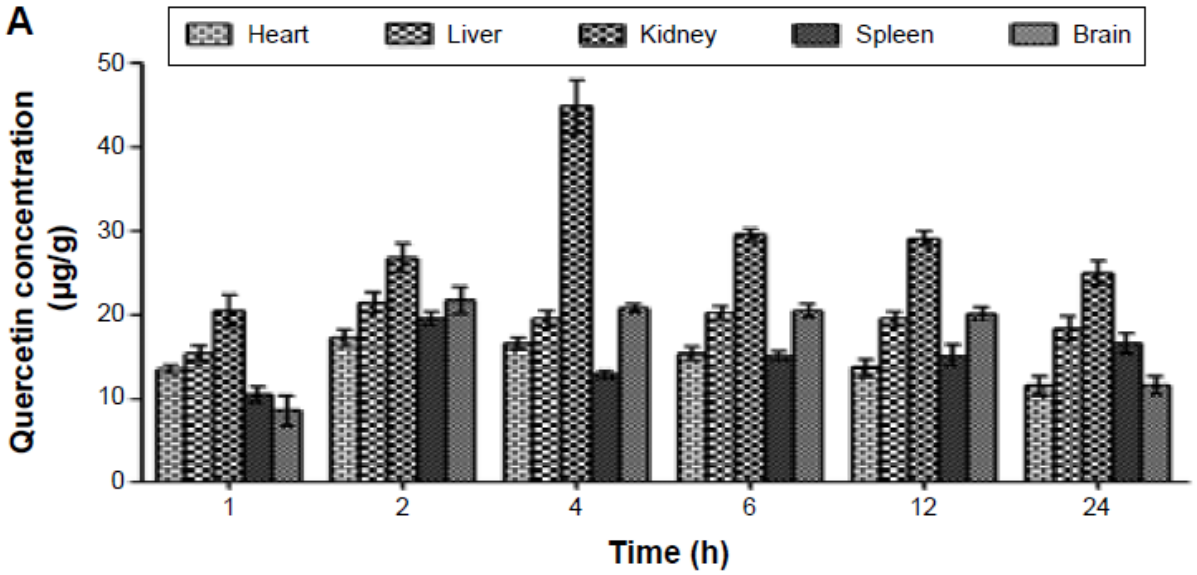


**Figure 5**. Tissue concentration-time profiles of quercetin after oral administration of free quercetin suspensions.

**Table 3**. Pharmacokinetics parameters of tissue distribution of quercetin after oral administration of quercetin suspensions to rats with dose of 50 mg/kg body weight.

| Tissue | $C_{max}$ (μg/mL) | $AUC_{total}$ (μg·h/mL) |
|---|---|---|
| **Brain** | 22.91 ± 3.35 | 201.76 ± 43.63 |
| **Heart** | 18.88 ± 2.09 | 124.29 ± 60.40 |
| **Liver** | 21.44 ± 3.97 | 248.91 ± 11.36 |
| **Kidney** | 43.67 ± 2.28 | 603.66 ± 35.23 |
| **Spleen** | 19.44 ± 1.35 | 284.09 ± 27.66 |

## CAPSAICIN AND ITS ANALOGUES

Peppers are popular around the world, which are often used as food additives to provide the hot and pungent taste. Capsaicinoids are flavor compounds in red chili peppers, mainly composed of capsaicin (C), dihydrocapsaicin (DHC), nordihydrocapsaicin (n-DHC), Homocapsaicin (h-C) and homodihydrocapsaicin (h-DHC) (*32*) (**Table 4**). Among these, capsaicin and dihydrocapsaicin contribute to around 80% to 90% of the total pungency in most chili peppers (*33*). Altogether, more than 20 capsaicinoids have been found in different pepper species (*34*). Capsaicinoids are biosynthesized in the placenta of the fruits by condensation of vanillylamine and medium chain length fatty acids (*35*).

**Table 4**. Chemical structures of capsaicinoids.

| Capsaicinoid Name | Abbreviation | Molecular Formula | Chemical Structure |
|---|---|---|---|
| Capsaicin (*trans*-8-methyl-*N*-vanillyl-6-nonenamide) | C | $C_{18}H_{27}NO_3$ | 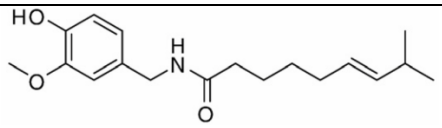 |
| Dihydrocapsaicin (8-methyl-*N*-vanillyl-nonanamide) | DHC | $C_{18}H_{29}NO_3$ | 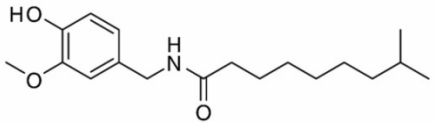 |
| Nordihydrocapsaicin (7-methyl-*N*-vanillyl-octamide) | n-DHC | $C_{17}H_{27}NO_3$ | 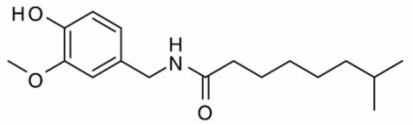 |
| Homocapsaicin (*trans* 9-methyl-*N*-vanillyl-7-decenamide) | h-C | $C_{19}H_{29}NO_3$ | 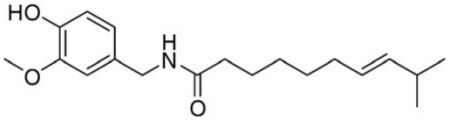 |

| | | | |
|---|---|---|---|
| Homodihydrocapsaicin<br><br>(9-methyl-*N*-vanillyl-decamide) | h-DHC | $C_{19}H_{31}NO_3$ | 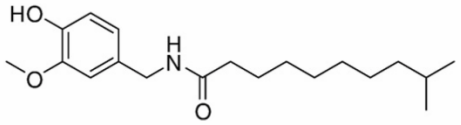 |

.

## BIOLOGICAL PROPERTIES OF CAPSAICIN AND MECHANISMS

*Anti-cancer*

Researches that were conducted on the anti-cancer and anti-tumor effects of capsaicin had demonstrated that capsaicin could induce apoptosis in cancer cells as well as suppress carcinogenesis in prostate, skin, breast, colon, lung and human bladder (*36-41*). According to F. Ziglioli *et al* (*42*), apoptosis in prostate cancer cells was triggered through two pathways: direct pathway (transient receptor potential vanilloid type 1 (TRPV-1) receptor-independent pathway) and indirect pathway (TRPV-1 receptor-dependent pathway). In the direct pathway, capsaicin was working as the coenzyme Q antagonist in controlling of the electron transport, resulting in an excess amount of reactive oxygen species (ROS). Consequently, cell damage and apoptosis mechanism was activated. In the indirect pathway, capsaicin interacted with receptor TRPV-1, which contained an ionotropic channel with regulatory functions of $Ca^{2+}$, leading to the accumulation of $Ca^{2+}$ within cancer cells and finally to the precocious and late elements of apoptosis. Moreover, Kim *et al* discovered that the apoptosis triggered by capsaicin was selectively happening in malignant cell lines instead of normal cell lines (*43*), the mechanism of which could be partially explained by different endoplasmic reticulum stress in malignant cells and normal cells in responses to the stimulation of capsaicin (*44*).

While most anti-cancer researches focused on mechanisms of capsaicin-induced apoptosis, only a few studies were concentrated on signaling pathways of capsaicin-induced cell cycle arrest. Experiments conducted by Kathleen C. Brown *et al.* revealed that capsaicin could induce G1 arrest in human small cell lung cancer cell lines, demonstrating an anti-proliferative effect in both cell culture models and mice models (*45*).

*Anti-oxidation*

Anti-oxidation activities of capsaicin had been proved by previous researches both in vitro and in vivo (*46-48*). The *in vitro* study using serum lipoproteins proved that capsaicin and dihydrocapsaicin increased the lag time before initiation of low-density lipoprotein (LDL) oxidation and decreased the oxidation rates, thereby reducing the lipid oxidation (*49*). Another study in human umbilical vein endothelial cells (HUVECs) demonstrated that capsaicin inhibited ROS generation and caspase-3 activation induced by oxidized low-density lipoprotein (oxLDL) (*50*). The oxidation of LDL was in relevance with the pathophysiology of atherosclerosis. Therefore, the antioxidant compound capsaicin could prevent cardiovascular diseases by protecting against oxLDL-induced endothelial dysfunctions.

In vivo, a reduction of oxidative stress in the liver, lung, kidney and muscle was reported in mice models after oral administration of capsaicin for 3 days (3 mg/kg body mass per day), showing that capsaicin could be an effective antioxidant in lowering oxidative

stress even when consumed for a short time (*51*). Experiments conducted by Bencsik *et al.* indicated that capsaicin could modulate the oxidative damage via reducing the formation of nitric oxide (NO) and peroxynitrite ($ONOO^-$) as well as increasing the superoxide dismutase (SOD) activities (*52*). Similar results could be found in the study by Hassan *et al.*, who revealed that capsaicin could protect the liver against carbon tetrachloride ($CCl_4$) - induced toxicity in rats by working as an antioxidant to reduce the production of free radicals and suppress the caspase-3 activities (*53*).

Therefore, the mechanism for antioxidative effects of capsaicin can be summarized as reducing the production of ROS and promoting the activities of antioxidant enzymes such as superoxide dismutase (SOD), catalase (CAT) and glutathione-S-transferases (GSTs), *etc.*

*Pain relief*

Capsaicin has been used to alleviate pain from neuropathic and musculoskeletal disorders, such as postherpetic neuralgia, diabetic neuropathy, osteoarthritis, and rheumatoid arthritis during topical applications (*54*). As was mentioned previously, after capsaicin binds to the TRPV1, intracellular $Ca^{2+}$ content will increase and inflammatory neuropeptides (substance P) will be released (*55*). Through this calcium-dependent process, neurons and nerve terminals are damaged and desensitized to further painful stimuli, leading to the analgesic effects or even the degeneration of nociceptive fibres (*56*). The reader is referred to several excellent reviews on this subject (*54, 57, 58*).

As an analogue to capsaicin, resiniferatoxin (RTX) can also activate TRPV1 and cause a large, prolonged increase in the intracellular $Ca^{2+}$. The excess amount of accumulated calcium will induce cytotoxicity and even apoptosis, resulting in the elimination of TRPV1-expressing neurons or cells (*59*). This process can be regarded as an alternative mechanism of pain relief.

In brief, capsaicin exerts analgesic effect by binding to the vanilloid receptor TRPV1 and regulating voltage activated calcium channels. Therefore, by understanding its mechanism of analgesics, we can develop capsaicin analogues and TRPV1 antagonists to better help with pain relief in the future.

*Cardioprotection*

Cardioprotective effects of capsaicin in animal models have been proved by studies performed during topical application, oral administration and intravenous injections. Researches by Jones, W.K. showed that topical application of capsaicin cream could result in significantly reduced infarcts following a 45-min coronary occlusion (*60*), demonstrating a cardioprotective activity in mice. Beneficial cardiovascular effects in rats of metabolic syndrome were also observed by feeding them 0.5mg/kg - 1.0mg/kg body weight of capsaicin together with regular diets (*61*). Those beneficial functions include heart rate variability improvement, increased vascular sympathetic drive and increased a-index (spontaneous baroreflex sensitivity). In addition, Gross *et al*. also reported that rats receiving capsaicin intravenously with doses ranging from 0.1 mg/kg to 1 mg/kg could reduce myocardial infarct sizes via TRPV1 channel (*62*).

In order to find out the mechanism of capsaicin's cardioprotective effects, Ma, L. *et al* proved that TRPV1 activation by capsaicin could reduce vascular lipid accumulation and ameliorate atherosclerosis in mice evoked by a high-fat diet through a calcium-dependent pathway (*63*). Therefore, the stimulation of TRPV1 by capsaicin could increase cytosolic calcium and therefore change cholesterol transporters expression, leading to enhanced cholesterol efflux and reduced cholesterol uptake into vascular smooth muscle cells, which lowered the major risk factor in the pathogenesis of atherosclerosis.

*Anti-obesity (Weight reduction)*

Consumption of chili peppers is known to increase the energy expenditure. And capsaicin as an active component in chili peppers has been proved to have thermogenic and anti-obesity properties (*64-67*). Reinbach *et al.* studied the effects of capsaicin on appetite, energy intake, body weight and heart rate in humans for six weeks (*64*). Results suggested that capsaicin could reduce the energy intake as well as help weight loss by relatively suppressing hunger and sustaining satiety.

To understand the mechanism underlying the weight reduction effect, Joo *et al.* fed the rats on a high fat diet with capsaicin and performed proteomic analysis to elucidate its molecular action in white adipose tissue (*67*). Results revealed that proteins related with lipid metabolism, redox regulations, and signal and energy transduction were significantly altered on the treatment of capsaicin, suggesting possible mechanism of anti-obesity effect of capsaicin.

Therefore, beneficial biofunctions of capsaicinoids have been reported with respect to anti-inflammation, anti-cancer, analgesic, cardioprotective, anti-oxidation and anti-obesity activities, which mainly function through activating the transient receptor potential vanilloid (TRPV) superfamily of cation-channel receptors (*36, 57*). However, direct ingestion of capsaicin can be lethal at a certain amount. Oral LD50 values of capsaicin are 161.2 mg/kg for rats and 118.8 mg/kg for mice. To alleviate its gastric mucosa irritation effects, many encapsulation methods have been employed with enhanced stability, bioaccesbility and bioavailability (*68-70*)

**EXTRACTION METHODS**

Various extraction methods of capsaicinoids from hot peppers have been developed during the past few decades. When designing an extraction process, the first step is the selection of appropriate solvent that can result in a high yield of desired compound. Among all solvents that have been used for extracting capsaicinoids, methanol, ethanol, acetonitrile and water are most common (*71*). In addition to the solvent selection procedure, there are many other influencing parameters to be considered in order to achieve high extraction efficiency, such as the temperature, extraction time, volume of solvent, quantity of sample, the repeatability and reproducibility of the methods. The extraction techniques that have widely been employed by researches include maceration (*72*), magnetic stirring (*73*), enzymatic extraction (*74*), microwave- (*75*) and ultrasound-assisted extraction (*76*), Soxhlet (*77*), supercritical fluid (*78*) and pressured liquids extraction (*79*). In this section, common extraction methods for capsaicinoids

have are reviewed and discussed.

*Enzymatic treatment*

Enzymatic processes have been proposed to increase yield and selectivity during extraction from fruits (*80*). In a study conducted by Santamaria et al, various commercially available enzymes were used to soften the tissues in Capsicum peppers and increase the extraction yield by 7%, with the final recovery of 80% of capsaicinoids (*74*). Enzymes used in this research include Olivex (mainly pectinase), Celluclast (mainly cellulase), Viscozyme L (mainly carbohydrase), and Peczyme 5XAL (mainly pectin esterase and arabanase). The treatment took place at 50 °C, required 7 h of agitation in a rotary shaker at 120 rpm, and the ratio of chili powder to water was 1:50. Later, a similar treatment method was adopted by Desikacharya *et al*. using Extrazyme (mainly pectinase and multiple carbohydrases) and Energex (mainly glucanase), which increased capsaicinoid extraction yield by 32% (*81*). In this case, the temperature was controlled at 37 °C for 12 h, and the ratio of chili powder to water was 1:1. Based on the treatment methods stated above, Salgado-Roman et al proposed a noncommercial enzymatic treatment using the enzymatic extracts derived from *Rhizopus nigricans* (*82*). After the enzymatic degradations, the chili fruit was dehydrated in a vacuum oven and later got milled. Then powdered samples were extracted in a Soxhlet system with tetrahydrofuran at 60 °C. A higher extraction yield above 85% was achieved for capsaicinoids, which demonstrated a more potent cellulose activity of this noncommercial enzymatic extract to soften the cell walls and facilitate the degradation of the cells.

*Ultrasound-assisted extraction (UAE)*

The ultrasound-assisted extraction (UAE) technique is effective due to the phenomenon of cavitation occurring when an ultrasonic wave is passing through the organic solvent, producing energy to enhance the mixing and penetration of solvent into the sample matrix (*76*). The application of UAE provides many advantages, such as the reduction of solvents, temperature and time for extraction, which is very important for the extraction of thermolabile and unstable compounds (*83*).

Barbero et al have developed a rapid and reproducible UAE method for capsaicinoids from three varieties of peppers in Spain using 25 mL of methanol as solvent at a temperature of 50 °C for 10 min (*1*). The quantificative analysis using HPLC is listed in **Table 5**.

*Soxhlet extraction (SOX)*

The soxhlet process is a traditional method that is widely applied to extract the oil from organic matrix, which is used when the desired compound has limited solubility in a solvent while the impurities are insoluble in this solvent (*77*). Bajer *et al.* extracted capsaicinoids from many chili samples using SOX method with methanol as solvent and an extraction time of 2 h (*84*). The extraction result is listed in **Table 5**. Same SOX method was used in a study by Liu *et al*. (*85*), in which extraction of 1.0 g of *Capsicum annuum* sample was performed with 50 mL methanol for 2 h. Though SOX is the

conventional method for extraction, it has disadvantages such as relative longer extraction time, higher energy consumptions and lower yields of capsaicinoids compared with other extraction methods, such as UAE, MAE and PLE.

*Supercritical fluid extraction (SFE)*

Supercritical fluids are substances at pressures and temperatures above their critical values, which are strong solvents for non-polar compounds (*86*). After pressure is adjusted to ambient pressure, the supercritical fluids will return to the gas phase and evaporate without leaving solvent residues. Supercritical fluids extraction (SFE) has been used as an alternative to traditional extraction method during extraction of bioactive compounds with the advantage of moderate temperatures, reduced energy consumptions and high purity extracts (*87*). Carbon dioxide $CO_2$ is frequently used as the supercritical solvent for extraction of capsaicinoids due to its low cost, nontoxicity, non-flammability, inertness and high extraction capacity (*78, 88, 89*).

Santos *et al*. *(90)* extracted capsaicinoids from malagueta pepper (Capsicum *frutescens* L.) using SFE assisted with ultrasound with $CO_2$ as solvent at pressure, temperature and flow rate of 15MPa, 40 °C and $1.673\times10^{-4}$ kg/s, respectively. The enhanced SFE rate was achieved when ultrasound power was applied at 360 W during 60 min (**Table 5**). Later in 2016, Dias *et al.* performed a similar SFE test on dedo de moça pepper with (25 MPa, 40 °C, 600W and 80 min) and without (25 MPa, 40 °C) application of ultrasound (*87*). The $CO_2$ flow rate was kept constant at $1.7569\times10^{-4}$ kg/s. Results showed that global yield of SFE was successfully increased. In summary, the application of ultrasound can

increase the SFE yield of capsaicinoids from peppers, which can work as an alternative for traditional extraction techniques that use toxic organic solvents.

*Pressurized liquids extraction (PLE)*

The operation of pressurized liquid extraction (PLE) is often conducted at high temperature and pressure, enabling high solubility of compound in the solvent while keeping the solvent below its boiling point, and therefore resulting in a high penetration of the solvent into the sample matrix (*79, 91*). Many researches have adopted the PLE method in the extraction of capsaicinoid from hot peppers (*84, 85, 92*). Barbero *et al*. developed a PLE method with the extraction solvent of water, methanol and ethanol; temperature of 200 °C and pressure of 100 atm. The result was analyzed by HPLC-MS. According to an experiment conducted by Liu *et al.* (*85*), three capsaicinoids (C; DHC; n-DHC) were extracted from dried *Capsicum annuum* samples through PLE method with methanol as the solvent; temperature at 100 °C and pressure at 1500 psi, combined with LC-MS/MS as the quantitative analysis method. Pressurized hot water extraction (PHWE) method was also used to extract capsaicinoids from ten chili samples following the procedures reported by Bajer et al (*84*). In this assay, water was selected as the environmentally friendly solvent and heated to 200 °C at pressure of 20 MPa. The quantitative analysis was performed by HPLC-MS. They also compared extraction efficiency of three capsaicinoids (C, DHC and n-DHC) through different extraction methods (UAE, MAE, PLE and SOX) and found that highest yields were achieved using PLE (**Table 6**).

*Microwave-assisted extraction (MAE)*

The technique of microwave-assisted extraction (MAE) is developed through the combination of microwave and traditional solvent extraction, which applies the energy generated through microwave radiation to heat the solvents and increase the kinetic of extraction. MAE has been employed for extraction of capsaicinoids from peppers in many studies (*75, 93, 94*). According to Williams et al (*75*), capsaicinoids yield through MAE method doubled and extraction time was significantly shortened compared with traditional reflux and shaking flask extraction methods. MAE conditions for extraction of capsaicinoids from fresh pepper samples was optimized by Barbero et al (*93*). In this study, extraction conditions of 125 °C extraction temperature, 0.5 g triturated pepper in 25 mL solvent (ethanol), 500 W of power and 5 min extraction time was found the optimum. The authors also compared the extraction efficiency of commonly used methods such as magnetic stirring, and confirmed that MAE is a much faster method. Chuichulcherm et al (*94*) made a comparison of three different extraction techniques (SOX, MAE and UAE) (**Table 7**). The amount of capsaicinoids derived from SOX, MAE and UAE methods at each optimum condition were 5.243, 5.282 and 4.014 mg/g dried chili, with the extraction time of 300, 20 and 20 min, respectively. The results showed that MAE method generated highest amount of capsaicinoids with 20 min extraction time and medium energy consumption, while SOX gave the highest energy consumption with extraction time of 300 min. The UAE method had the minimum energy consumption per capsaicinoids and shortest extraction time among three methods.

**Table 5**. Quantification of capsaicinoids extracted from peppers through different extraction methods. Capsaicin (C), dihydrocapsaicin (DHC); nordihydrocapsaicin

(n-DHC); homocapsaicin (h-C); homodihydrocapsaicin (h-DHC). n.d.: not detected;

| Method | Solvent | Conditions | Pepper | C | DHC | n-DHC | h-C | h-DHC | Unit | Refs |
|---|---|---|---|---|---|---|---|---|---|---|
| UAE | Methanol | Temp: 50 °C; Time: 10 min; Pressure: 1 atm (14.696 psi). | Cayenne | 448 ± 28 | 265 ± 15 | 94 ± 6 | 30 ± 1 | 47 ± 2 | µmol/kg of fresh pepper | (*71*) |
| | | | Bolilla Redondo pepper | 370 ± 23 | 190 ± 11 | 40 ± 3 | n.d. | 20 ± 1 | | |
| | | | Bollila Largo pepper | 275 ± 17 | 122 ± 7 | 25 ± 2 | n.d. | 14 ± 1 | | |
| SOX | Methanol | Time: 2h; Pressure: 1 atm (14.696 psi). | Trinidad Scorpion Moruga fruit | 42.88 ± 0.403 | 18.09 ± 0.16 | 0.42 ± 0.03 | n.d. | n.d. | g/kg of dried ground sample | (*84*) |
| | | | Yellow Bedder fruit | 2.49± 0.09 | 2.53 ± 0.09 | 0.29 ± 0.02 | n.d. | n.d. | | |
| | | | Ring of Fire fruit | 1.74 ± 0.06 | 1.73 ± 0.04 | 0.51 ± 0.02 | n.d. | n.d. | | |
| | | | Jamaican Hot Red fruit | 2.08 ± 0.08 | 1.17 ± 0.06 | 0.20 ± 0.02 | n.d. | n.d. | | |
| | | | Yellow Habanero fruit | 0.54 ± 0.02 | 0.41 ± 0.02 | 0.027±0.01 | n.d. | n.d. | | |
| | | | Tabasco fruit | 3.19 ± 0.03 | 2.50 ± 0.09 | 0.94 ± 0.04 | n.d. | n.d. | | |
| | | | Chiltepin fruit | 0.29 ± 0.02 | 0.22 ± 0.02 | 0.07 ± 0.01 | n.d. | n.d. | | |
| | | | Bhut Jolokia spice | 8.50 ± 0.07 | 5.74 ± 0.05 | 0.18 ± 0.02 | n.d. | n.d. | | |
| | | | Trinidad Scorpion Moruga spice | 20.42 ± 0.09 | 12.26 ± 0.07 | 0.45 ± 0.02 | n.d. | n.d. | | |
| | | | Fatalii Red spice | 10.64 ± 0.10 | 3.06 ± 0.09 | 0.10 ± 0.01 | n.d. | n.d. | | |
| | Ethyl acetate | Time: 6 h; Temp: 25°C; | Malagueta pepper (Capsicum *frutescens* L.) | 2.16 ± 0.20 | 1.20 ± 0.09 | 0.10 ± 0.01 | n.d. | 0.04± 0.003 | g/kg of dried sample | (*90*) |
| | Dichloromethane | | | 2.27 ± 0.30 | 1.22 ± 0.17 | 0.10± 0.015 | n.d. | 0.04± 0.006 | | |
| | Ethyl ether | | | 1.76 ± 0.12 | 0.97 ± 0.07 | 0.08± 0.003 | n.d. | 0.03± 0.006 | | |
| | Hexane | | | 1.88 ± 0.17 | 1.05 ± 0.09 | 0.09± 0.015 | n.d. | 0.03± 0.004 | | |
| SFE | Carbon dioxide | Temp: 40°C; Pressure: 25 MPa (3625.94psi) | Dedo de moça pepper | 0.88 ± 0.11 | 0.37 ± 0.04 | 0.06 ± 0.01 | 0.04 ± 0.00 | 0.01 ± 0.00 | g/kg of raw material | (*87*) |
| | Carbon dioxide | Temp: 40°C; Pressure: 15 MPa (2175.57 psi) | Biquinho peppers (C. *chinense*) | 0.30 ± 0.01 | 0.075 ± 0.007 | n.d. | n.d. | n.d. | g/kg of dried ground sample | (*89*) |
| | | Temp: 50°C; Pressure: 15 MPa (2175.57 psi) | Biquinho peppers (C. *chinense*) | 0.22 ±.0.001 | 0.042 ± 0.001 | n.d. | n.d. | n.d. | | |
| SFE+US | Carbon dioxide | Ultrasound power: 600W; Temp: 40°C; Time: 80 min; Pressure: 25 MPa (3625.94psi) | Dedo de moça pepper | 0.94 ± 0.09 | 0.39 ± 0.04 | 0.06 ± 0.00 | 0.04 ± 0.00 | 0.01 ± 0.00 | g/kg of raw material | (*87*) |

| | | | | | | | | | | |
|---|---|---|---|---|---|---|---|---|---|---|
| | Carbon dioxide | Ultrasound power: 360W; Temp: 40°C; Time: 60 min; Pressure: 15 MPa (2175.57 psi) | Malagueta pepper (Capsicum *frutescens* L.) | 1.93 ± 0.05 | 1.01 ± 0.03 | 0.07± 0.021 | n.d. | 0.03 ±0.003 | g/ kg of raw material | (*90*) |
| PLE | Methanol; Ethanol; Water | Temp: 200 °C; Pressure: 10 atm (146.96 psi) | Long marble pepper | 369.8 ± 23.3 | 190.1 ± 10.9 | 40.3 ± 2.7 | n.d. | 19.7 ± 0.9 | µmol/kg of fresh pepper | (*92*) |
| | | | Round marble pepper | 275.2 ± 17.3 | 122.5 ± 7.0 | 25.3 ± 1.7 | n.d. | 14.5 ± 0.7 | | |
| | Methanol | Temp: 100 °C; Pressure: 1500 psi | Capsicum *annuum* samples | 0.75 | 0.34 | 0.13 | n.d. | n.d. | g/kg of dried pepper | (*85*) |
| | | | | 1.17 | 0.68 | 0.14 | n.d. | n.d. | | |
| | | | | 0.73 | 0.32 | 0.064 | n.d. | n.d. | | |
| | | | | 0.56 | 0.24 | 0.047 | n.d. | n.d. | | |
| | | | | 1.49 | 0.89 | 0.19 | n.d. | n.d. | | |
| | Water | Temp: 200 °C; Pressure: 20 MPa (2900.75 psi) | Trinidad Scorpion Moruga fruit | 46.45 ± 0.41 | 15.54 ± 0.16 | 0.30 ± 0.02 | n.d. | n.d. | g/kg of dried ground sample | (*84*) |
| | | | Yellow Bedder fruit | 3.96 ± 0.09 | 3.10 ± 0.09 | 0.50 ± 0.03 | n.d. | n.d. | | |
| | | | Ring of Fire fruit | 1.86 ± 0.06 | 1.82 ± 0.04 | 0.61 ± 0.03 | n.d. | n.d. | | |
| | | | Jamaican Hot Red fruit | 2.55 ± 0.08 | 1.35 ± 0.05 | 0.26 ± 0.02 | n.d. | n.d. | | |
| | | | Yellow Habanero fruit | 0.74 ± 0.03 | 0.51 ± 0.02 | 0.02 ± 0.01 | n.d. | n.d. | | |
| | | | Tabasco fruit | 3.94 ± 0.04 | 2.70 ± 0.09 | 1.07 ± 0.05 | n.d. | n.d. | | |
| | | | Chiltepin fruit | 0.31 ± 0.02 | 0.22 ± 0.02 | 0.08 ± 0.01 | n.d. | n.d. | | |
| | | | Bhut Jolokia spice | 9.13 ± 0.08 | 4.83 ± 0.08 | 0.22 ± 0.02 | n.d. | n.d. | | |
| | | | Trinidad Scorpion Moruga spice | 20.26 ± 0.21 | 10.57 ± 0.10 | 0.52 ± 0.03 | n.d. | n.d. | | |
| | | | Fatalii Red spice | 12.40 ± 0.10 | 3.12 ± 0.09 | 0.14 ± 0.01 | n.d. | n.d. | | |
| MAE | Ethanol | Temp: 125°C; Time: 5 min Pressure: 1 atm (14.696 psi) | Cayenne | 451.6 ± 32.8 | 265.4 ± 18.1 | 93.8 ± 6.6 | 29.6 ± 1.7 | 46.9 ± 2.4 | µmol/kg of fresh pepper | (*93*) |
| | | | Long marble pepper | 378.8 ± 24.3 | 185.6 ± 10.3 | 40.3 ± 2.7 | nd | 18.9 ± 0.8 | | |
| | | | Round marble pepper | 265.2 ± 16.8 | 132.4 ± 8.0 | 23.2 ± 1.4 | nd | 15.3 ± 0.6 | | |

**Table 6.** Extraction efficiency (%) of capsaicinoids from Capsicum *annuum* sample using different extraction methods (*28)* . Capsaicin (C), dihydrocapsaicin (DHC); nordihydrocapsaicin (n-DHC).

| Extraction method | C | DHC | n-DHC |
|---|---|---|---|
| UAE | 85.26 ± 1.35 | 89.46 ± 1.31 | 86.72 ± 1.31 |
| MAE | 86.36 ± 1.12 | 88.26 ± 1.21 | 87.46 ± 1.27 |
| PLE | 98.31 ± 1.46 | 97.27 ± 1.13 | 97.91± 1.05 |
| SOX | 88.31 ± 1.03 | 87.32 ± 1.22 | 1.13 |

**Table 7.** Energy consumption to capsaicinoids ratio of Capsicum *frutescens* Linn using different extraction methods. (*37)*

| Extraction method | Extraction time (min) | Energy Consumption (KJ) | Capsaicinoid (mg/g dried chili) | Energy consumption per capsaicinoid (kJ/mg) |
|---|---|---|---|---|
| UAE | 20 | 102 | 4.014 | 25.411 |
| MAE | 20 | 384 | 5.282 | 72.700 |
| SOX | 300 | 21600 | 5.243 | 4119.779 |

## BIOAVAILABILITY OF CAPSAICINOIDS

### *Absorption and Metabolism*

The absorption, distribution, metabolism and elimination of capsaicinoids (mainly capsaicin and dihydrocapsaicin) have been reported for a long time (*95-99*). According to Kawada et al (*99*), about 85% capsaicin and dihydrocapsaicin were rapidly absorbed from stomach and small intestine after administration in male Wistar rats. The absorbance efficiency of 1mM capsaicin in stomach, jejunum and ileum was 50%, 80% and 70%, respectively; indicating that absorption of capsaicin was higher in the small intestine than in the stomach. They suggested that a small amount of dihydrocapsaicin was hydrolyzed to vanillylamine and 8-methyl nonanoic acid when passing through the epithelial cells of the jejunum after absorption. The majority of capsaicin and dihydrocapsaicin were metabolized in the liver after being transported via the hepatic portal vein. In a similar study, Donnerer *et al*.(*95*) examined the metabolism and

absorption of capsaicinoids in the anaesthetized male Sprague-Dawley rats through intragastric administration. They reported that capsaicin and dihydrocapsaicin were almost completely metabolized in the liver before entering the systematic and general circulation. Recently, Kuzma et al (*96*) analyzed the intestinal absorption and metabolism of capsaicinoids in male Wistar rats using *ex vivo* perfusion of standard *Capsicum* extraction through proximal jejunum. Results showed that capsaicinoids were fast absorbed in jejunum and metabolized into capsaicin glucuronide and dihydrocapsaicin glucuronide by the UDP-glucuronyltransferse (UGT) enzymes, which were then excreted back into the intestinal lumen. While hepatic metabolism of capsaicin and dihydrocapsaicin had been illustrated in previous studies, this study reported for the first time the detailed intestinal metabolism of two capsaicinoids.

The hepatic metabolism of capsaicin was described in a work by Chanda et al (*100*), in which the biotransformation of capsaicin in rat, dog, and human hepatic microsomes and S9 fractions was examined. 5 primary metabolites were detected after incubations. Major side chain-hydroxylated metabolites of capsaicin included 16-hydroxycapsaicin and 17-hydroxycapsaicin. 16,17-dehydrocapsaicin was produced by oxidation of capsaicin or dehydration of the hydroxylated metabolites. Vanillylamine was generated by hydrolysis of the amide bond of capsaicin, part of which was further metabolized to form vanillin. Metabolism of capsaicinoids by cytochrome p450 enzymes was also reported by Reilly et al (*101, 102*). 5,5'-capsaicin, part of which was further metablized were also capable of oxidizing capsaicin to produce free radical intermediates.

The *in-vitro* and *in-vivo* metabolism of dihydrocapsaicin in rats was studied by Kawada *et al*. (*99*). 48 hours after the oral administration of dihydrocapsaicin in male Wistar rats at a dose of 20 mg/kg body weight, the unchanged dihydrocapsaicin (8.7% of total dose) and its metabolites were detected in urine, which included vanillylamine (4.7%), vanillin (4.6%), vanillyl alcohol (37.6%) and vanillic acid (19.2%). In addition, 10% of unchanged dihydrocapsaicin was also identified in feces. The *in vitro* study was performed using cell-free extracts of rat liver, which contained dihydrocapsaicin-hydrolyzing enzymes to transform dihydrocapsaicin to vanillylamine and 8-methyl nonanoic acid. The vanillylamine was further transformed to vanillin *in situ*.

The pharmacokinetics study of capsaicin in human subjects has also been studied and evaluated. When taken orally, capsaicin is absorbed in stomach and whole intestine, and metabolized in liver. The absorption and first-pass metabolism of capsaicin after oral administration in humans is demonstrated in **Figure 6 (A)**.

In 2009, Chaiyasit *et al.*, investigated the human pharmacokinetics of orally administrated Capsicum frutescens, which contains 26.6 mg of pure capsaicin (*103*). He reported that the peak plasma concentration of capsaicin was 2.47 ± 0.13 ng/ml, half-life $t_{1/2}$ was 24.9 ± 5.0 min. $T_{max}$ was 47.1 ± 2.0 min, which was in correspondence to the $T_{max}$ in rats (0.75 ± 0.35 h) as was shown in **Table 8**.

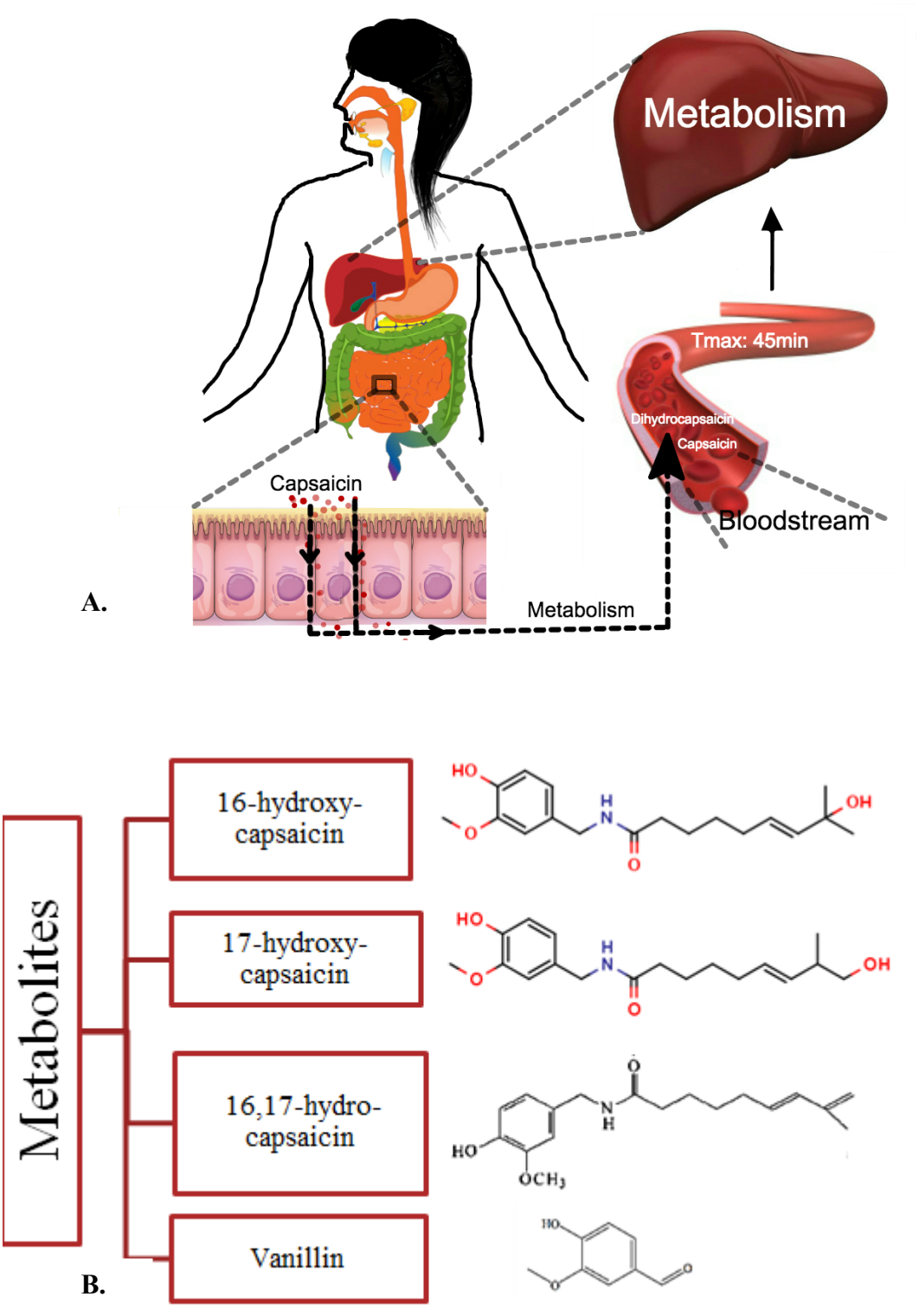


**Figure 6. (A)** Absorption and first-pass metabolism of capsaicin after oral application in

humans; **(B)** Proposed biotransformation pathway for capsaicin after first-pass metabolism in liver

*Tissue distribution and elimination*

The study of *in vivo* tissue distribution and subsequent elimination after oral administration of capsaicin to Wistar male albino rats (30 mg/kg of body weight) were carried out by Suresh et al (*98*). During each time internal at 1 h, 3 h, 6 h, 1 d, 2 d, 4 d and 8 d following the oral gavage of capsaicin, six rats were sacrificed and serum were separated from blood samples for HPLC analysis. Liver, kidney and intestine were excised for distribution study. Urine and faecal samples were collected for elimination study. According to the tissue distribution result in **Table 8**, the highest concentration was shown at 1 h in blood and intestine, 3 h in liver and 6 h in kidney. The total concentration of 24.4% of administered capsaicin was seen after 1 h, which was reduced to 1.24 % in 24 h and 0.057 % in 48 h. After 96 h, no capsaicin was detected in all tissues.

The elimination result of orally administered capsaicin is shown in **Table 9**. Within 4 days, the amount of capsaicin excreted in faeces and urine was 6.34 % and 0.095%, respectively. Therefore, about 94% of capsaicin was absorbed through oral administration. After 5 days, no capsaicin was detected in urine and faeces. This result was consistent with previous bioavailability study (*99*), which proved that 85% of capsaicinoids were quickly absorbed from the GI tract following oral administration .

**Table 8.** Tissue distribution of orally administered capsaicin in rats at dosage of 30 mg/kg body weight (n = 6) (*98*).

| Time (h) | Serum (µg/ml) | Blood (µg/total blood) | Liver (µg /whole tissue) | Kidney (µg/whole tissue) | Intestine (µg/whole tissue) |
|---|---|---|---|---|---|
| 1 | 1.90 ± 0.18 | 11.11 ± 1.05 | 24.7 ± 2.1 | 3.61 ± 0.32 | 1057.0 ± 157.0 |
| 3 | 1.47 ± 0.09 | 8.59 ± 0.53 | 44.7 ± 3.37 | 5.71 ± 0.33 | 700.2 ± 42.2 |
| 6 | 0.93 ± 0.10 | 4.85 ± 0.59 | 14.8 ± 1.50 | 6.73 ± 0.45 | 249.3 ± 24.0 |
| 24 | 0.05 ± 0.01 | 0.29 ± 0.06 | 8.71 ± 2.55 | 3.35 ± 0.45 | 43.5 ± 3.75 |
| 48 | 0.006 ± 0.001 | 0.035 ± 0.006 | 0.60 ± 0.03 | 0.48 ± 0.09 | 1.14 ± 0.21 |
| 96 | 0.00 | 0.00 | 0.045 ± 0.005 | 0.00 | 0.72 ± 0.01 |
| 192 | 0.00 | 0.00 | 0.00 | 0.00 | 0.00 |

**Table 9.** Elimination of orally administered capsaicin in rats at dosage of 30 mg/kg body weight (n = 6) (*98*).

| Day | Feces | Urine |
|---|---|---|
| 1 | 174.0 ± 11.3 | 4.05 ± 0.45 |
| 2 | 99.8 ± 5.03 | 0.225 ± 0.035 |
| 3 | 11.3 ± 1.25 | 0 |
| 4 | 0.375 ± 0.032 | 0 |
| 5 | 0 | 0 |
| Total | 285.5 (6.34% of administered dose) | 4.275 (0.095% of administered dose) |

## ENCAPSULATION METHODS FOR CAPSAICIN

Encapsulation is a process to entrap different amount of active agents within a thin film of polymer that forms a solid wall (*104, 105*). The encapsulation of capsaicin not only provides a better control release property than coarse compound, but also relieves the irritation by preventing the direct contact between capsaicin and human skin, oral and gastric mucosa. Currently, capsaicin content during topical application is either 0.025% or 0.075% within the cream, patch or gels. The research advances concerning the encapsulation of capsaicin are discussed in this section.

*Encapsulated capsaicin for transdermal delivery systems*

Dermal and transdermal applications played an important role in the delivery of drugs. According to statistics, approximately 33% of drugs in clinical trials were designed for topical applications (*106, 107*). Transdermal delivery systems for capsaicin was proved to have several advantages over oral delivery systems because of the reduction in abdominal irritations, avoidance of first-pass metabolism in liver and increase in the solubility as a lipophilic drug (*108*). Delivery systems of capsaicin for skin penetration had been investigated in formulations such as gels, lipid vesicles, microemulsions, nanoemulsions and nanocapsules.

### Formulated gels

Cubic phase gels containing capsaicin were designed by Peng *et al.* (*109*) using glycerol monooleate (MO), propylene glycol (1,2-propanediol, PG) and water with capsaicin concentration of 2.5mg/g. The internal structure and transdermal control-release

mechanisms of cubic phase gels were investigated, indicating that sustained capsaicin release relied on the water migration through water channels and drug diffusion within the swelling matric system simultaneously. This capsaicin encapsulated cubic phase gel could be applied to pain relief after incision with an enhanced skin penetration and continued release of drug reaching the target site.

Hydrogels were produced and found to possess control-release property, tissue compatibility and permeability by Kim *et al. (110)*. Nanoencapsulated capsaicin hydrogels were later designed using various kinds of polymers, for example, chitosan, Pluronic F-127 and carboxymethyl cellulose, etc (*111, 112*), which presented a reduced *in vivo* skin irritation and enhanced *in vitro* skin permeation compared with commercialized capsaicin formulations, indicating that those capsaicin hydrogels had the potential to be further developed into drugs with sustained release properties during topical application.

In order to find out the proper percentage of capsaicin within hydrogels that was both safe and efficient for patients during topical therapy, researchers tried and evaluated various capsaicin concentrations in recent years. Brodsky *et al.* (*113*) conducted a randomized, double-blind and placebo-controlled experiment on the efficacy of 0.1% capsaicin hydrogel patch in alleviation of chronic myofascial neck pain. According to the result, although the difference between capsaicin group and placebo group was not obvious, application of 0.1% capsaicin hydrogel patch did relieve the neck pain effectively. In addition, the capsaicin content in treatment of painful diabetic neuropathy (PDN) was also studied by various scholars. Previous researches on the concentration of

0.075% demonstrated moderate efficacy for PDN with burning sensation. Kulkantrakorn *et al.* (*114*) tried a capsaicin content of 0.025%, which was later proved to be safe and well tolerated for patients with PDN. However, no analgesic effect could be observed in this clinical trial.

Organolgels containing 0.05% capsaicin were explored by Allen Jr (*115*). Ketamine HCl, ethanol, lecithin and Pluronic F127 20% gels were added and used as anesthetic, antimicrobial preservative, emollient and solubilizing agent, separately. Finally, all ingredients got thoroughly mixed using a shear-mixing technique. This type of organogel applies to relieving orofacial neuropathic pain.

**Lipid vesicles**

Capsaicin-loaded flexible membrane vesicles (FMVs) and liposomes were prepared using thin-film hydration method by K. Raza *et al*. for the study of topical delivery of capsaicin (*116*). Physiochemical characters of two formulations were evaluated in transmittance, entrapment efficiency, deformability, stability, skin permeation and compatibility, and pharmacodynamics *etc*. Results showed that even though both vesicles had lower skin penetration than conventional formulations, the analgesic effect was enhanced and skin irritation was reduced.

Analogous to liposomes, noisomes had closed bilayer structures that were formed through the self-assembly of nonionic amphiphiles in aqueous media (*117*). Capsaicin-loaded niosomal formulations were prepared by Tavano *et al*. using Tween 80

and Span 80 with certain HLB values (*118*). Noisomes were in the size range of 162-576nm and encapsulation efficiency (EE) range of 39.42- 86.71%. The diameter increased with surfactant hydrophilicity and formulations' surface energy; and EE was dependent on the ratio between surfactant. Therefore, results indicated that niosomes could be used to promote the transdermal delivery of capsaicin.

Besides liposomes and niosomes, solid-lipid nanoparticles were also exploited as potential drug carrier systems. Desai *et al.* designed a novel biodegradable lipid-polymer hybrid nanoparticle, encapsulating capsaicin and anti-TNFα siRNA (siTNFα), both of which are anti-inflammation agents, to treat chronic skin inflammatory diseases (*119*). Enhanced skin permeation was observed by using fluorescently labeled siRNA. Moreover, both capsaicin and siTNFα were successfully delivered to the deeper dermal milieu. Similar efficacy was achieved by another capsaicin-loaded nano-lipidal carrier (NLCs) (*120*), illustrating that solid-lipid nanoparticles could be a new pharmaceutical delivery system with a wide application spectrum.

**Microemulsions and nanoemulsions**

Microemulsions were homogenous liquid mixtures of water, oil and surfactant, frequently with a cosurfactant. As amphiphilic compounds, surfactants could enhance the skin permeation during dermal and transdermal delivery of microemulsions. Different 0.75% capsaicin microemulsion formulations were prepared using water, ethanol, isopropyl myristate, Tween 80 and Span 80 with different HLB values ranging from 10-14 (*118*). *In vitro* Franz diffusion cells that were used to explore the percutaneous permeation demonstrated that capsaicin microemulsions had an enhanced transdermal delivery

compared with conventional drugs, which was partly affected by HLB values and ratios of Tween 80/Span 80. Similarly, another capsaicin microemulsion was made using soybean oil as the oil phase，a mixture of water and glycerol as liquid phase, Span 80 as surfactant and ethanol as cosurfactant (*121*). The microemulsion system was proved to be an efficient vehicle for topical application of capsaicin.

Compared with microemulsions, nanoemulsion system had much smaller particle sizes, better solubilization for hydrophobic compounds, higher thermodynamic stability and skin penetration ability (*108, 122*). Jee Hye Kim*, et al.* developed a capsaicin o/w nanoemulsion using Tween 80 and Span 80 as surfactant and water as liquid phase (*123*). Skin penetration experiments were conducted using Franz diffusion cells, which showed that capsaicin nanoemulsion with a droplet size of 62.98 nm could successfully penetrate all skin layers from the stratum corneum to the dermis.

**Coacervation method based nanocapsules**

A simple coacervation method for encapsulation of capsaicin was established by Wang, *et al.* (*105*). During the process, gelatin was used as the wall material and glutaraldehyde as a cross-linking reagent. The physiochemical properties of formulated nanocapsule were evaluated, demonstrating an improved melting point and thermal stability. Besides, the mean particle size was controlled at around 100 nm. The successful synthesis of capsaicin nanoparticles could be mainly attributed to the cross-linking reaction between gelatin and glutaraldehyde, which resulted in the formation of nanocapsule shell. Apart from that, the process conditions, such as high shearing force, low gelatin viscosity and

addition of tannins, also helped in the formation of the nanocapsule. Later on, this technique was developed into a complex coacervation method by synthesizing the gelatin and acacia to form a shell for capsaicin encapsulation (*124*). Compared with the simple coacervation method, the addition of acacia improved the interfacial activity and controlled release property of nanocapsulated drug. This technique was also expected to reduce the irritation, enhance the biocompatibility and biodegradation of capsaicin.

*Encapsulated capsaicin for oral administration*

Oral administration for food and drugs was the most traditional and widely used method due to its convenience and high bioavailability. However, direct oral ingestion of capsaicin would provoke irritations to the stomach, such as abdominal pain and burning diarrhea owing to its intensely pungent flavor. Therefore, encapsulation methods for oral delivery of capsaicin were developed to not only reduce the irritation, but also ensure the high bioavailability.

**Liposomes, micelles and colloidal nanocapsules**

In 2014, a capsaicin-loaded liposome was successfully prepared by Zhu *et.al.* using cholesterol, sodium cholate and isopropyl myristate with particle sizes ranging from 50-60 nm (*125*) with the highest loading of 15 $mg \cdot mL^{-1}$. This formulated liposome demonstrated an improved solubility, stability and dissolution rate as well as relieved gastric mucosa irritation caused by capsaicin in rats. The alleviation in the irritation was mainly due to the high EE ($81.9 \pm 2.43$ %), which prevented the immediate contact

between capsaicin and the gastric mucosa. Finally, the liposomal nanoformulation was proved to have an advanced oral bioavailability for capsaicin oral administration, which would also be a promising delivery system for poorly water-soluble drugs.

Different to liposomes that had lipid bilayer structures, micelles were closed lipid monolayers with a hydrophilic head in contact with water and hydrophobic tail in the interior. Zhu *et al*. later designed a mixed polymeric micelle using a thin-film dispersion method (*126*). This capsaicin-loaded micelle was composed of polyvinylpyrrol- idone (PVP)/sodium cholate/phospholipid mixed micellar system with the capsaicin content around 3.70 mg/mL, EE around 92.3% and particle sizes below 50 nm. The irritation test proved that the nanoformulation had reduced the irritation of capsaicin due to high EE, which prevented its adherence to gastric mucosa. More importantly, the *in vivo* bioavailability study revealed that formulated micelles had enhanced the oral bioavailability of capsaicin due to reduced particle sizes and increased solubility in gastrointestinal tract. Consequently, this nanoformulated micelle demonstrated an improved oral bioavailability and reduced irritation on gastric mucosa.

Goycoolea *et al.* designed a novel colloidal capsaicin nanocapsule containing an oily core of lecithin and hydrophilic shell of chitosan for transmucosal drug delivery with the EE of 72-96% and particle size of 150-200nm (*127*). By studying the biophysical properties and colloidal stability, they concluded that both the molecular weight and the degree of *N*-acetylation affected the EE of capsaicin. Besides, the major forces to incorporate the chitosan to the capsaicin nanoparticles were electrostatic attractions between $–NH^{3+}$

groups in chitosan and phospholipidic heads of lecithin, as well as hydrophobic interactions between hydrophobic parts of polysaccharide and lipid. This formulation could be utilized as a nanocarrier for transport of capsaicin both *in vitro* and *in vivo*, as well as a regulator for TRPV receptors in body tissues.

**Microemulsions and Nanoemulsions**

A capsaicin-containing microemulsion with the concentration of 8 mg/mL was developed by *Zhu, et al* in 2014 (*128*), which was prepared by dissolving capsaicin into medium-chain triglycerides (oil phase) and Cremophor EL. After addition of absolute ethanol as cosurfactant, water was added to the mixture under agitation until a clear and transparent system was achieved. This microemulsion had demonstrated an enhanced stability, higher dissolution rate as well as significantly increased oral bioavailability through pharmacokinetic study. In the meantime, reduced gastric mucosa irritation was also observed in rats compared with free capsaicin after oral administration. Therefore, this formulation was effective in orally carrying capsaicin into the digestive system with less irritation to stomach.

In addition to microemulsions, nanoemulsion delivery systems had also been widely used to enhance the oral bioavailability of lipophilic compounds in the food and pharmaceutical industry, which were often prepared by high-pressure valve homogenizers or microfluidizers (*129*). Double and triple-layer nanoemulsions were prepared through self-assembly emulsification method (*130*). By adding alginate and chitosan into single-layer capsaicin nanoemulsions, double-layer nanoemulsions were made. And the triple-layer emulsions were formed based on the electrostatic interactions

between the carboxylic groups of alginate and the amine groups of chitosan. The particle sizes of the nanoemulsions that contained alginate and chitosan were 20 nm or smaller. Physiochemical characterizations demonstrated that this capsaicin-loaded emulsion system had reduced particle sizes and enhanced stability compared with other food delivery systems. A pharmacokinetics study was conducted using rats (*18*). And results demonstrated that nanoemulsions had a relative bioavailability of 131.7 times higher than unformulated capsaicin emulsion with prolonged half-life and decreased distribution.

**Nanoparticles**

A biodegradable polymeric vehicle for oral delivery of capsaicin was made through CAP-containing methoxy poly (ethylene glycol)-poly (ε-caprolactone) nanoparticles (CAP/NPs) (*131*). Characterization results showed that this nanoparticle had small size of 82.54±0.51 nm, high drug-loading capacity and stability. After oral administration in rats, there was an increased amount of capsaicin detected in the serum compared with the raw capsaicin suspension. Apart from that, the irritation in gastric mucosa was significantly reduced. The capsaicin nanoparticles showed an increased bioavailability through oral delivery.

**SUMMARY**

In this brief review, common extraction methods for capsaicinoids were examined, including enzymatic pretreatment, UAE, SOX, PLE, SFE and MAE. Recently, combined methods have been developed to further enhance the extraction yields of capsaicinoids

and reduce the energy consumption, such as SFE assisted by ultrasound, and multiple-stage extraction methods, etc.

Bioavailability of capsaicinoids were reviewed and explained. After oral administration, capsaicin and dihydrocapsaicin are absorbed in the GI tract and almost completely metabolized in the liver. Biological studies have shown that capsaicinoids has anti-inflammation, anti-cancer, anti-oxidation, pain-relief, cardioprotective and anti-obesity effect. Therefore, these nutraceuticals can be further developed into multi-functional foods with great potential in the food industry. However, how to reduce the extreme pungency and enhance the bioavailability of capsaicinoids should be a major focus in the future work.

# CHAPTER II. FABRICATION OF QUERCETIN-LOADED NANOFORMULATIONS THROUGH WET-MILLING PROCESS

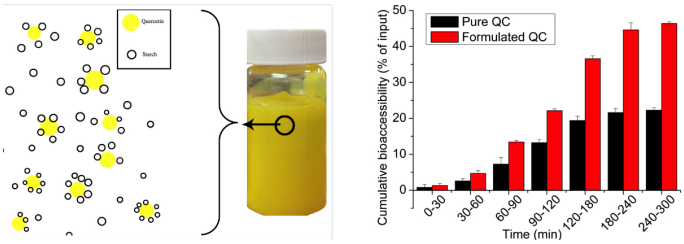


## PROJECT TITLE: IMPROVING QUERCETIN DISSOLUTION AND BIOACCESSIBILITY THROUGH WET-MILLING TECHNIQUE


## ABSTRACT

Quercetin (QC) is a common bioflavonoid with very low water solubility and dispersity, which limits its oral bioavailability and beneficial functions *in vivo*. In order to overcome these drawbacks, the wet-milling technology was used to disintegrate micron-sized QC crystals into nanoparticles. Hydrophobically modified starch (HMS) was added to the formulation in the same ratio of QC dihydrates before processing, which acted as the stabilizer to prevent the agglomeration of the particles. Then nanodispersions were spray-dried and freeze-dried separately after wet milling. The physicochemical characteristics of formulated QC were measured through Dynamic Light Scattering (DLS), Fourier Transform Infrared Spectroscopy (FTIR), Dissolution Test and Powder X-ray Diffraction (PXRD). In addition, a TNO gastro-Intestinal Model (TIM-1) was utilized to show the improved *in vitro* bioaccessibility of QC formulation compared with unformulated suspension. This study suggested that wet-milling technique combined with spray-drying or freeze-drying treatment would be an excellent processing method for the

development of QC-based functional food products with enhanced solubility, dissolution and bioaccessibility.

## INTRODUCTION

Flavonoids were polyphenolic compounds rich in fruits, vegetables and plant-derived beverages such as tea and red wine (*26*). Quercetin (QC, 3,3′,4′,5,7-pentahydroxyflavone) as one of abundantly consumed flavonoid had been reported to have many biological activities, including antioxidative (*27*), anticarcinogenic (*28*), anti-arthritic (*29*), anti-inflammatory, anti-proliferative and anti-atherosclerotic effects (*30*). However, the poor water solubility of QC limits its bioavailability. In order to improve this situation, researchers attempted various encapsulation methods to increase its dissolution rate. According to Kakran (*2*), QC nanocrystals have been fabricated by means of three methods, including high-pressure homogenization, wet bead milling, and cavi-precipitation. The smallest nanocrystals were fabricated by wet bead milling with a saturation solubility of 25.59 ± 1.11 μg/mL, about nine times higher than coarse QC. Niwa (*3*) also reported that the technique of wet-milling and spray & freeze-drying processes could enhance the dissolution for poorly water-soluble drugs. In addition, hydrophobically modified starch (HMS), which was synthesized from waxy maize and n-octenyl succinic anhydride (n-OSA), is widely used as wall material to encapsulate flavors in spray-drying process (*132*). Therefore, in this research, HMS was added as a stabilizer to prepare the QC formulation. Then the combination of wet-milling technique and different drying methods in processing QC formulations was studied. The formulated QC nanoparticles were proven to have an increased water solubility, enhanced rate of dissolution and increased bioaccessibility.

## MATERIALS AND METHODS

*Materials.*

Quercetin dehydrate (purity 85%) was purchased from VWR Scientific (Seattle, WA, USA). Hydrophobically modified starch (HMS) with the brand name of Hi-Cap 100 was obtained from National Starch and Chemical Company (Bridgewater, NJ, USA). HPLC grade-methanol and acetonitrile were purchased from Sigma-Aldrich Company (St. Louis, MO, USA). Milli-Q water (18.3 MΩ) was used in all experiments.

*Hydrophobically modified starch (HMS)*

Hydrophobically modified starch (HMS) is synthesized from waxy maize and n-octenyl succinic anhydride (n-OSA). It is widely used as wall material to encapsulate flavors in spray-drying process (*132*). Its chemical structure can be found in **Figure 7**.

Therefore, in this research, HMS was added as a stabilizer to prepare the QC formulation. Then the combination of wet-milling technique and different drying methods in processing QC formulations was studied. The formulated QC nanoparticles were proven to have increased water solubility, enhanced rate of dissolution and increased bioaccessibility.

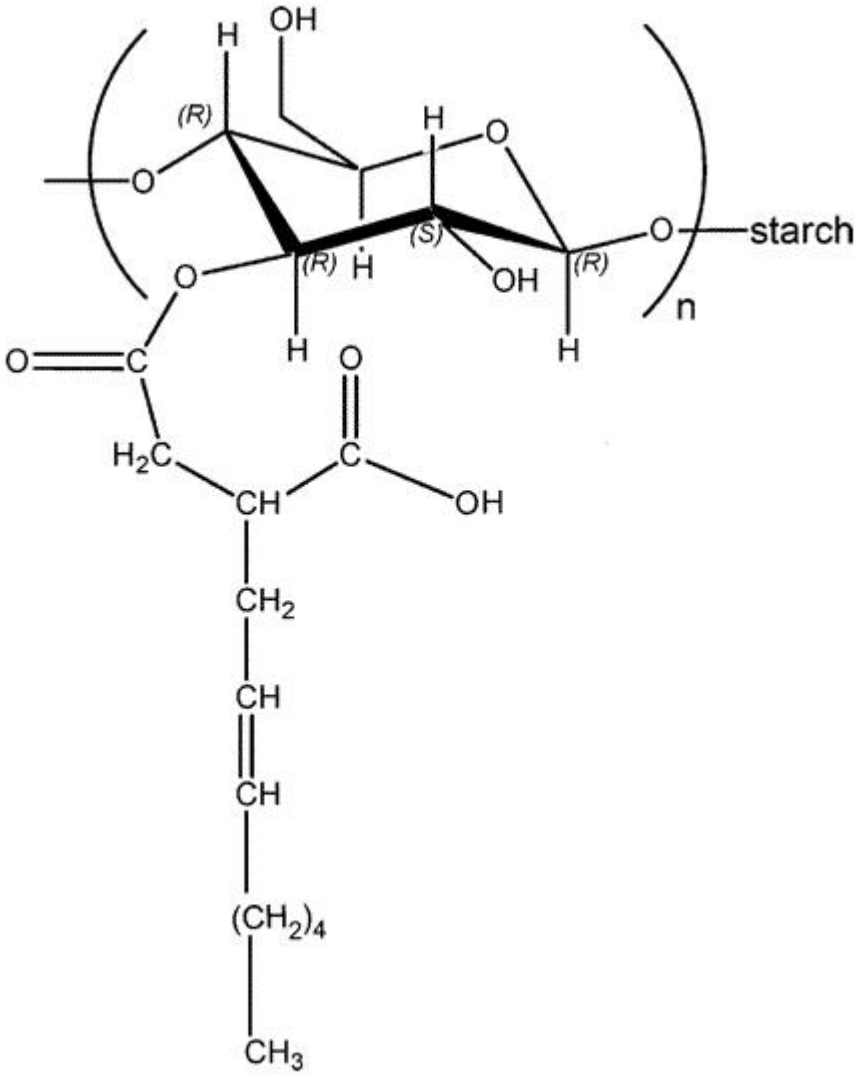


**Figure 7**. Chemical structure of hydrophobically modified starch.

*Preparation of formulated QC Microdispersions.*

QC micro-sized formulations were prepared by dispersing 15 g of QC dehydrate and 15 g of HMS in 300 mL-deionized water. The suspension was under agitation overnight at room temperature.

*Wet-milling Processing.*

This high-shear beads milling machine is developed by the company NanoSystems (Collegeville, USA). The media mill consists of milling chamber, milling shaft and recirculation chamber as depicted in **Figure 8**. The milling media is composed of glass, zirconium oxide or highly cross-linked polystyrene resin. As the mill starts to run, the drug, stabilizer and milling media rotate at a very high sheer rate, producing excessive energy and sheer forces to disintegrate microparticulate drug into nano-sized particles. A cooling system is attached to the recirculation chamber to control the temperature.

This wet-milling technique is efficient in producing uniformed particle sizes in nano scale, as well as prevents the agglomeration and precipitations by processing at a liquid environment (i.e. water, buffer solutions, etc.).

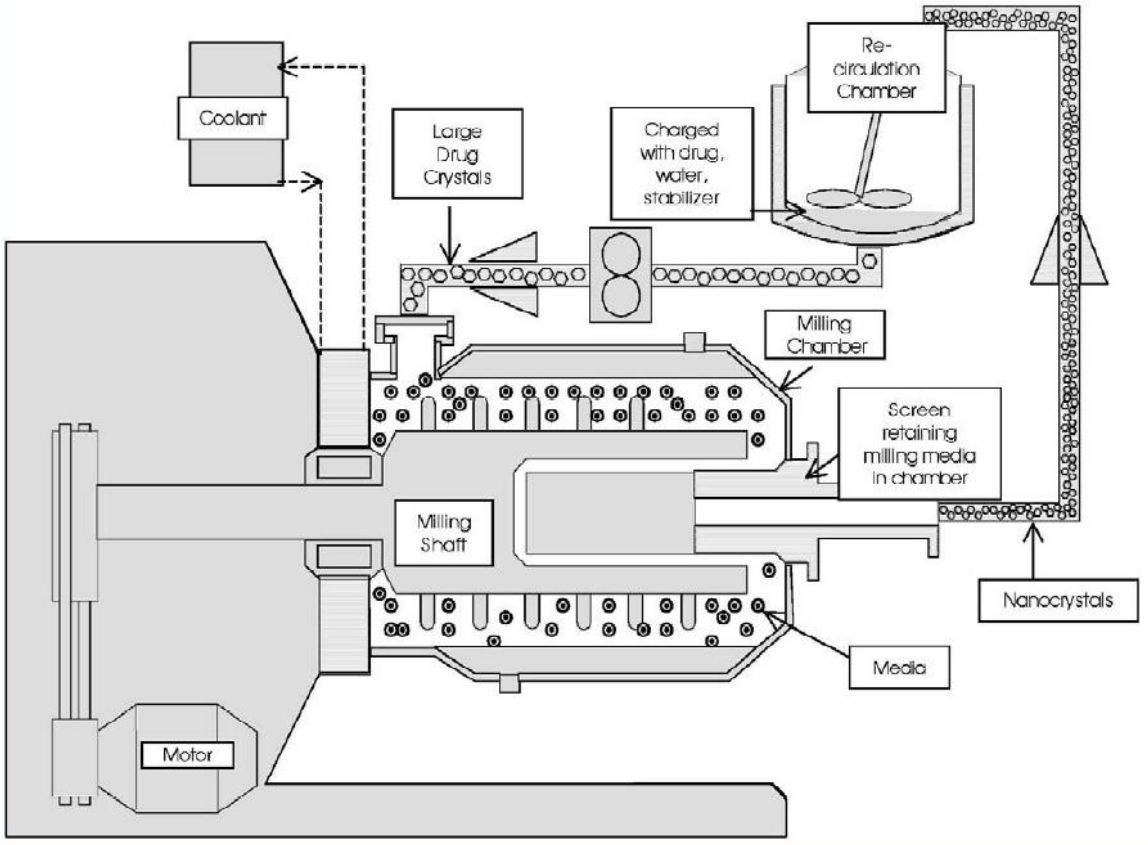


**Figure 8.** A schematic representation of wet milling process

The formulated QC suspension was fed to a milling chamber before being milled. The wet-milling machine (MiniCer, NETZSCH-Feinmahltechnik GmbH, Staufen, Germany) was used in this research to disintegrate the microsized QC crystals into nanoparticles. During the milling process, Yttrium-stabilized zirconium oxide grinding beads with a diameter of 0.8-1.0 mm performed as the milling media. As the mill started running, the formulation was under agitation of grinding beads at the speed of 3100 rpm and recycled by a pump at the speed of 100 rpm. The milling temperature was controlled at 20 °C by a cooling system. Samples were collected every 5 minutes for particle size analysis.

*Spray-drying.*

150 mL of wet-milled QC nanodispersions were spray-dried in the model Pulvis GB22 fluid bed spray dryer (Yamato, Santa Clara, CA). The drier conditions were: drying air flow 0.43-0.45 $m^3$/min, inlet temperature 110 °C; outlet temperature 200 °C; air pressure 6 bar; aspirator 100%. Each preparation was carried out in triplicate (*133*). All spray-dried QC powders were then collected from the filter chamber and stored at 4 °C.

*Freeze-drying.*

The remaining 150 mL of wet-milled QC nanodispersions were frozen overnight and freeze-dried using the freeze dryer (Freezone 4.5, Labconco, Kansas City, MO, USA), open to the system and under vacuum until all moisture was removed and a dry solid mass remained (*134*). Then dried powders were stored in 50 mL sterile centrifuge tubes at 4 °C until further evaluation.

## CHARACTERIZATION

*Particle Size Measurements*

The particle size of the wet-milled QC dispersions were measure by dynamic light scattering particle size analyzer (Model 90 Plus, Brookhaven Instrument Corp., Holtsville, NY, USA) at a fixed scattering angle of 90° and temperature of 25.0 °C. Each time, 5 µL

of dispersed samples were collected from the recirculation chamber during the wet-milling process within a certain time interval and diluted by 5 mL distilled water. All samples were measured in triplicate to ensure accuracy.

*Fourier-Transform Infrared Spectroscopy (FT-IR)*

Infrared absorption spectra of pure QC, HMS and formulated QC powders were recorded using a Thermo Nicolet Nexus 670 FT-IR system with attenuated total reflection set-up (ATR-FTIR) (Thermo Fisher Scientific, Waltham, MA, USA) (*135*). Absorption spectra at a resolution of one data point every 4 $cm^{-1}$ were obtained in the region between 4000 and 600 $cm^{-1}$ using a clean crystal as the background. 512 repeated scans for each sample were collected. All experiments were carried out at room temperature. The absorption spectra were averaged and smoothed, and their baselines were calibrated with the Spectra Manager software. The ATR crystals were cleaned with organic solvent (acetone).

*Loading Capacity*

20 mg of QC-loaded formulation powders were dissolved in 10 ml methanol and diluted by 10 times. Then the dispersion was filtered by a 0.45 μm filter and the drug concentration was measured using HPLC at 370 nm. Absorbance values of the solution were used to calculate the drug-loading capacity according to the following formulae (*136*):

$$\% \text{ Loading Capacity} = \frac{\text{Total mass of QC in the formulation}}{\text{Total mass of the formulation}} \times 100\% \quad .$$

*Solubility Studies*

The solubility of QC formulations in Milli-Q water was determined by using an incubating orbital shaker (VWR Scientific, Cornelius, OR, USA). Saturated solutions of QC formulation were prepared by dispersing an excessive amount of formulated QC powders into distilled water. Then solutions were collected into 40 ml capped vials to avoid evaporation and shaken at 25 °C for 1 day. After the equilibrium was reached, suspensions were filtered through a 0.45 μm filter and analyzed by HPLC. Experiments were carried out in triplicate.

*Dissolution Studies*

The dissolution rates of pure QC dihydrate powders, wet-milled pure QC dihydrate powders, QC/HMS (1:1) physical mixtures and wet-milled QC formulations were measured using flow-through cell USP apparatus 4 (SOTAX Corporation, Westborough, MA, USA). 10 mg of powdered samples were introduced into the dissolution medium containing 400 mL of DI water at 37±0.5 °C at a speed of 3 mL/min. Samples were collected from the reservoir every 5 min within an hour and analyzed through HPLC at 370 nm. All studies were carried out in triplicate.

*X-ray Diffraction on Powder (PXRD)*

The X-ray diffraction patterns of pure QC, spray-dried QC and freeze-dried QC were analyzed using a D/M-2200T X-ray powder diffractometer (Ultima+, Rigaku) with nickel filtered Cu Kα radiation (λ=1.54056 Å). The scanned radiation was detected in the angular range of 5° to 40° (2θ) with a step of 0.02° (2θ) per second. Graphite monochromator was used and the generator power settings were at 40 kV and 40 mA (*137*).

*TNO intestinal model (TIM-1)*

The dynamic, computer-controlled in vitro gastrointestinal model TIM-1 (TNO, Zeist, The Netherlands) was used to mimic the human upper gastrointestinal tract using four compartments, which are stomach, duodenum, jejunum, and ileum (*138, 139*). The temperature of water, pH conditions and secretion of digestive fluids are controlled by computer programs to resemble the human physiological gastrointestinal conditions.

**Figure 9** shows a schematic representation of TIM-1 system. As can be seen from this figure, the top compartment represents stomach, where the sample solutions can be injected and mixed with gastric acid, lipase and pepsin. The following section is the small intestine divided into 3 parts: duodenum, jejunum, and ileum, where the sodium bicarbonate ($NaHCO_3$) is secreted to neutralize the pH, and bile & pancreatic enzymes are added to digest the fat, carbohydrate and proteins. At the end of this system (H), the undigested components are collected as efflux for further analysis. By far, the TIM model

is recognized as one of the most sophisticated and precise model for evaluate the bioaccessibility of nutraceuticals through oral administration.

In this research, the TIM-1 system is used to mimic the digestion process of quercetin, and compare the difference in bioaccessibility of free quercetin and formulated quercetin nanoparticles.

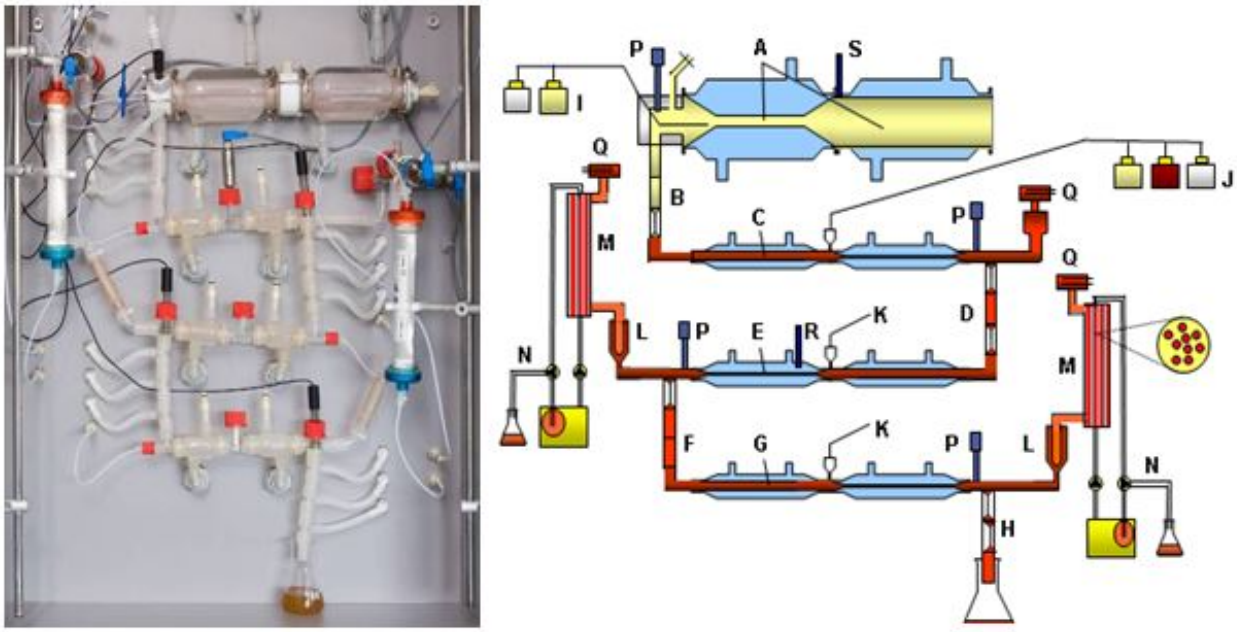


**Figure 9.** A schematic representation of TIM-1 *in vitro* dynamic gastrointestinal model system.

Samples were fed into the system and tested for 5 hours. Suspensions containing same content of quercetin (0.1%) were prepared by dissolving coarse QC and formulated QC powders into the DI water respectively. The QC bioaccessibility was analyzed by

collecting dialysates from jejunal and ileal filtrates at 30, 60, 90, 120, 180, 240 and 300 minutes. Bioaccessible QC nanoparticles were able to pass through the hollow fiber filtration device (Spectrum Milikros modules M80S-300-01P, with 0.05 μm pore size) and got absorbed in the jejunum and ileum. In the meantime, ileal efflux samples were also collected, which represented the percentage of compound that would theoretically be delivered to the colon. Samples obtained from TIM-1 were immediately stored at -20 °C until HPLC analysis. The experiments were performed in duplicate and samples were analyzed in triplicate.

For HPLC analysis, 400 μL of sample was inoculated with an internal standard (Morin, 10 μg/mL) was then extracted by mixing with 600 μL of ethyl acetate and centrifuge at 16000 g for 30 min at room temperature. After centrifuge, the 400 μL of supernatant was obtained and mixed with equal amount of DMSO for use in HPLC analysis. The percent cumulative bioaccessibility of QC was calculated using equation below:

$$\%\, Bioaccessibility = \frac{Total\ mass\ of\ solubilized\ QC}{Total\ mass\ of\ QC\ in\ original\ samples} \times 100\%$$

*Quantitative Analysis of QC using high-performance liquid chromatography (HPLC)*

Quercetin was quantified by an automated high-performance liquid chromatograph system (Dionex, Sunnyvale. CA, USA). The system consists of a quaternary solvent delivery system, an UV–vis diode array detector and an automated injection system. The column used in this study is Supelco's RP-Amide C18, 15 cm x 64.6 mm, 3 μm

(Bellefonte, PA, USA). The mobile phase consists of (A) acetonitrile and (B) 0.2 % acetic acid in water (HPLC grade). 10 μL samples were injected each time and then eluted under gradient conditions: 0-2 min, 40% A and 60% B; 2-8 min, linear gradient from 40 to 55% A; 9-12 min, linear gradient from 55 to 70% A; 12-13 min, linear gradient from 70 to 90% A; 14-6 min, held at 90% A; 17-18 min, A went back to 40% linearly; 19-20 min, held at 40% to balance the column. The flow rate was set at 1.0 mL/min and the eluent was detected with UV wavelength at 370 nm. Different standard concentrations (5, 10, 15, 20, 40, 60, 80 and 100 μg/mL) of QC were dissolved in methanol and analyzed using the HPLC to generate the calibration curve. Each measurement was carried out in triplicate.

## RESULTS AND DISCUSSION

### *Effect of the wet-milling process on particle sizes of QC*

In this research, the wet-milling technique was used to produce QC nanodispersions. According to Figure 10, the average particle size decreased from approximately 1.1 μm to 340 nm after the processing.

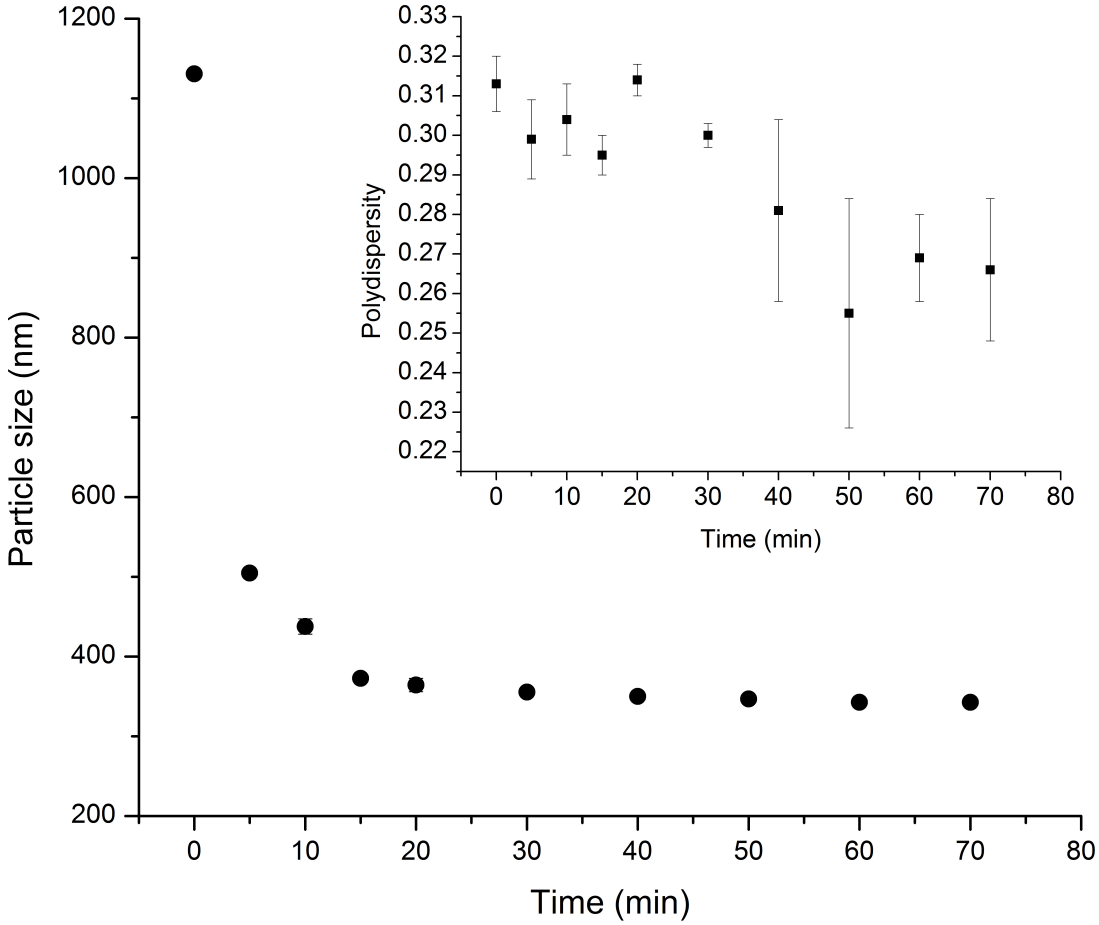


**Figure 10.** Change in particle size and polydispersity of formulated QC dispersion as a function of time.

The reduction of the particle size was mainly owing to the intense shear forces during the wet-milling process. Apart from that, the modified starch also functioned as the stabilizer to prevent the agglomeration of QC particles due to its hydrophobic property. In 2008, Pongpeerapat (*140*) proposed a formation mechanism of colloidal nanoparticles. According to his theory, the adsorption behavior between two hydrophobic molecules helped the stabilization of the ground mixture. Therefore, the hydrophobically modified starch would adsorb to the hydrophobic surface of dispersed QC nanoparticles, reducing the contact between QC themselves. Therefore, the hydrophobically modified starch

might effectively contribute to the reduction of particle size of the nanodispersion after the milling process.

*FTIR spectroscopy*

The FTIR spectra of HMS, pure QC dihydrate powder and formulated QC powder were shown in Figure 11. There were many FTIR bands in the fingerprint region from 1700 to 700 $cm^{-1}$: 1618 $cm^{-1}$, 1339 $cm^{-1}$, 1664 $cm^{-1}$, 1450 $cm^{-1}$, 1262-1168 $cm^{-1}$and 1130-1014 $cm^{-1}$ (*141*) (*142*). The band at 3100-3500 $cm^{-1}$ of the pure QC powder was attributed to QC—OH stretching. In the physical mixture this band shape did not change and peaks at 3323 and 3405 $cm^{-1}$ could still be identified. However, the formulated powders showed broad peaks at 3000-3600 $cm^{-1}$ that were similar to the bands of HMS powders. It might be the intermolecular hydrogen bonding between QC and the HMS that led to the broadening of this peak, which disrupted the QC crystalline structure. Besides, most of the characteristic peaks of both HMS and pure QC powders could be found in formulated ones, though with less intensity. Apart from that, no new peak or band shift was found in the FTIR spectra for formulated ones, reflecting that there might be no covalent interactions between the pure QC and HMS powders. These results indicated that neither wet-milling process nor addition of modified starch would influence the chemical properties of QC significantly.

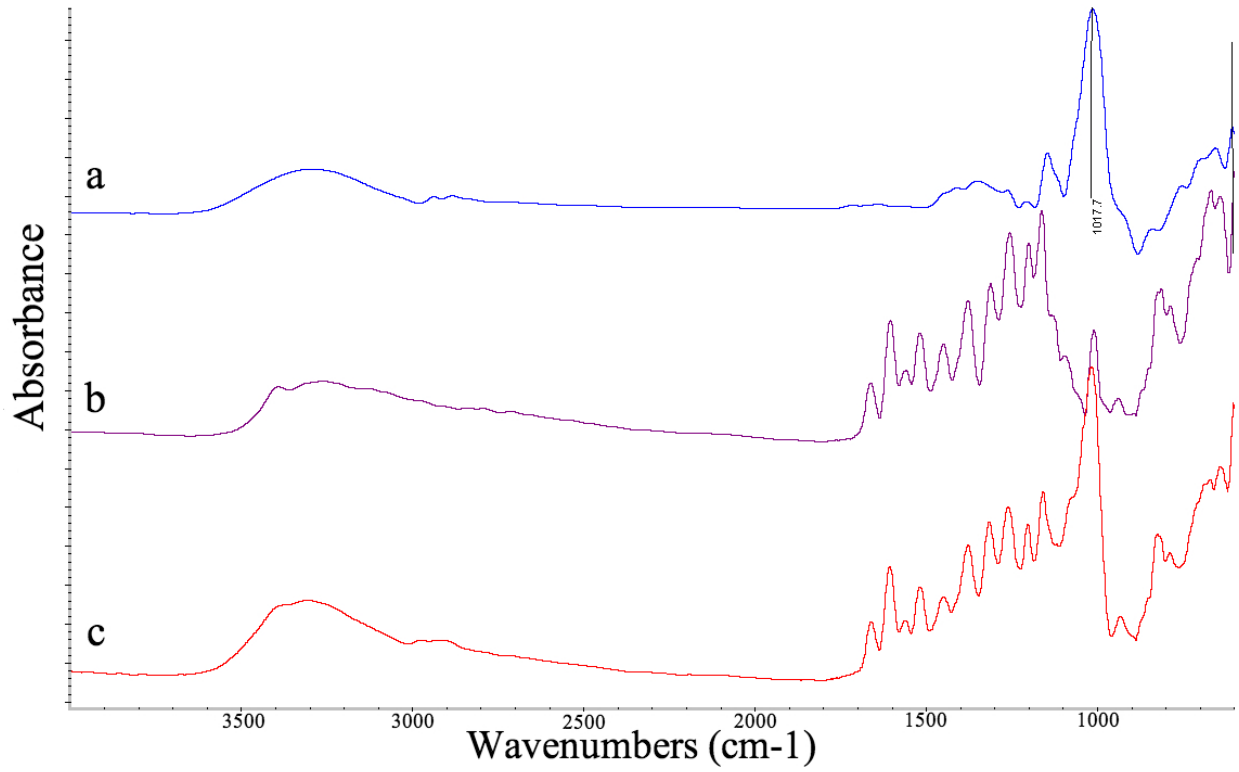


**Figure 11.** FTIR spectra of HMS (a), Pure QC powder (b) and Formulated QC powder (c).

*Loading Capacity and Solubility Studies*

The excess amount of the wet-milled QC powder was dispersed into distilled water and gently agitated for 1 day at room temperature to reach full saturation. According to the HPLC analysis, the water dispersity of the formulated QC was 28.78 ± 0.31 μg/mL. Compared with the pure QC's water solubility of 2.63 μg/mL at 25 °C (*143*), this formulation can enhance the water solubility by approximately eleven times. Besides, the loading capacity of the formulation powder was 48.74% after calculation, which theoretically should be 50%. This result demonstrated that quercetin and HMS were well mixed; and there was almost no loss in the amount of quercetin during processing.

*Dissolution Studies*

The dissolution rate of pure QC powders, wet-milled pure QC powders, physical mixtures of QC and HMS with the ratio of 1:1, and the formulated QC powders were shown in **Figure 12**. The wet-milled QC referred to powders that only went through the wet-milling and drying process without the addition of HMS. For the dissolution processes of different solutions, only about 1.09% of the coarse QC was dissolved after one hour. While the dissolution rate of wet-milled pure QC was stable around 5.37%, which was slightly higher than the original one. Compared with pure QCs, both physical mixtures and formulated powders had higher dissolution rates of 36.86% and 98.76%, respectively. Therefore, the addition of modified starch can function as a stabilizer to increase the solubility. The significant increase of the formulated QC powder in dissolution rate might be attributed to the formation of soluble complex of QC and starch.

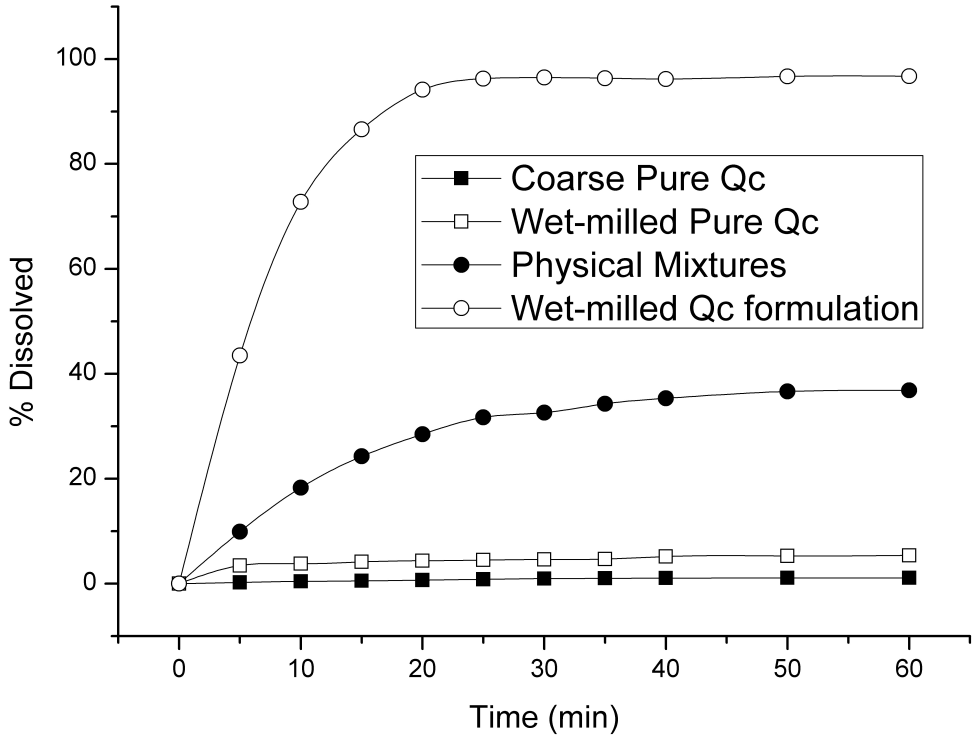


**Figure 12.** Dissolution profiles of coarse pure QC, wet-milled pure QC, physical mixture and wet-milled QC formulations.

*The PXRD Analysis*

The powder X-ray diffractogram of pure QC, wet-milled pure QC and formulated ones were illustrated in **Figure 13A**. The characteristic peaks of pure QC samples corresponded to the one in the Cambridge Structure Database (CSD), which included some characteristic peaks of 2θ at 10.68°, 12.42°, 16.15°, 24.46°, etc. The percent crystallinity of spray-dried and freeze-dried samples containing amorphous starch were determined by subtraction of pure QC pattern from normalized starch containing pattern.

As is shown in **Figure 13B**, the area under the difference curve between the pure QC pattern and freeze-dried QC pattern was proportional to the total weight ratio of amorphous starch, which was measured by the Peak Paint Cursor function in MDI program JADE7. The pure QC curve compared very well with the amorphous starch background-subtracted curve of the freeze-dried QC samples, as was shown in **Figure 13C**. The area under the difference curve between the background-subtracted pattern and manually determined background-containing pattern was proportional to the weight ratio of QC crystals in the freeze-dried samples. Using this method, the percent crystallinity of freeze-dried and spray-dried QC samples calculated were 50.2% and 52.3%, respectively, which was consistent with the weight ratio of QC in the formulated samples. This result implied that the 1-hour wet-milling process didn't reduce the level of crystallinity of QC particles.

Furthermore, based upon the peak widths β for 12 intense low angle peaks on different θ positions corresponding to single reflections, the crystallite sizes and strain information were computed using the Fit Peak Profile routine in JADE7. During this process, we used the *Williamson- Hall* plot (*144*):

$$\beta \times cos\theta = \frac{K\lambda}{D} + 4 \times \varepsilon \times sin\theta$$

Where β is the peak width; θ is the Bragg angle; K is the Scherrer Constant; λ is the X-ray wavelength; D is the crystallite size; and ε is the strain. B*cosθ was plotted with respect to sinθ for the peaks of quercetin in each samples (**Figure 13D**). Strain in crystals created by dislocations, domain boundaries and deformations, *etc*., was defined as relative lattice displacement (*145*). Crystallite sizes and strain were calculated from the

y-intercept and slope of the fitted line. Results were shown in **Table 10**. According to calculations, crystallite sizes for pure QC, wet-milled QC, spray-dried formulated QC and freeze-dried formulated QC were 49.4, 39.5, 24.3 and 20.4 nm respectively, implying that combination of wet-milling process and addition of modified starch could help reduce the QC crystallite sizes. Moreover, freeze-drying process was more efficient in producing QC dried powders with smaller crystallite sizes than spray-drying process.

A

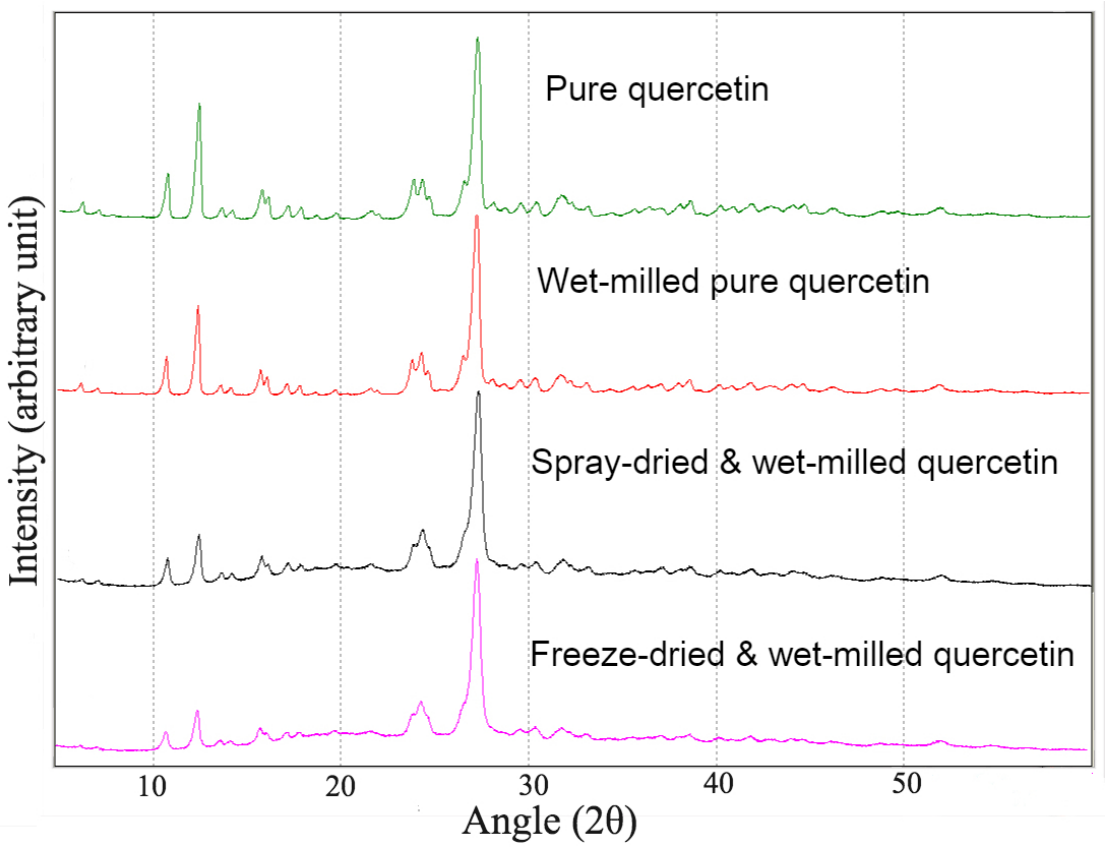
Pure quercetin
Wet-milled pure quercetin
Spray-dried & wet-milled quercetin
Freeze-dried & wet-milled quercetin
Intensity (arbitrary unit)
10
20
30
40
50
Angle (2θ)

B

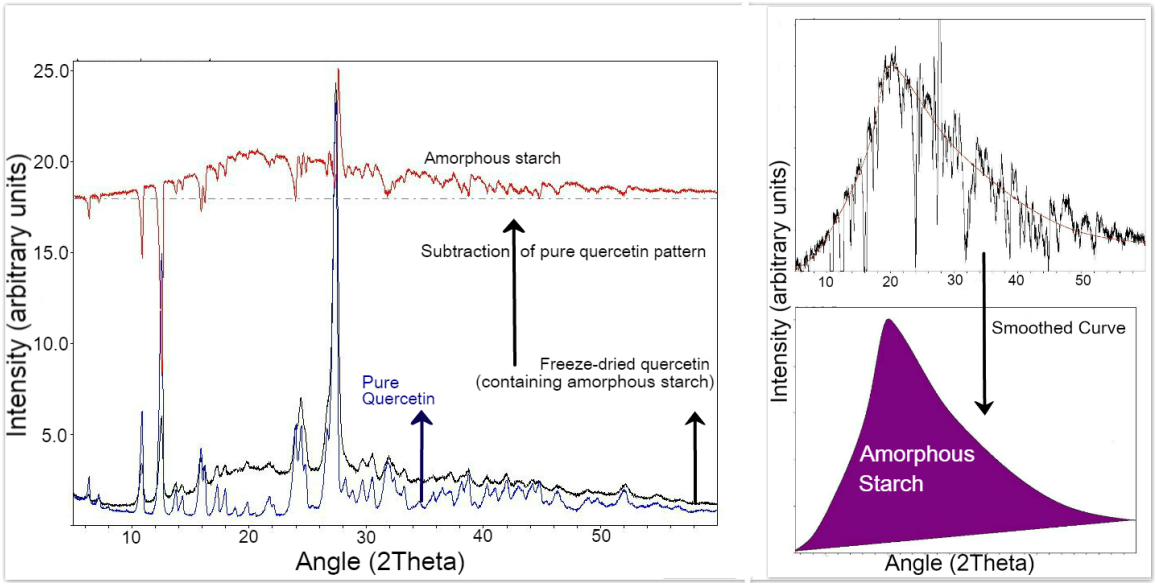
25.0
20.0
15.0
10.0
5.0
Intensity (arbitrary units)
Amorphous starch
Subtraction of pure quercetin pattern
Freeze-dried quercetin
(containing amorphous starch)
Pure
Quercetin
10
20
30
40
50
Angle (2Theta)
Intensity (arbitrary units)
Smoothed Curve
Amorphous
Starch
Angle (2Theta)

C

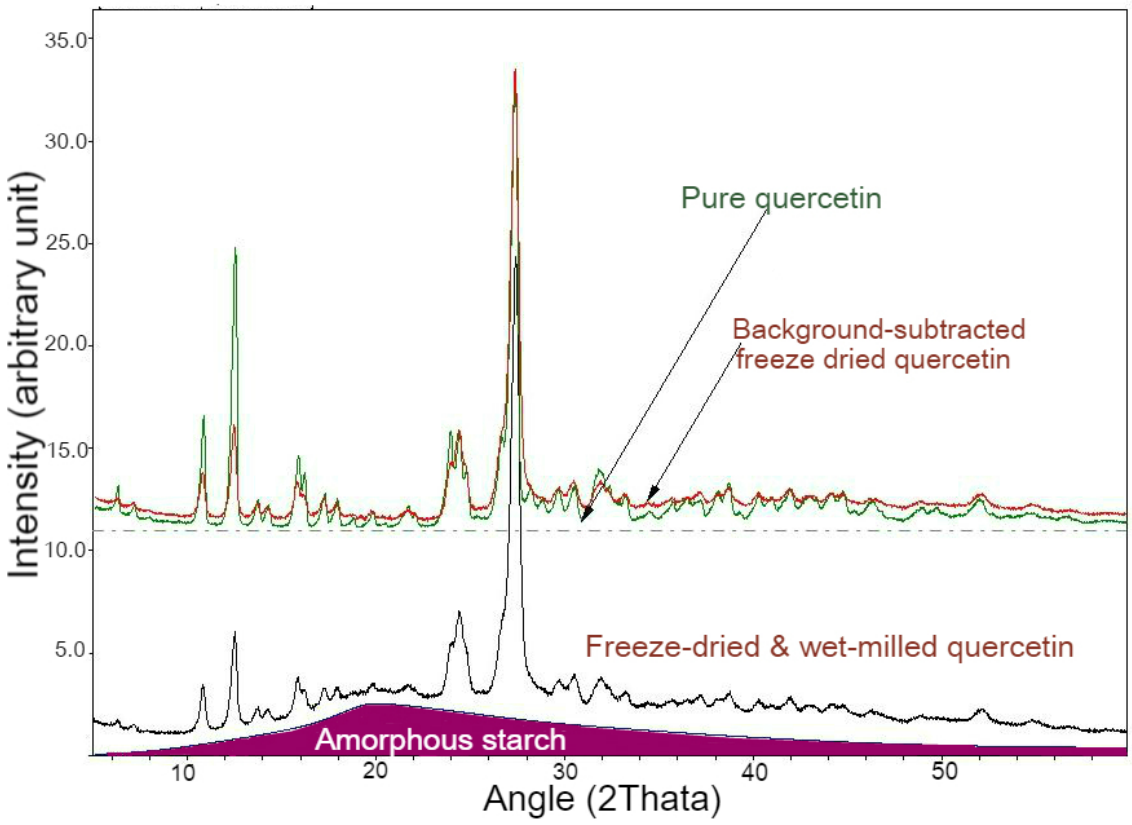
35.0
30.0
25.0
20.0
15.0
10.0
5.0
Intensity (arbitrary unit)
Pure quercetin
Background-subtracted
freeze dried quercetin
Freeze-dried & wet-milled quercetin
Amorphous starch
10
20
30
40
50
Angle (2Thata)

D

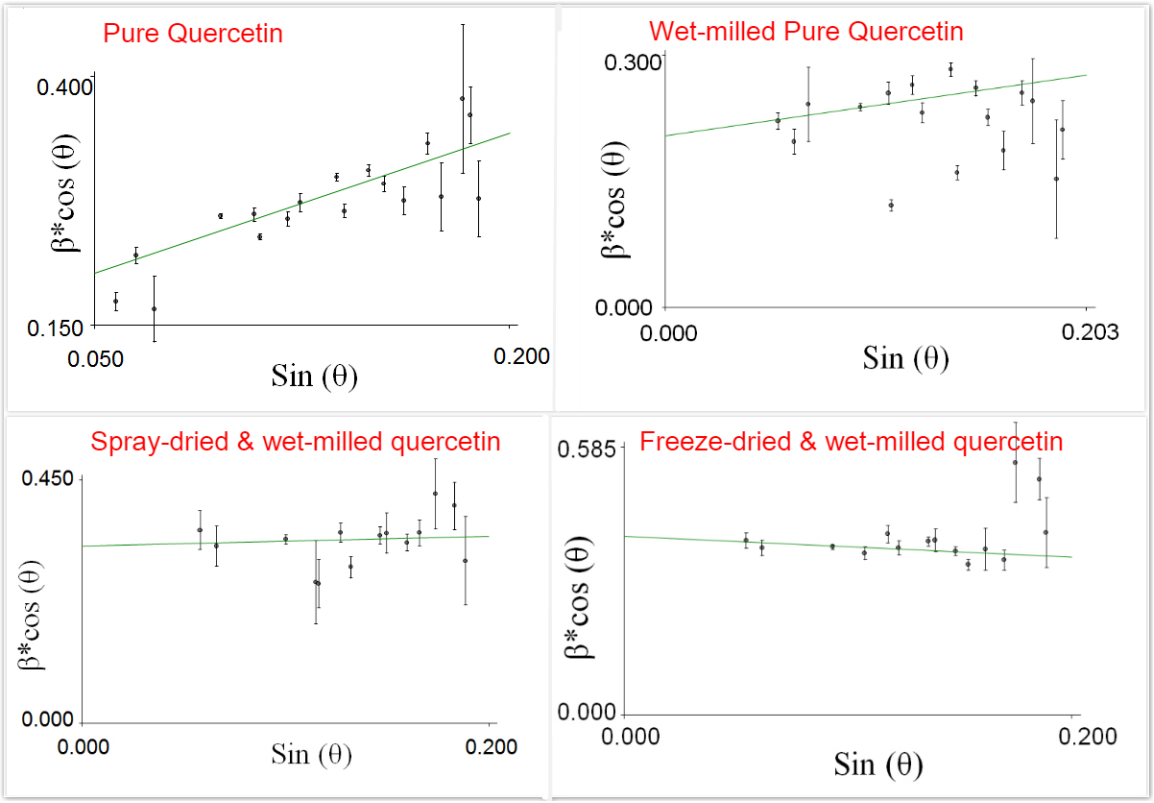


**Figure 13.** (A) The XRD diffractogram of pure QC powder, wet-milled pure QC powder, spray-dried & wet-milled QC powder and freeze-dried & wet-milled QC powder; (B) Subtraction of pure QC pattern from normalized starch containing pattern;(C) Comparison of pure QC with the background-subtracted curve of the freeze-dried QC samples; (D) The Williamson and Hall analysis of QC crystals in each group. Fitted to the data, the strain is extracted from the slope and the crystalline size is extracted from the y-intercept of the fit.

**Table 10.** The structure parameters of QC crystals in each group.

| **Samples** | **Crystallite Size (nm)** | **Strain (%)** | **ESD[a] of Fit** |
|---|---|---|---|
| Pure QC | 49.4 | 0.39 | 0.00054 |
| Wet-milled pure QC | 39.5 | 0.15 | 0.00081 |
| Spray-dried & wet-milled QC | 24.3 | 0.04 | 0.00034 |
| Freeze-dried & wet-milled QC | 20.4 | -0.10 | 0.00030 |

**Abbreviations:** a) ESD, estimated standard deviations.

*Comparison of in vitro gastrointestinal digestion between pure QC suspension and QC formulations*

The bioaccessibility of quercetin for both pure QC suspension and formulation was studied through the Tim-1 system. After the HPLC analysis, the bioaccessible QC content in Jejunum dialysate, Ileum dialysate and Ileum effluent was calculated and shown in **Figure 14.** As was demonstrated from **Figure 14 (A)**, for coarse QC samples, the quercetin digested in Jejunum gradually increased during first 2 hours, and reached the maximum in 90-120 minutes. Then bioaccessible QC content started to decrease until the end of the 5-hour period. While for QC formulations, the maximum bioaccessibility was achieved in 120-180 minutes, meaning that the formulation continued to be digested and absorbed in Jejunum and Ileum after 2 hours. The sustained digestion process can be explained by the reduced particle size and stabilization function of modified starch in the formulated quercetin suspension. Besides, comparing **Figure 14 (A)** with **(B)**, the bioaccessible QC in Jejunum dialysate was higher than the amount detected in Ileum in both cases, which demonstrated that Jejunum was the major location for quercetin digestion. Moreover, the overall bioaccessibility was defined as the combined bioaccessible QC content in Jejunum and Ileum dialysates. And according to **Figure 14 (C)**, compared with the coarse samples, the formulated ones had an increased amount of overall bioaccessibility during almost every time interval.

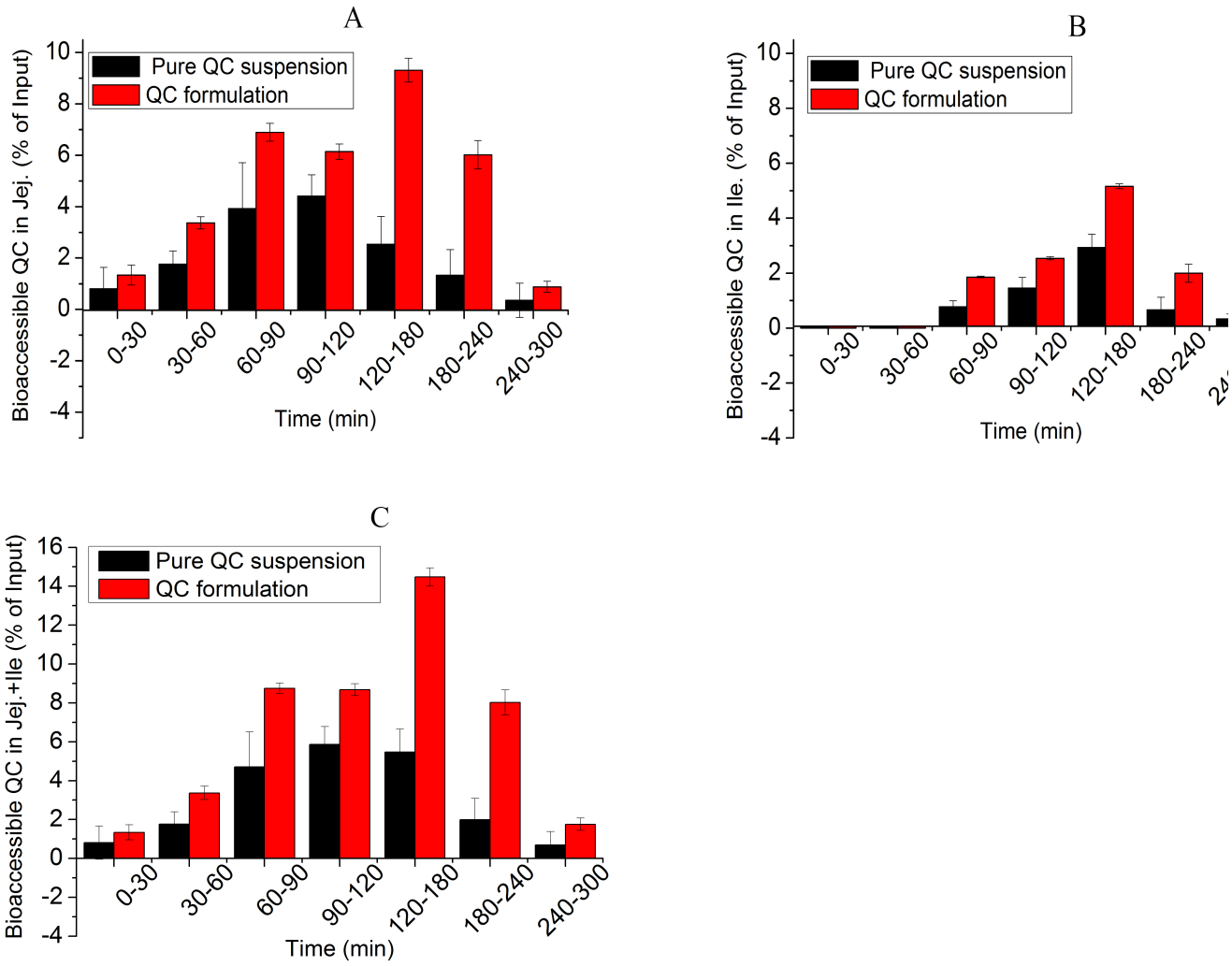


**Figure 14.** Bioaccessible QC (% of input) accumulated in every 30 minutes during first 2 hours and every 60 minutes during 2-5 hours from different parts of the TIM-1 model. (A) Bioaccessible QC in jejunum dialysate from pure QC suspension and QC formulation; (B) Bioaccessible QC in ileum dialysate from pure QC suspension and QC formulation; (C) Total bioaccessible QC in both jejunum and ileum dialysate from pure QC suspension and QC formulation.

Meanwhile, a cumulative bioaccessibility profile of quercetin in the Jejunum, Ileum and Jej+Ile was analyzed and plotted in **Figure 15.** According to the cumulative bioaccessibility in Jejunum dialysate, the amount of quercetin derived from formulations (33.96%) was about twice the amount from pure suspensions (15.14%) after the 5-hour

Tim-1 test. Same trend was observed for the Ileum dialysate, where 12.43% of its original input was produced from the formulation through digestion and absorption; while only 6.16% of input was obtained from the unformulated sample. Combining results from Jejunum and Ileum together, we had observed that the cumulative bioaccessibility of quercetin doubled for the formulation (46.39%) compared with the pure sample (22.29%). Therefore, we can come to the conclusion that wet-milling process combined with the addition of modified starch could effectively increase the bioaccessibility of quercetin through the dynamic *in vitro* gastrointestinal digestion model.

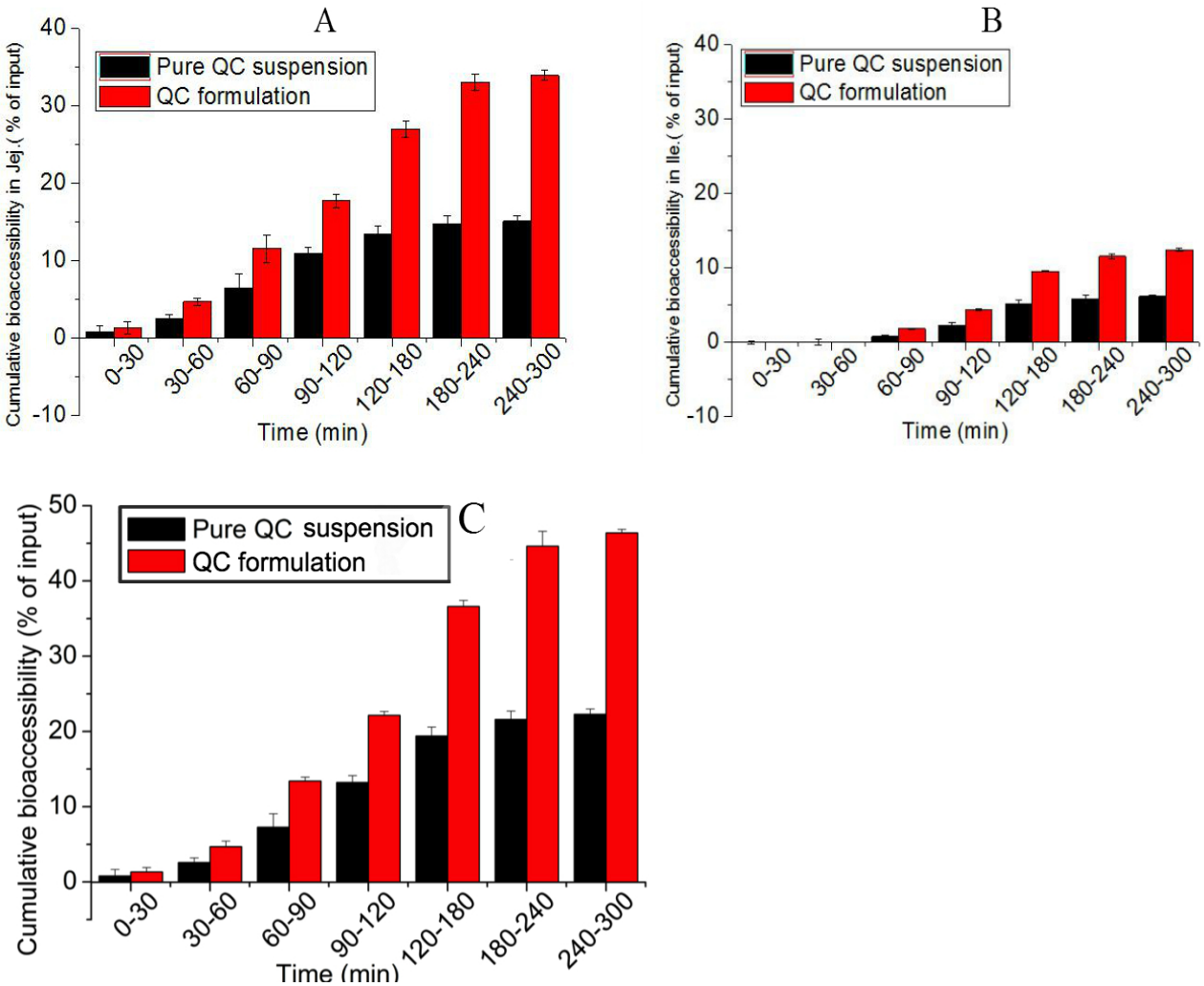

**Figure 15.** Cumulative bioaccessibility profile of QC (% of input) accumulated in every 30 minutes during first 2 hours and every 60 minutes during 2-5 hours from different parts of the TIM-1 model. (A) Cumulative bioaccessibility of QC in jejunum dialysate from pure QC suspension and QC formulation; (B) Cumulative bioaccessibility of QC in ileum dialysate from pure QC suspension and QC formulation; (C) Cumulative bioaccessibility of QC in both jejunum and ileum dialysate from pure QC suspension and QC formulation.

## CONCLUSIONS

Quercetin nanocrystals were successfully fabricated by means of wet-milling and spray & freeze drying process. The particle size was reduced to around 340 nm with a saturation solubility of 28.78 ± 0.31 μg/mL, about eleven times higher than coarse quercetin. The addition of hydrophobically modified starch could help reduce the particle size by working as a stabilizer to prevent the agglomeration of QC nanosuspensions after wet milling. FTIR spectroscopy results illustrated that neither wet-milling nor drying process would affect the chemical properties of QC. And we learned from DSL and XRD results that wet-milling process with modified starch not only reduced the particle size to nano-range, but also transferred some degree of crystal quercetin into the amorphous state, which would enhance solubility and dissolution rate. Moreover, the freeze-dried nanoquercetin powders had more degree of amorphous state than that of the spray-dried ones. And the *in vitro* digestion model, which simulated the upper GI tract, had determined an increased bioaccessibility of quercetin for the formulated nanoparticles. In conclusion, the QC nanoparticles were proved to have increased water solubility,

dissolution rate, enhanced the bioavailability and bioaccessibility.

# CHAPTER III. DEVELOPMENT OF ORGANOGEL-DERIVED CAPSAICIN NANOEMULSIONS

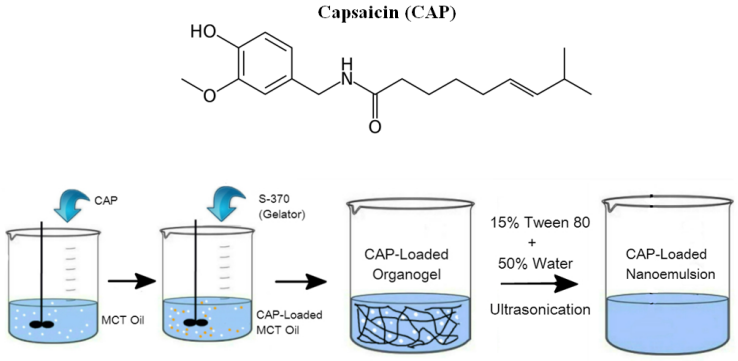


## PROJECT TITLE: DEVELOPMENT OF ORGANOGEL-DERIVED CAPSAICIN NANOEMULSION WITH IMPROVED BIOACCESSIBILITY AND REDUCED GASTRIC MUCOSA IRRITATION

*The work in this chapter has been published in the title of "*Development of Organogel-Derived Capsaicin Nanoemulsion with mproved Bioaccessibility and Reduced Gastric Mucosa Irritation*" in the Journal of agricultural and Food Chemistry (Volume 64,*

*Pages from 4735 to 4741) on May 2016.*

**ABSTRACT**

Capsaicin (CAP) is the major active component found in chili peppers that gives its pungent and spicy flavor. Its beneficial functions have been reported in anti-inflammation, anti-cancer, cardio-protective and anti-obesity activities. However, CAP's low water solubility greatly limits its bioavailability. In addition, CAP is known as an irritant compound that induces anxiety-like behaviors with prolonged stress-response in rats and cough response in humans. In order to increase the dissolution, bioaccessibility of CAP and overcome its irritating qualities, a nanoemulsion system was developed. Oil samples (medium-chain triacylglycerol (MCT), corn oil and canola oil) were used to dissolve the CAP and evaluated on in-vitro digestion test. Lipolysis results showed that MCT system had both the highest bioaccessibility of CAP and the largest extent of lipolysis. Sucrose stearate S-370 was chosen as the gelator to form the CAP-loaded organogel. After the addition of Tween 80 as the emulsifier, the organogel-derived nanoemulsion was formed with CAP's loading of 80 mg/ml. In-vitro dissolution test and in-vitro digestion test of CAP-loaded nanoemulsion proved that the dissolution rate and bioaccessibility of CAP were enhanced significantly. In addition, gastric mucosa irritation test was carried out using specific-pathogen-free (SPF) rats as animal models. The result showed that the nanoemulsion system significantly alleviated the gastric mucosa irritation caused by CAP compound. This emulsion system has been proved to be an excellent delivery system for CAP-based functional food products.

## INTRODUCTION

Capsaicin (8-methyl-*N*-vanillyl-6-nonenamide) (CAP) (structure shown in **Figure 1**) is a naturally occurring alkaloid that exists in placental tissue, the internal membranes as well as other parts of fruits of capsicum plants (*146*), which is responsible for its hot and spicy taste (*147*). Researches on CAP's beneficial effects have demonstrated its anti-inflammation (*148*), anti-cancer (*149-152*), analgesic (*153*), cardioprotective (*66*), anti-oxidation (*154*) and anti-obesity activities (*155*), which function through activating the transient receptor potential vanilloid (TRPV) superfamily of cation-channel receptors (*153, 156*).

However, as a lipophilic substance, CAP's low aqueous solubility greatly hinders its oral bioavailability (*157*). Moreover, the intensely pungent flavor results in a burning sensation for mammals, including humans. Choi *et al.* demonstrate that repeated oral exposure to CAP significantly increases anxiety-like behaviors with a prolonged stress-response in rats (*158*). In recent years, various lipid-based formulations for capsaicin have been developed, such as capsaicin-loaded liposomes (*159*), mixed polymeric micelles (*160*) and lecithin-based colloidal capsaicin nanocapsules (*161*), which proved to be very efficient in increasing oral bioavailability and relieving gastric mucosa irritations. The main issue of the above- mentioned delivery systems is their relatively low load, which limits its broad applications as dietary supplement. CAP-loaded organogel system, as a relatively new delivery system, has been applied to

the transdermal delivery of CAP in order to relieve orofacial neuropathic pain (*162*). Previous researches have demonstrated that organogels can be used for not only dermal, transdermal delivery, but also oral delivery of nutraceuticals (*163*). Therefore, the lipid-based organogel system was adopted in the first part of this research to increase the dissolution and stability of CAP in oils. To further enhance the bioaccesibility of CAP during oral administration, the organogel-derived nanoemulsion system was developed.

In this study, the organogel-derived capsaicin nanoemulsion was prepared. The *in-vitro* lipid digestion test was carried out using lipolysis experiment to determine the bioaccessibility of CAP entrapped by the lipid-based nanoemulsion system. In addition, the *in-vitro* dissolution rate was also tested using the Flow-Through Cell Apparatus (USP Apparatus 4). Moreover, the gastric mucosa irritation test was conducted using rats as animal model to study if the irritation caused by CAP could be relieved after it was encapsulated into the nanoemulsion system.

## MATERIALS AND METHODS

*Materials.*

Capsaicin (purity ~99%) was purchased from Ji'an Shengda Fragrance Oils Company (Ji'an, Jiangxi, China). Analytical standards for capsaicin (> 99%) were purchased from Sigma (St. Louis, MO, USA). Medium chain triacylglycerol (MCT) (Neobee 1053) was provided by Stepan Company (Northfield, IL, USA). Canola oil and corn oil were

purchased from Walmart. Tween 20 (polyoxyethylenesorbitan monolaurate), Tween 40 (Polyoxyethylenesorbitan monopalmitate), Tween 60 (polyoxyethylenesorbitan monostearate) and Tween 80 (polyoxyethylenesorbitan monooleate) were obtained from Sigma-Aldrich. Sugar ester (i.e., sucrose stearate S-370) was provided by Mitsubishi-Kagaku Foods Company (White Plains, NY, USA). Pancreatin with 8X USP specification, tris maleate and sodium taurodeoxycholate (NaTDC) were obtained from Sigma-Aldrich Company (St. Louis, MO, USA). PC75 rapeseed lecithin containing 75% phosphatidylcholine was provided by American Lecithin Co. (Oxford, CT, USA). HPLC-grade water was from Alfa Aesar (Lawrence, KS, USA). HPLC grade-methanol and acetonitrile were also purchased from Sigma-Aldrich Company.

*Preparation of the CAP-Loaded Organogel and Organogel-Derived Nanoemulsion.*

The CAP-loaded oil was first prepared by adding 2.3g CAP into 5.7g MCT (w/w), the oil mixtures were then heated up to 70 °C under stirring to achieve complete dissolution. Subsequently, two grams of sucrose stearate S-370 were added as gelator into the oil mixtures to form the CAP-loaded organogel. The loading for CAP in organogel was 23%.

The organogel-derived nanoemulsion was formed by mixing CAP-loaded organogel as the oil phase, Tween 80 as the emulsifier and water with the ratio of 35%: 15%: 50% (w/w/w). Then ultrasonication technique was used at 250W for 5 min to reduce the size of emulsion droplet into nano-scale. The final organogel-derived nanoemulsion was

formed with CAP loading of 80 mg/mL and droplet sizes of 167.9 ± 0.3 nm. This loading is by far the highest reported among CAP emulsion formulations.

*Particle Size Measurement*

Nanoemulsions were diluted 200 times into deionized water and mixed well. The average particle sizes (hydrodynamic diameters) of the lipid droplets were determined with dynamic light scattering (DLS) method using a BIC 90 Plus particle size analyzer (Brookhaven Instrument, NY) at a fixed scattering angle of 90° at ambient temperature, with a solid-state laser. The scattering signals were detected by a high-sensitivity avalanche photodiode detector.

*Lipolysis Experiment.*

Lipolysis is the digestion process of lipids, which involves the lipid triglycerides being catalyzed and hydrolyzed into 2-monoglyceride and 2 free fatty acids. Through this process, the capsaicin that is initially entrapped into the lipid oils will be redistributed into micelles or mixed micelles. Therefore, lipophilic bioactive compounds with poor water solubility become bioaccessible in the gastrointestinal tract. To mimic this process, an *in-vitro* lipolysis model was developed to test the bioaccessibility as well as the extent of lipolysis of the formulation before its further application in animal studies (*164*). The schematic explanation of this lipolysis model can be found from the work by Yu, *et al* (*163*).

Before the test, two lipolysis buffer solutions were prepared to mimic the fasted-state and fed-state chemical environment. The components in those buffer solutions were shown in **Table 10**. At the beginning of the test, 250 mg oil samples were added into 9 mL buffer solutions. Then by adding 1 mL pancreatin into the mixtures, the lipolysis process was initiated. During the digestion process, the triacylglycerols went through hydrolysis and released free fatty acids, causing a pH drop. To maintain the pH of the oil samples at 7.50 ± 0.2, 0.25 N sodium hydroxide solutions (NaOH) were added into the oil mixtures. The volume of NaOH was recorded by a computer program that can be used to analyze the extent of lipolysis. The lipid oil suspensions were being agitated during this 2-hour test at a fixed temperature of 37 °C. After the lipolysis test, samples were ultracentrifuged at 50,000 rpm (Type 60 Ti rotor, about 180,000g, Beckman Coulter) for 40 min. Finally, the supernatants were filtered through 220 nm filters and mixed with acetonitrile for HPLC analysis. Experiments were carried out in triplicate.

**Table 11.** Recipe of lipolysis buffer (1000 mL) for fasted and fed states.

| Components | Fasted-State Buffer | Fed State Buffer |
|---|---|---|
| Tris Maleate | 11.86 g | 11.86 g |

| | | |
|---|---|---|
| NaCl | 8.7664 g | 8.7664 g |
| $CaCl_2.2\ H_2O$ | 0.7351 g | 0.7351 g |
| NaTDC | 2.6084 g | 10.4336 g |
| Phosphatidylcholine | 0.9501 g | 3.8004 g |

*Determination of Bioaccessibility and Extent of Lipolysis for Different Oil Samples.*

The bioaccessibility refers to the potential for CAP to interact with (and be absorbed by) the GI tract, which can be calculated as follows:

$$\%\ \text{Bioaccessibility} = \frac{\text{Total mass of solubilized CAP}}{\text{Total mass of CAP loaded in original system}} \times 100\%$$

The mass of CAP was calculated according to the concentration of capsaicin, the density of samples and mass of the oil or emulsion system.

The extent of lipolysis was determined as the percentage of triacylglycerols digested in the system, which could be computed using the amount of NaOH added during the experiment and theoretical amount of NaOH needed to neutralize the fatty acids released from the complete digestion of triacylglycerols. Theoretically, complete digestion of 1 mole of triglyceride releases 2 moles of fatty acids, which needed 2 moles of NaOH to neutralize. The calculation method could be found as follows:

$$\text{Extent of lipolysis} = \frac{\text{Amount of NaOH added}}{\text{Theoretical amount of NaOH needed}} \times 100\%$$

Before each test, a mock lipolysis test was conducted without the addition of lipid oil

samples. And the amount of NaOH added in this test was subtracted when calculating the extent of lipolysis.

*In Vitro Dissolution Test.*

The dissolution rates of unformulated CAP, CAP-loaded organogels and organogel-derived nanoemulsion were measured using flow-through cell USP apparatus 4 (SOTAX Corporation, Westborough, MA, USA). 10 mg of samples (referring to the content of CAP) were introduced into the dissolution medium containing 100 mL of phosphate-buffered medium (PBS) at 37 ± 0.5 °C at a speed of 10 mL/min. To better mimic the dissolution environment of GI tract, pH was set at 1.2 during 0-1 hour (pH in stomach) and 7.5 during 1-3 hours (pH in small intestine). Samples were collected from the reservoir every 5 min during 0-1 hour, every 10 min during 1-2 hours, and every 30 min during 2-3 hours. Collected samples were analyzed using HPLC at 280 nm. All studies were carried out in triplicate.

*In Vitro Lipid digestion Test.*

One of the advantages of novel delivery systems is to increase the solubility and bioaccessibility of nutraceuticals when passing through the gastro-intestinal tract, being incorporated into the micelles or mixed micelles. Lipolysis was the digestion process of lipids, which involved the lipids being hydrolyzed and turned into glycerol and free fatty acids. Through this process, the capsaicin that was initially entrapped into the lipid oils

would be dissolved in micelles or mixed micelles. Therefore, the bioaccessibility of this bioactive compound would be increased in the gastrointestinal tract. To mimic the process, an *in-vitro* lipolysis model was used to test the bioaccessibility as well as the extent of lipolysis of the formulation before its further application in animal studies (*165*). The schematic representation of this model could be found in **Figure 16**. Theoretically, during the digestion of lipid oils, one molecule of triglyceride releases two molecules of free fatty acid and one molecules of glycerol under the enzymatic actions. And the pH of this model system is maintained at 7.5, with sodium hydroxide (NaOH) solution being used for titration.

As is shown in **Figure 16**, 1 mL of pancreatin is added into the oil dispersions at the beginning of the lipolysis test. And temperature is controlled at 37°C by oil bath. A pH meter is used to measure the pH of oil mixtures, and volume of NaOH consumed during titration process is recorded using a computer program. The extent of lipolysis is defined as the percentage of triglycerides digested through this process, which can be calculated according to the volume of NaOH consumed as a matter of time. And the bioaccessibility is determined by the content of nutraceuticals in the aqueous solutions after the lipolysis process.

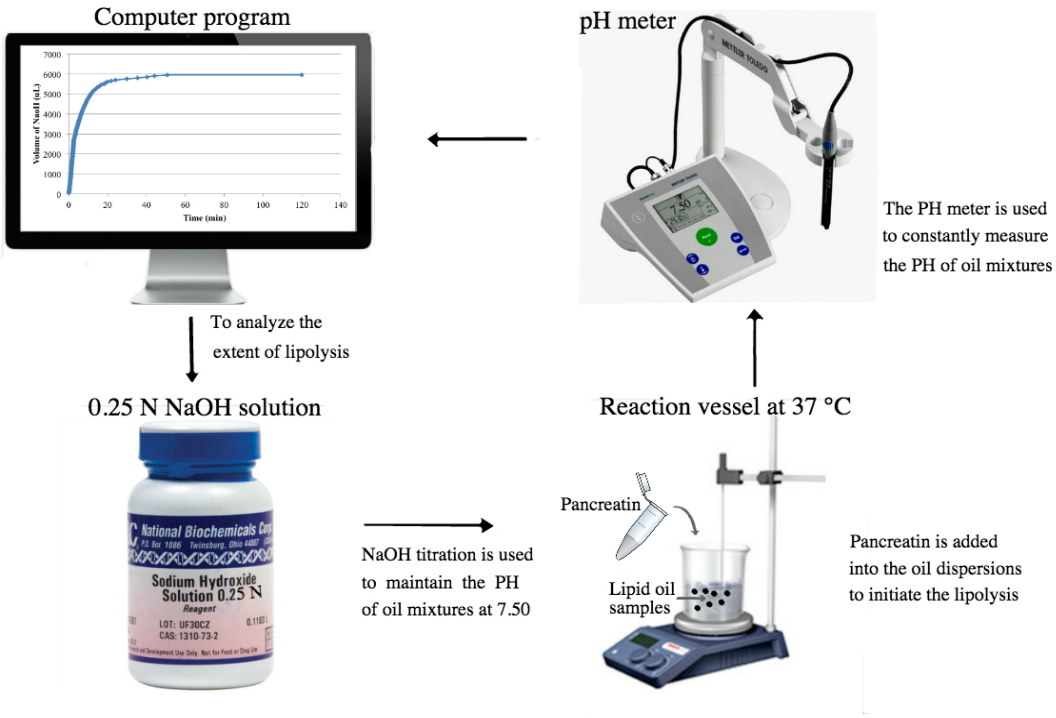


**Figure 16**. The *in vitro* lipolysis model.

The bioaccessibility of unformulated CAP, CAP-loaded MCT oils, CAP-loaded organogels and organogel-derived nanoemulsion were studied through the lipolysis experiment. Each test was conducted using fed-state and fasted-state buffer solutions to better mimic the lipid digestion process when meal was taken or several hours after the meal. Experiments were carried out in triplicate.

*High-Performance Liquid Chromatography (HPLC).*

Capsaicin was quantified by an automated high-performance liquid chromatography

system (Dionex, Sunnyvale, CA, USA). The system was consisted of a quaternary solvent delivery system, an UV–vis diode array detector and an automated injection system. The column used in this study is Dionex C18 column (150 x 4.6 mm, 3.5 μm) (Bellefonte, PA, USA). The mobile phase consists of (A) acetonitrile and (B) water (HPLC grade). 10 μL samples were injected each time and then eluted under gradient conditions: 0-2 min, 45% A and 55% B; 2-13 min, linear gradient from 45 to 90% A; 13-16 min, held at 90% A; 17-18 min, A went back to 45% linearly; 19-20 min, held at 45% to balance the column. The flow rate was set at 1.0 mL/min and the eluent was detected with UV wavelength at 280 nm. Different standard concentrations (5, 10, 20, 40, 60, 80 and 100 μg/mL) of CAP were dissolved in methanol and analyzed using HPLC to generate the calibration curve. Each measurement was carried out in triplicate.

*Gastric Mucosa Irritation Test.*

This study protocol was reviewed and approved by the South China Agriculture University Animal Ethics Committee. Male SPF Wistar rats (250g-300g) were obtained from Guangdong Medical Laboratory Animal Center (Guangzhou, Guangdong, China). Rats were adapted for 5 days to the experimental conditions: temperature 25 ± 2 °C, humidity 60 ± 5% and light/dark cycles of 12 h. Three groups of rats, each consisting of three rats, were orally administrated physiological saline (negative control group), free CAP suspended in physiological saline (positive control group) and CAP-loaded nanoemulsions (test group), respectively, at a dose of 90 mg/kg of body weight (referring to only capsaicin content). The rats were fasted but allowed free access to water for 12 h before and 2 h after oral administration. Then they were sacrificed for autopsy, and the intact stomachs were removed and fixed in 10% formaldehyde solution. All samples were

dehydrated and embedded in paraffin. The pathological section of the stomach, stained with hematoxylin and eosin, were observed under light microscope equipped with computer-controlled digital camera.

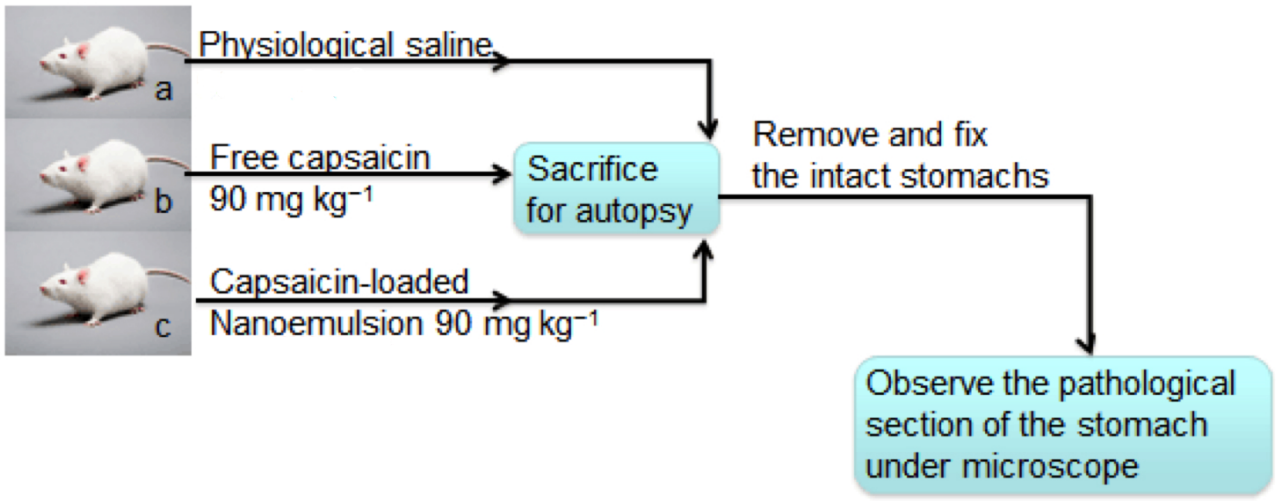


**Figure 17.** Gastric mucosa irritation test procedure.

## RESULTS AND DISCUSSION

*Determination of the Lipid Oil for the CAP-Loaded Organogel.*

To decide which lipid oil to use, three oil samples (medium-chain triacylglycerol (MCT), canola oil and corn oil) containing 5% CAP were tested based on their bioaccessibility and extent of lipolysis through the lipolysis tests in both fasted state and fed state. According to **Figure 18A**, capsaicin dissolved in MCT had the highest level of bioaccessibility among all oils in both fasted state (77.99 ± 2.74%) and fed state (76.19 ± 1.92%), followed by canola oil and corn oil. The same trend can be observed in **Figure 18B**, where the extent of lipolysis of MCT was much more complete than that of corn oil and canola oil in both fasted state (92.82 ± 2.22%) and fed state (76.86 ± 2.55%).

Therefore, MCT was most effective in providing a high bioaccessibility and extent of lipolysis among all lipid oils, which was chosen as the oil for capsaicin. This result agreed with previous researches concerning the digestion, absorption and metabolism of MCT as edible oils, which demonstrated that MCT could be hydrolyzed into fatty acids and glycerol in the small intestine with a rapid digestion rate (*166*).

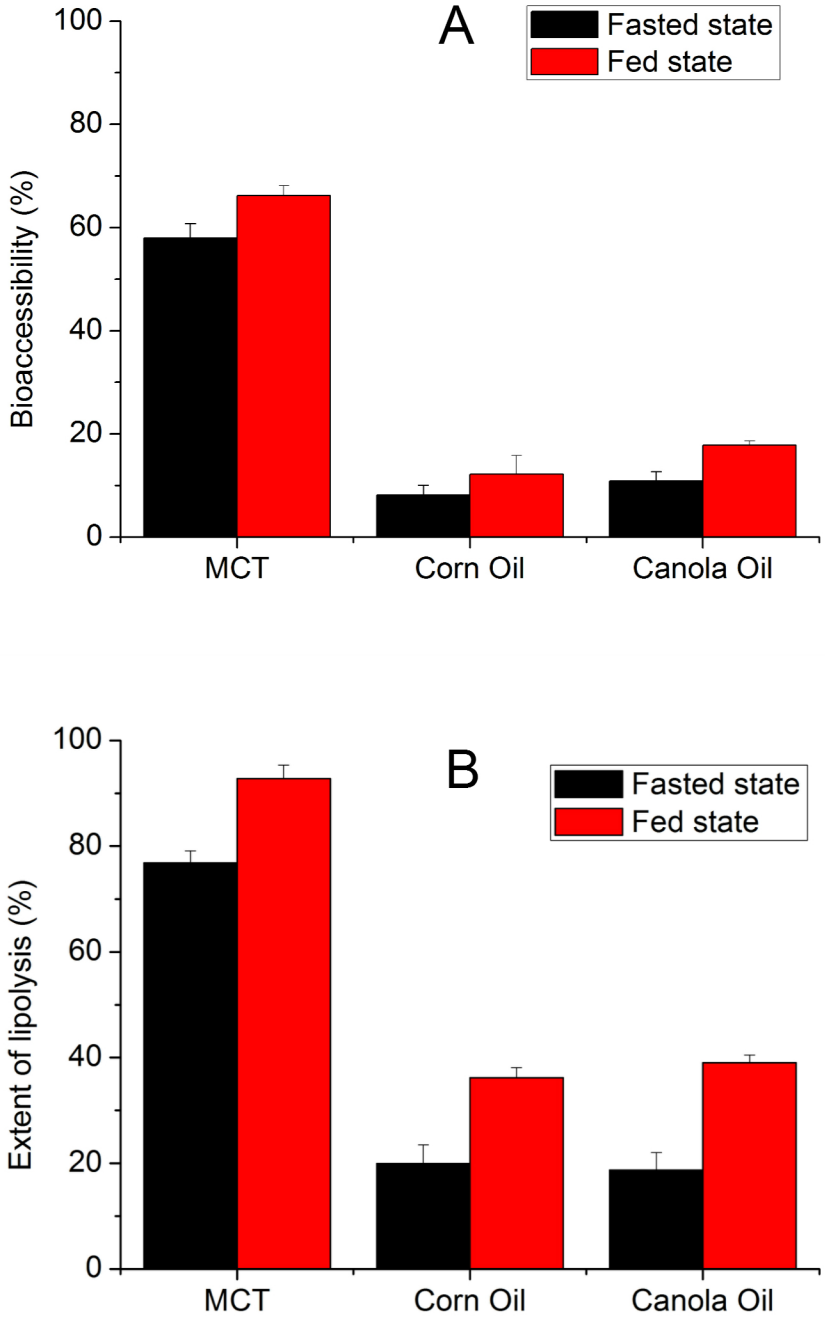


**Figure 18.** Comparison of the lipolysis of CAP in three oils. (A) The percent bioaccessibility of CAP after lipolysis of three oils; (B) the extent of lipolysis of three oils. Data from fasted- and fed-state lipolysis are combined. Error bars represent standard deviation (n = 3).

*Selection of the Gelling Agent.*

Previous researches showed that phytochemicals dissolved in MCT were metastable (*163*), so an organogel system was developed to increase its stability and dissolution rate as well as to prevent precipitations during storage. In order to form an organogel, the gelling agent is the key-contributing factor to the cross-linked network. Researches revealed that sugar-derived compounds present organo-gelation properties through the formation of certain intermolecular hydrogen bonds (*167, 168*). Therefore, sugar derivatives, such as sugar esters, were chosen in our experiment as the gelator to help create the organogel.

Food-grade sucrose stearates with different HLB values (between 1 to 9) were added to the preheated CAP-loaded MCT oil under stirring. The content of sucrose stearates in oil ranged from 15% to 25%. The result of the gel formation was shown in **Table 11**. According to the result, gels could be formed by adding 15 – 20% S-270 and 15 – 25% S-370 to the system. However, only the gel formed by 20% S370 was most stable without phase separations or precipitations during one-month storage. Therefore, the CAP-loaded organogel was successfully formed with 20% surcrose stearate S-370 working as the gelling agent. And the final loading of CAP in the organogel was 5.23%.

**Table 12.** Formation of the organogel system using different sucrose stearates of different weight ratios. (√ stands for the successful formation of gels; × stands for the failure in formation of gels.)

| **Sucrose Stearate** | **Weight Ratio** | | |
|---|---|---|---|
| | 15% | 20% | 25% |
| S170 | × | × | × |
| S270 | √ | √ | × |
| S370 | √ | √ | √ |
| S570 | × | × | × |
| S770 | × | × | × |
| S970 | × | × | × |

According to the result, gels could be formed by adding 15 - 20 % S-270 and 15 - 25 % S-370 to the system. However, only the gel formed by the addition of 20% S-370 was most stable without phase separations or precipitations during one-month storage. The formed gel using 20% S-370 can be found in **Figure 19**.

Therefore, the CAP-loaded organogel was successfully formed with 20 % surcease stearate S-370 working as the gelling agent. And the final loading of CAP in the organogel was 5.23%.

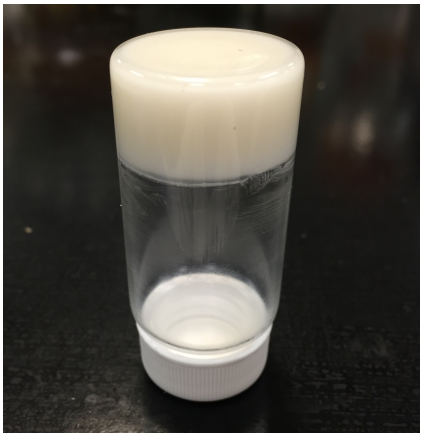

**Figure 19.** The photograph of the developed capsaicin-loaded organogel.

*Selection of Emulsifier for the Formation of Organogel-Derived Nanoemulsion***.**

A series of organogel-derived emulsions was formulated using non-ionic, oil-in-water emulsifiers (Tween 20, 40, 60 and 80). **Figure 20** shows the particle size and polydispersity index (PDI) of organogel-derived emulsion prepared at 15% (w/w) with different Tween surfactants. PDI is used to measure the heterogeneity of sizes of particles or molecules in a mixture (*169*), which is denoted as PDI = $M_w$ / $M_n$, where $M_w$ is the weight average molecular weight and $M_n$ is the number average molecular weight. The lower the PDI for an emulsion, the higher its degree of uniformity. An emulsion is called uniform if the oil droplets have the same size, shape, or mass. Among four different emulsifiers tested, Tween 80 produced the smallest mean droplet size (687.2 ± 63.7 nm, **Figure 20(A**) with the lowest PDI (0.22, **Figure 20B**), meaning that the formation of emulsion with Tween 80 is most uniform and stable. The difference in the oil droplet sizes may be owing to the hydrophilic - lipophilic balance (HLB) of

emulsifiers, which can influence the stability and formation of emulsions. HLB values for Tween 20 and 40 are 16.7 and 15.6, respectively, which are relatively higher than Tween 60 (14.9) and Tween 80 (15.0). Furthermore, even though Tween 60 and 80 have similar HLB values and molecular structures, the hydrophobic chain of Tween 80 has a double bond yet the hydrophobic chain of Tween 60 is saturated. Previous researches have reported that the presence of a double bond in the chain favors the formation of emulsions with smaller droplet sizes (*170, 171*). Therefore, Tween 80 as the emulsifier can help produce the emulsion with smallest particle sizes and highest stability among all tested emulsifiers.

In the following experiments, after ultrasonication at 250 Watt for 5 minutes, the organogel-derived nanoemulsion using Tween 80 as the emulsifier was formed with mean droplet sizes of 167.9 ± 0.3 nm.

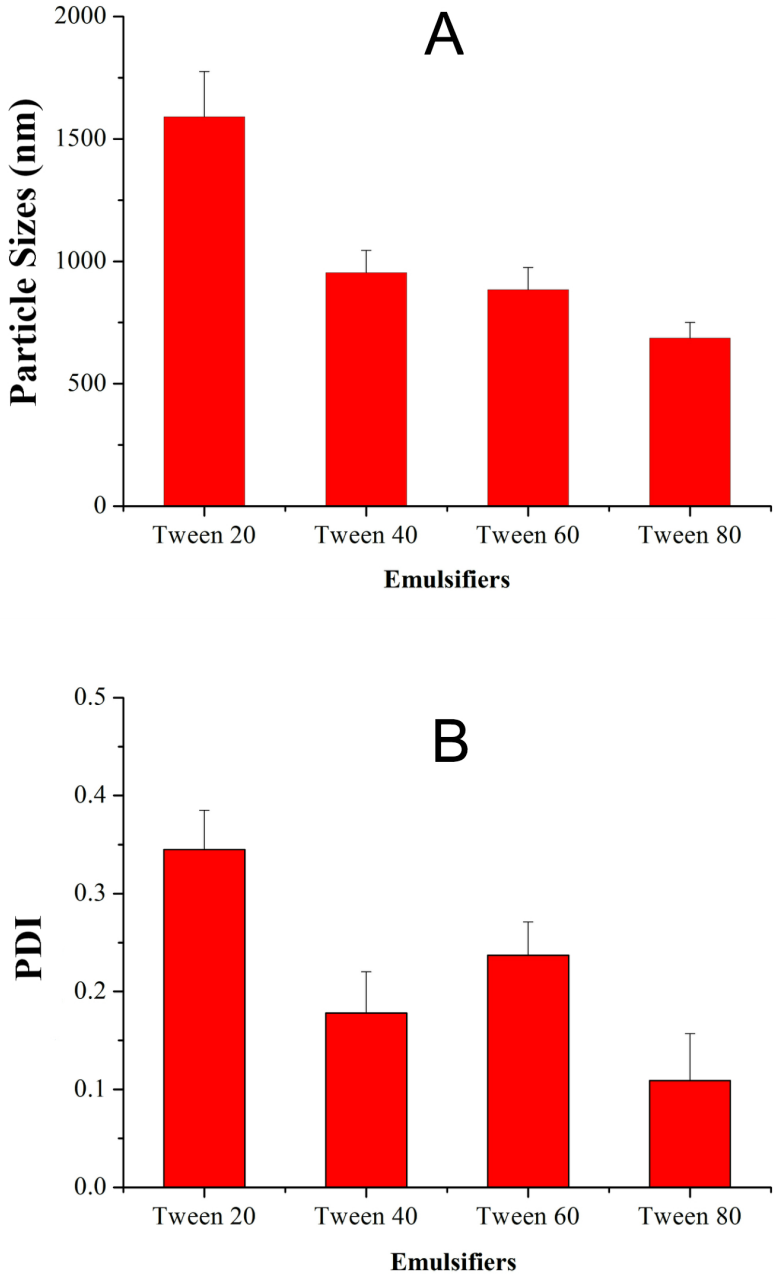


**Figure 20.** Effect of the emulsifier's type on (A) the particle size and (B) the polydispersity (PDI) of organogel-derived CAP-loaded emulsion before ultrasonication. Emulsifiers were Tween 20, 40, 60 and 80, from the left to the right (data shown are the mean ± SD).

*In Vitro Dissolution Test.*

To compare the *in-vitro* dissolution rate of CAP-loaded nanoemulsion, CAP-loaded organogel and free unformulated CAP after oral administration, the dissolution test was carried out in two consecutive pH environments. During first 60 minutes, the pH was set at 1.2 to mimic the acidic environment in the stomach. And Between 60 to 180 minutes, the pH was changed to 7.5 using the phosphate buffer solution (PBS) to simulate the pH evolution in the small intestine. As shown in **Figure 21**, the dissolution processes when pH was set at 1.2, only 3.19 ± 0.38 % of the free CAP was dissolved after one hour. While the dissolution rates of organogel and nanoemulsion were stable around 10.08 ± 2.55% and 64.48 ± 2.85%, which were more than 3 folds and 20 folds higher than free unformulated ones, respectively.

After one hour, the dissolution process continued as pH changes from 1.2 to 7.5. By the end of the 3-hour dissolution test, free CAP, formulated organogel and nanoemulsion had stable dissolution rates of 4.02 ± 0.45, 16.50 ± 3.02 and 75.74 ± 4.10%, respectively. Therefore, the organogel system had increased the *in-vitro* dissolution rate of CAP by 4 times compared with coarse samples, which might be attributed to the formation of soluble CAP-loaded micelles through agitation during the dissolution process. However, by the end of dissolution test, a large portion of CAP in the gel still remained undissolved, which might be attributed to the cross-linked network structure of the formed gel, requiring CAP to find its way out through the holes in the gel matrix before it was dissolved in the solution. Furthermore, the CAP-loaded nanoemulsion had the highest

dissolution rate among all tested samples, which was more than 10 times higher than free CAP and 4 times higher than organogel. This was mainly due to the reduced emulsion droplet sizes and enhanced surface area of the nanoemulsion, enabling more CAP-loaded nano-scale oil droplets to get access to the PBS buffer solutions. In addition, by comparing the dissolution result between CAP-loaded organogel and gel-derived nanoemulsion, it is obvious that the transformation from the gel system into nanoemulsion system is necessary in order to achieve a high dissolution rate of CAP compound.

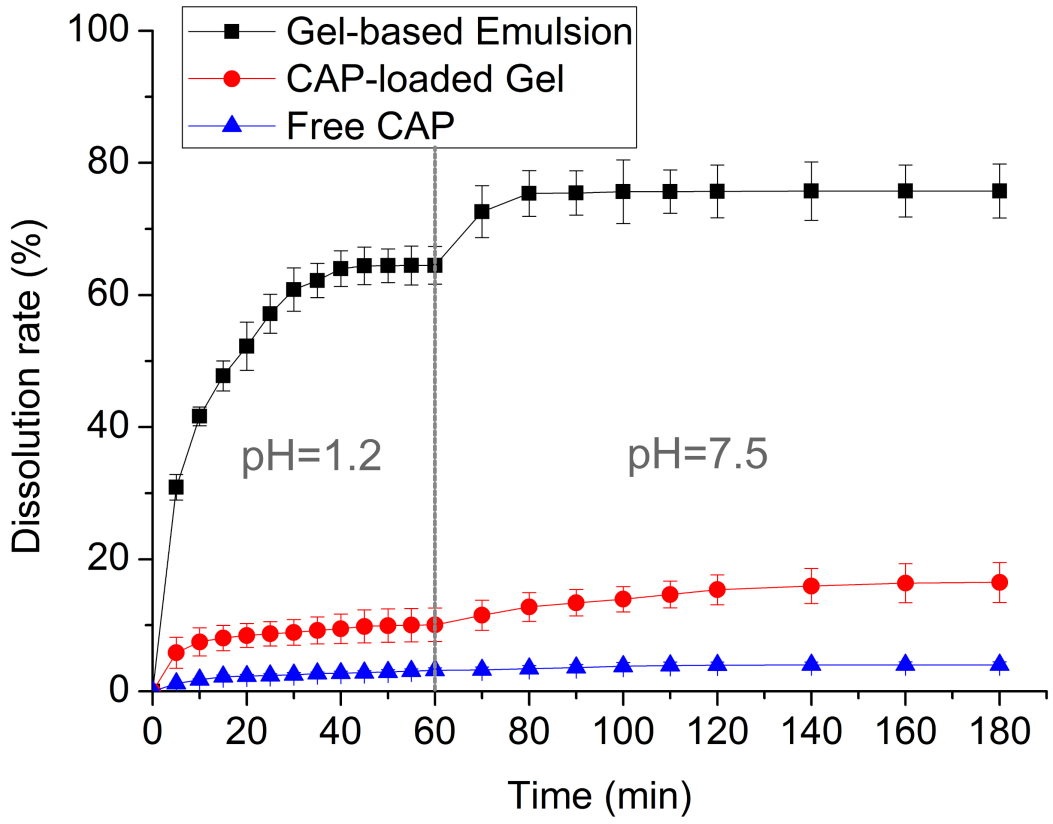


**Figure 21.** Dissolution profiles of CAP-loaded organogel and free CAP. Between 0 to 60

min, pH was 1.2; between 60 to 180 min, pH was 7.5 (data shown are the mean ± SD).

*In Vitro Bioaccessibility.*

To evaluate the *in-vitro* bioaccessibility of CAP from different formulation systems, the lipolysis experiment was carried out among CAP-loaded nanoemulsion, CAP-loaded gel, CAP-loaded MCT and free unformulated CAP in both fasted and fed state buffer solutions. The result was shown in **Figure 22**. The bioaccessibility of CAP-loaded gel was 56.53 ± 4.16% in fasted state and 63.89 ± 1.50% in fed state, which increased by approximately 10 times compared with free CAP (5.71 ± 1.82% in fasted state and 6.86 ± 0.19% in fed state). The major increase in the biaccessibility was owing to the rapid digestion ability and high dissolution rate of MCT. In addition, no major difference was observed for the bioaccessibility between CAP-loaded organogel and CAP-loaded MCT oil in both situations, showing that the formation of gel by adding gelling agent S-370 would not significantly reduce the *in-vitro* bioaccessibility of CAP. Moreover, after forming the nanoemulsion based the organogel structure, the bioaccessibility of CAP was further increased to 71.93 ± 1.33% in fasted state and 79.54 ± 0.64% in fed state. Also, by comparing the fed-state lipolysis titration profiles in **Figure 22C**, the initial lipid digestion rate for nanoemulsion was higher than the gel. After 25 minutes, the extent of digestion for the gel started to become stable and eventually reached 79.38 ± 3.23%, while the nanoemulsion continued to be digested and reached a final digestion extent of 99.54 ± 1.26%. Therefore, the nanoemulsion system had a much more complete lipid digestion and more sustained lipolysis rate compared with the orgaongel system, which can be attributed to the small droplet sizes and high surface area for lipase-catalyzed lipid

hydrolysis. Additionally, it was evident that the bioaccessibility and extent of lipolysis in fasted state was higher than fed state for all samples, reflecting that the developed CAP nanoemulsion and organogel should be taken with meal in order to guarantee a high bioaccessibility.

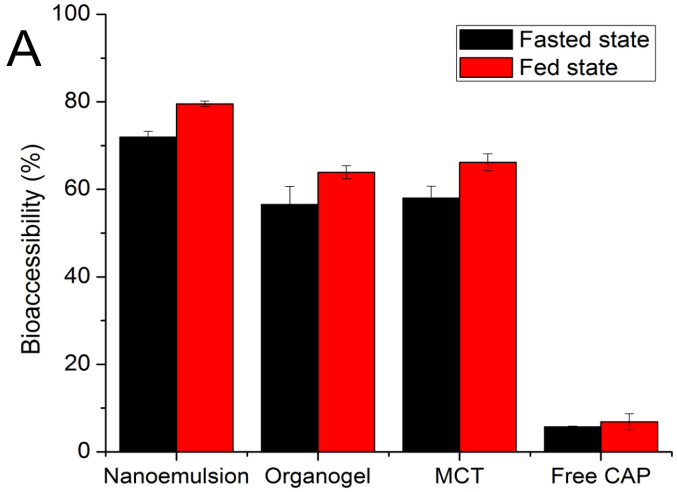
A
Bioaccessibility (%)
100
80
60
40
20
0
Fasted state
Fed state
Nanoemulsion
Organogel
MCT
Free CAP

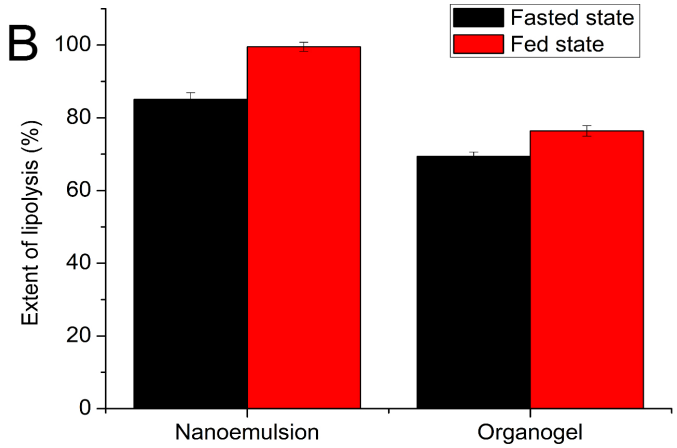
B
Extent of lipolysis (%)
100
80
60
40
20
0
Fasted state
Fed state
Nanoemulsion
Organogel

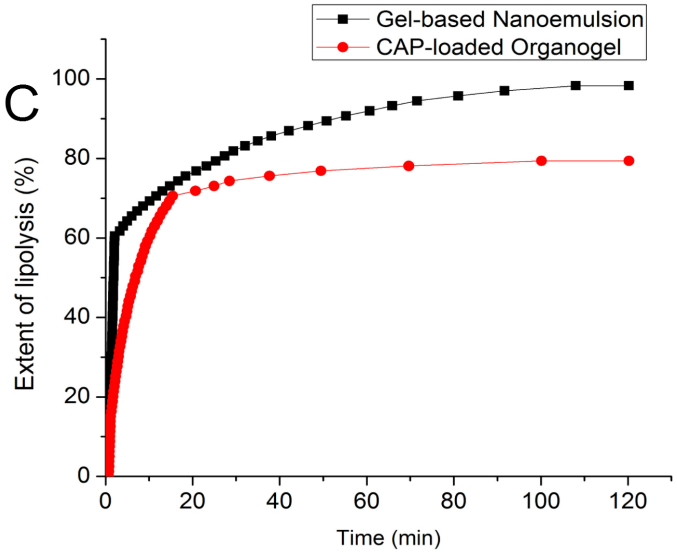
C
Extent of lipolysis (%)
100
80
60
40
20
0
Gel-based Nanoemulsion
CAP-loaded Organogel
0
20
40
60
80
100
120
Time (min)

**Figure 22.** Comparison of the *in-vitro* lipolysis result of free CAP, CAP-loaded MCT, CAP-loaded organogel and organogel-derived nanoemulsion, in the aspect of (A) the lipolysis profile and (B) the extent of lipolysis (C) the lipolysis profile of organogel and nanoemulsion in fed state (data shown in (A) and (B) are the mean ± SD).

*Morphological and Histological Evaluation of Gastric Mucosal Irritation.*

In this experiment, Male SPF Wistar rats (250g-300g) were used to study if the gastric mucosal irritation response caused by CAP could be relieved after CAP was encapsulated into the nanoemulsion system. Saline group (A) was used as negative control, while CAP suspension group (B) and CAP nanoemulsion group (C) with same dosage of capsaicin content (90 mg/kg of body weight) were used as positive control and test group, respectively. Oral administration of CAP suspension for 6 h induced marked hemorrhagic and ulcerative lesions on the gastric mucosal surface in rats according to **Figure 23B**; while in other groups, hardly any hyperemia was observed (**Figure 23 A and C**). The protective effect of the organogel-derived nanoemulsion system was further confirmed by histological examination. For the positive control group fed with free CAP suspension at dose of 90 mg/kg, infiltration of inflammatory cells was clearly seen in the gastric mucosa of rats as showed in **Figure 23 B1 and B2**. Rupture of membranes could also be seen in **Figure 23 B3**. However, for the negative control group A and test group C, which were given physiological saline and CAP-loaded nanoemulsion respectively, there was little evidence of gastric mucosal irritation **(Figure 23 A and C)**. Also, no

inflammatory cell infiltration was seen in the histological sections of gastric mucosa for rats fed with CAP nanoemulsion.

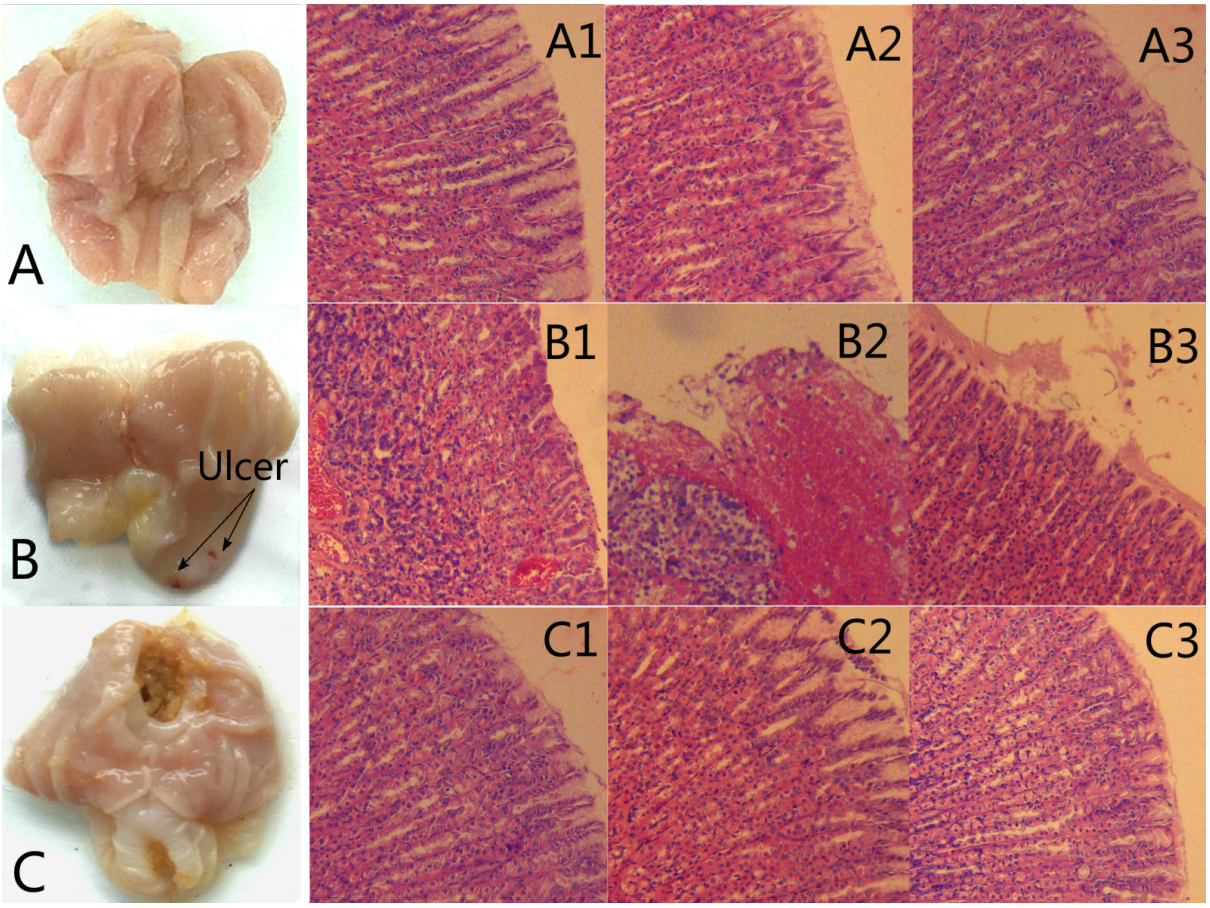


**Figure 23.** Stomach and gastric mucosa. (A) Stomach of rats treated with physiological saline; (A1) - (A3) Histological tissues of gastric mucosa in group A without damage. (B) Stomach of rats treated with pure capsaicin suspension; (B1) - (B3) Histological tissues of gastric mucosa in group B with damage; (C) Stomach of rats treated with capsaicin-loaded nanoemulsion; (C1) - (C3) Histological tissues of gastric mucosa in group C without damage. Only group B showed gastric ulcer and irritation response in gastric mucosa.

The above results suggested that the organogel-derived nanoemulsion possessed a reducing effect against irritation in rat stomach tissues induced by CAP. This could be explained by the encapsulation of CAP compound in the nanoemulsion system, reducing the direct contact between CAP and surface of gastric mucosa. In addition, the nano-scale lipid droplet might be able to biologically adhere to gastric tract, prolonging the retention time and avoiding the sudden release of CAP into the stomach. Furthermore, after the lipid hydrolysis in the gastric fluid, the CAP nanoemulsion could be digested into micelles with even tiny droplet sizes (13.4 ± 0.4 nm, according to the fasted state lipolysis model), thereby preventing the irritation caused by CAP crystals getting in contact with gastric mucosa.

## CONCLUSIONS

In summary, the organogel-derived CAP nanoemuslion with high *in-vitro* dissolution rate and lipid digestibility was developed and evaluated. The MCT was chosen as the lipid oil not only because of its high bioaccessibility and extent of lipolysis, but also for its ability to increase fat oxidation, energy expenditure and weigh loss as edible oil, which could work synergistically with CAP as the anti-obesity agent. Then with the addition of sucrose stearate S-370, which was working as the gelling agent to increase the stability of CAP-loaded MCT, the organogel was formed. To better enhance the bioaccessibility of

CAP, Tween 80 was added into organogel and water with the ratio of 15 %: 35 %: 50 %, which was functioning as emulsifier to produce a formulation with small droplet sizes and high stability. After ultrasonication process, the nanoemulsion was developed with mean droplet sizes of 167.9 ± 0.3 nm and CAP loading of 80 mg/mL. Animal studies using SPF rats showed that the gastric mucosa irritation caused by CAP was alleviated effectively. These results indicated that the organogel-derived nanoemulsion could be used as a promising carrier system for poorly water soluble nutraceuticals with reduced irritation in the stomach. This CAP-loaded nanoemulsion could also be further developed into multi-functional beverages with weight-loss and cardio-protection effects.

# CHAPTER IV. ANTI-OBESITY EFFECT OF CAPSAICIN LOADED NANOEMULSION (C-NE) IN RATS TREATED WITH HIGH-FAT DIET

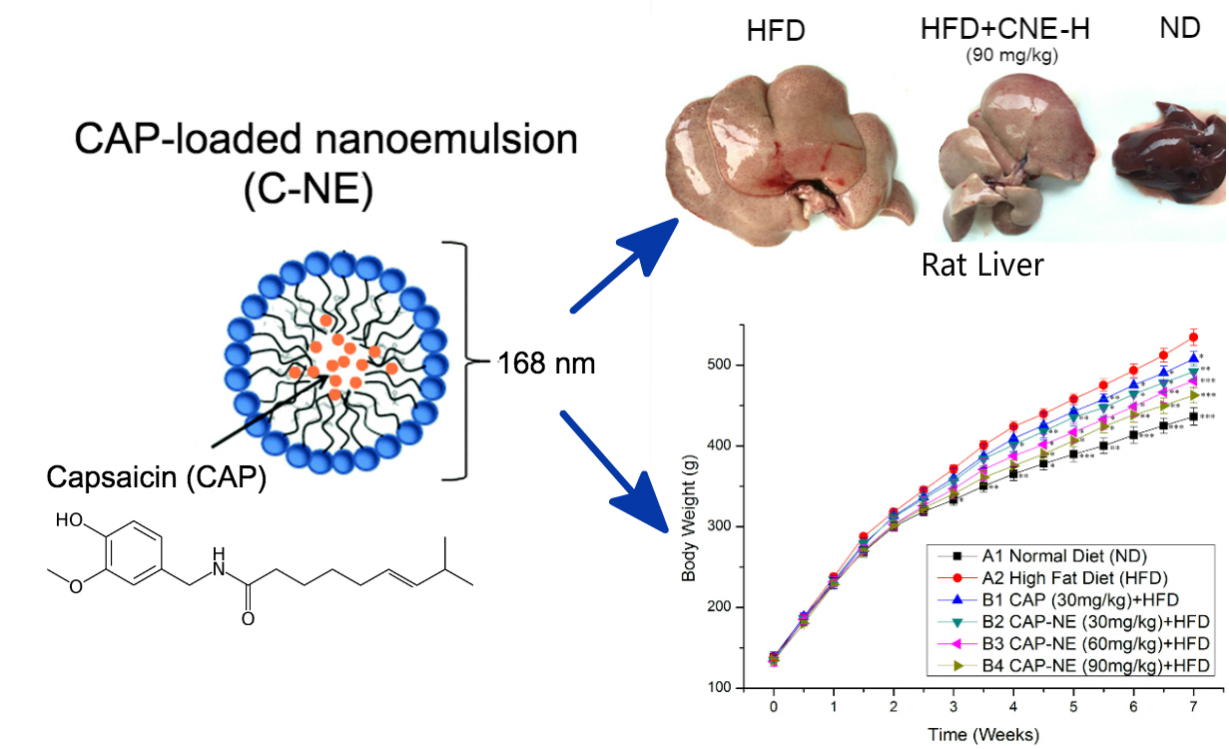


## PROJECT TITLE: ENHANCED ANTI-OBESITY EFFECT AND REDUCED GATRIC MUCOSA IRRITATION OF CAPSAICIN-LOADED NANOEMULSION

*The work in this chapter has been published in the title of "*The Enhanced Anti-obesity Effect and Reduced Gastric Mucosa Irritation of Capsaicin-loaded Nanoemulsions*" in the Food & Function (Volume 8, Pages from 1803 to 1809) on May 2017.*

**ABSTRACT**

Capsaicin (CAP), the major active component in chili peppers, is known to have thermogenetic and weight-loss potentials. The aim of this study was to investigate the anti-obesity effects of capsaicin-loaded nanoemulsions (C-NE) on male Sprague Dawley (SD) rats treated by high-fat diet (HFD). The food grade C-NE was prepared using capsaicin, medium chain triacylglycerol (MCT) (Neobee 1053), sucrose stearate S-370, Tween 80 and distilled water with emulsion droplet sizes of 168 nm and loading of capsaicin 80.4 mg/mL. Results showed that C-NE effectively decreased body weight gain and hypercholesterol induced by HFD in a dose-dependent way. Histological evaluations of liver and adipose tissue confirmed that C-NE had significant effects on inhibiting diet-induced hepatic steatosis, reducing epididymal adipocyte size and tissue mass. Gastric mucosa irritation test demonstrated that C-NE was effective in alleviating the gastric inflammations caused by free unformulated CAP crystals.

**INTRODUCTION**

Obesity has become one of global health issues negatively affecting the quality of human lives. Obesity is the consequence of a high level of energy intake and a low level of energy expenditure, which has a strong association with numbers of metabolic syndromes, such as hypertension, hyperlipidemia, fatty liver, type 2 diabetes, insulin resistance and cancer. Numerous researches on obesity were conducted to find out the food-grade nutraceuticals with weight loss potentials, including isolated compounds from natural products, such as 5-demethylated polymethoxyflavones (5-OH PMFs) extracted from

citrus peels (*172*) and epigallocatechin gallate (EGCG) isolated from green tea (*173*), etc.

Consumption of chili peppers is known to increase the energy expenditure. Capsaicin (8-methyl-*N*-vanillyl-6-nonenamide) (CAP) as an active component in chili peppers has been proved to have thermogenic and anti-obesity properties (*64-66*). Reinbach *et al.* (*174*) reported that capsaicin could reduce the energy intake and reduce weight gain by relatively suppressing hunger and sustaining satiety. Joo *et al.* (*67*) fed the rats on a high fat diet with capsaicin and performed proteomic analysis to elucidate its molecular action in white adipose tissue. Results revealed that proteins related with lipid metabolism, redox regulations, and signal and energy transduction were significantly altered on the treatment of capsaicin, suggesting possible mechanism of anti-obesity effect of capsaicin.

Recently, we developed a food-grade capsaicin-loaded nanoemulsion (C-NE) system for oral delivery with enhanced stability, dissolution rate, bioaccessibility and gastro-protective effect compared with free unformulated CAP water suspensions (*68*).

In this study, our goal was to investigate the effects of C-NE on body weight gain after a 7-week high-energy diet in male Sprague Dawley (SD) rats. Previous research indicated that the oral $LD_{50}$ (lethal dose that causes the death of 50% of a group of test animals) value of CAP for male rats is 161.2 mg/kg (*175*). Different amount of C-NE were applied to different groups of rats to evaluate if the anti-obesity effect got enhanced with the increase of doses. Histological sections of liver and adipose tissues from each group were prepared to examine if C-NE could inhibit hepatocytes vacuolation and suppress the HFD-induced increase in adipocyte mass and size. Gastro-protective potential of C-NE was compared with free unformulated CAP water suspensions by evaluation of the

gastric tissue sections of rats.

## MATERIALS AND METHODS

*Materials.*

Capsaicin (purity ~99%) was purchased from Ji'an Shengda Fragrance Oils Company (Ji'an, Jiangxi, China). Medium chain triacylglycerol (MCT) (Neobee 1053) was provided by Stepan Company (Northfield, IL, USA). Tween 80 (polyoxyethylenesorbitan monooleate) was obtained from Sigma-Aldrich. Sugar ester (sucrose stearate S-370) was provided by Mitsubishi-Kagaku Foods Company (White Plains, NY, USA). Milli-Q water (18.3 MΩ) was used in all experiments.

We prepared the C-NE in our laboratory using a previously reported procedure (*68*). Briefly, The CAP-loaded oil was first prepared by adding 2.3g of CAP into 5.7g of MCT (w/w). Then the oil mixtures were heated up to 70 °C under magnetic stirring to achieve complete dissolution. 2.0g of sucrose stearate S-370 were added as gelator into the oil mixtures to form the CAP-loaded organogel. Then by mixing CAP-loaded organogel, Tween 80 and water with the ratio of 35%: 15%: 50% (w/w/w), after ultrasonication process at an output power of 250W for 5 min, the organogel-derived nanoemulsion was formed with CAP loading of 80.4 mg/mL and droplet sizes of 167.9 ± 0.3 nm. This loading is by far the highest reported among CAP emulsion formulations. All other reagents and solvents were of analytical grade.

Animals and Experimental Design.

Male specific-pathogen-free Sprague Dawley (SD) rats (100-150 g) were purchased from

Guangdong Medical Laboratory Animal Center (Guangzhou, Guangdong, China). Rats were housed four per cage and maintained in a temperature/humidity-controlled room with a 12 h light/dark cycle. After 5 days, 56 rats were randomly divided into 7 groups (n = 8). Group A1 was the normal diet (standard rodent chow) group (ND); rats in this group were fed with a standard diet. Rats in group A2, B1, B2, B3, B4, B5 were fed with a high-fat diet (HFD), which contained 15% lard; 20% sucrose; 10% casein; 1.2% cholesterol; 0.2% bile; 1% calcium hydrogen phosphate ($CaHPO_4$); 0.2% sodium chloride (NaCl); 0.5% egg yolk powder, 51.9% basic feed. From group A2 to group B5, rats were fed through oral gavage with HFD (group A2), HFD and pure CAP suspended in water at dose of 30 mg/kg of body weight (group B1); HFD and C-NE at dose of 30 mg/kg of body weight (group B2); HFD and C-NE at dose of 60 mg/kg of body weight (group B3); HFD and C-NE at dose of 90 mg/kg of body weight (group B4); HFD and wall materials of C-NE (medium chain triglycerides, S-370, Tween 80 and water, without CAP) at the same dosage with group B4 (group B5). The diet and dosage of CAP formulations in each group are epitomized in Table 12.

This animal study protocol was reviewed and approved by the South China Agriculture University Animal Ethics Committee.

**Table 13.** The diet and dosage of capsaicin formulations in each group.

| Group name | | Number of rats | Diet | Compound | Dosage/day |
|---|---|---|---|---|---|
| Control Group | A1 | 8 | ND | - | - |
| | A2 | 8 | HFD | - | - |
| Experimental Group | B1 | 8 | HFD | CAP water suspension | 30 mg/kg |

| | | | | | |
|---|---|---|---|---|---|
| | B2 | 8 | HFD | C-NE | 30 mg/kg |
| | B3 | 8 | HFD | C-NE | 60 mg/kg |
| | B4 | 8 | HFD | C-NE | 90 mg/kg |
| | B5 | 8 | HFD | wall materials of C-NE | Equal to 90 mg/kg |

Determination of food intake, water intake and body weight.

Rats were allowed free access to water and food throughout the experiment. Body weight of rats was weighed twice a week, food and water intake levels for each group were recorded daily. The results are presented as the mean ± standard deviation (n = 8).

*Measurement of liver, retroperitoneal fat, and epididymal fat tissue weight.*

At the end of the experiment, all groups of rats were fasted overnight, and blood samples were withdrawn from the orbital vein using a capillary. The rats were then subjected to cervical dislocation, sacrificed, and necropsied. The liver, retroperitoneal fat and epididymal fat tissue of each mouse were removed and weighed on ice. Tissue samples were stored in liquid nitrogen for further analysis.

*Serum Biochemical Analysis.*

Serum samples collected from 7 groups of rats were sent to the Division of Hematology at the First Affiliated Hospital of Ji'nan University (Guangzhou, Guangdong) for the measurement of alanine aminotransferase (ALT), triglyceride level (TG), total cholesterol (TC), high-density lipoprotein cholesterol (HDLC), low-density lipoprotein cholesterol (LDLC),and alanine transaminase (ALT).

*Histological analysis.*

Liver, epididymal fat and stomach tissues were dissected and fixed in 10% (v/v) formaldehyde solution for 24 hours. The fixed samples were dehydrated and embedded in paraffin. The pathological sections of the liver, epididymal fat and stomach tissues, stained with hematoxylin and eosin, were observed under an optical microscope (Olympus, Tokyo, Japan) equipped with a computer-controlled digital camera.

*Statistical Analysis.*

All of the data are expressed as means ± standard error. Differences between groups were analyzed by one-way ANOVA using IBM SPSS Statistics, version 21.0 (SPSS Inc., Chicago, IL, USA). Significance level at $p < 0.5, 0.05, 0.001$ were considered to indicate statistical significance.

## RESULTS AND DISCUSSION

*C-NE Reduced the Body Weight Gain Induced by HFD*

To examine the anti-obesity effect of capsaicin-loaded nanoemulsion (C-NE), male SD rats were treated with HFD to induce fat accumulation and body weight increase. As shown in Supplementary Material (Table S1), the initial body weights of rats were not different among all seven groups in the beginning of the experiment. After 7 weeks of experiment, the rats fed with HFD alone developed the highest final body weight (534.8 ± 9.9 g) among all groups (Fig. 2A). While rats treated with CAP-containing formulations showed reductions in the final body weights. In group B1, after the oral feeding of CAP water suspensions at dose of 30 mg/kg/day, the final body weight was

reduced to 508.0 ± 9.1 g. The C-NE exhibited better weight-loss properties by further decrease the final body weight to 492.3 ± 9.7 g with a statistically significant difference from group B1 (Fig. 2B, $P<0.05$). Moreover, as the dose of C-NE increased from 30 mg/kg to 90 mg/kg per day, the final body weight of rats continued to be decreased. C-NE at dose of 90 mg/kg/day (group B4) significantly controlled the weight gain by 13.5% in comparison with that of HFD group (group A2), demonstrating an effective inhibitory activity on obesity induced by high-energy intake. The wall material (WM) of C-NE, which contained medium chain triacylglycerols (MCT), sucrose ester S-370, Tween 80 and water, also decreased the body weight by 8.7% compared to HFD. The weight reduction effect of WM might be due to MCT's ability in suppressing energy intake, which was documented in a number of studies (*176-179*). Comparing group B4 with B5, we could observe that the anti-obesity effect of C-NE was better than that of the wall materials at CAP dose of 90 mg/kg. The results above implied that C-NE had enhanced weight-loss activity in rats fed by HFD compared with free unformulated CAP and wall material group, which might be attributed to the fact that CAP bioaccessibility was promoted by the nanoemulsion system and additive effects existed between CAP and the encapsulation materials. Additionally, no apparent difference in daily food intake was observed among six groups fed with HFD (Table S1), indicating that weight-loss effects of C-NE were not influenced by the reduced energy consumption. The weight loss efficacy of C-NE got improved with the increase of the doses.

**Table 14.** Changes in body weight, food intake, and tissue weight among groups in male SD rats.

| Variables | | ND [a] (A1) | HFD [b] (A2) | HFD+C [c] 30mg/kg (B1) | HFD+C-NE [d] 30mg/kg (B2) | HFD+C-NE 60mg/kg (B3) | HFD+C-NE 90mg/kg (B4) | HFD+WM [e] (B5) |
|---|---|---|---|---|---|---|---|---|
| Initial body weight (g) | | 138.300±6.700 | 138.700±3.800 | 137.100±7.300 | 134.900±3.200 | 133.000±5.500 | 134.900±4.900 | 138.700±5.7 |
| Final body weight (g) | | 436.600±10.900 | 534.800±9.900 | 508.000±9.100 | 492.300±9.700 | 480.800±8.6700 | 462.900±9.7500 | 488.100±9.1 |
| Water intake (g/day) | | 53.600±5.500 | 33.300±0.100 | 36.800±2.000 | 35.000±3.600 | 37.100±1.400 | 34.100±2.300 | 34.700±1.20 |
| Food intake (g/day) | | 29.100±0.800 | 24.500±0.600 | 22.700±0.400 | 23.000±0.700 | 22.300±0.900 | 22.700±0.300 | 22.600±0.10 |
| Food efficiency (g gain/g consumed) | | 0.183±0.002 | 0.289±0.007 | 0.292±0.003 | 0.278±0.007 | 0.278±0.013 | 0.262±0.008 | 0.275±0.002 |
| Total food intake (kg/8 weeks) | | 1.630±0.080 | 1.370±0.060 | 1.270±0.040 | 1.290±0.070 | 1.250±0.090 | 1.260±0.030 | 1.270±0.010 |
| Liver weight (g/100g body weight) | | 3.130±0.540 | 4.380±0.510 | 4.170±0.570 | 4.180±0.510 | 3.930±0.360 | 3.800±0.530 | 4.100±0.550 |
| Adipose tissue weight(g/100g body weight) | 1.390±0.360 | 2.020±0.410 | 1.740±0.240 | 1.700±0.260 | 1.630±0.330 | 1.640±0.270 | 1.650±0.340 | 1.65±0.34 |
| | 1.670±0.490 | 2.750±0.320 | 2.570±0.410 | 2.550±0.290 | 2.200±0.380 | 2.300±0.410 | 2.180±0.390 | 2.18±0.39 |

**Notes:** Data are presented as mean ± standard error (n=8).

**Abbreviations:** a) ND, normal diet; b) HFD, high fat diet; c) C, capsaicin; d) C-NE, capsaicin nanoemulsion; e) WM, wall material.

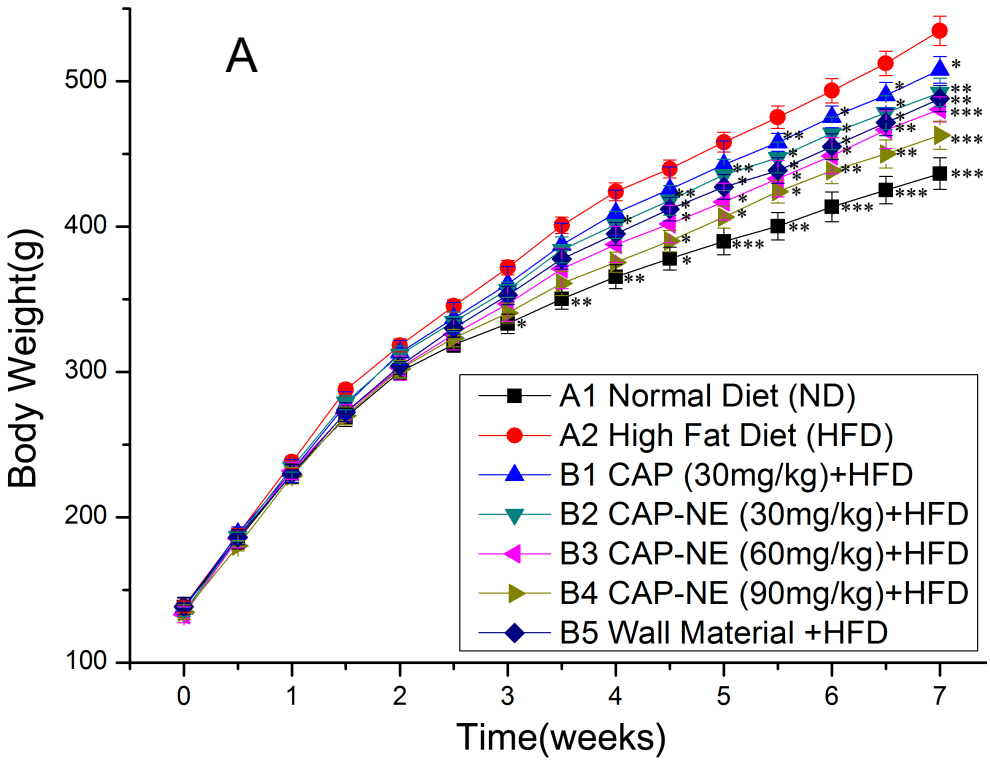
A
Body Weight(g)
Time(weeks)
100
200
300
400
500
0
1
2
3
4
5
6
7
A1 Normal Diet (ND)
A2 High Fat Diet (HFD)
B1 CAP (30mg/kg)+HFD
B2 CAP-NE (30mg/kg)+HFD
B3 CAP-NE (60mg/kg)+HFD
B4 CAP-NE (90mg/kg)+HFD
B5 Wall Material +HFD

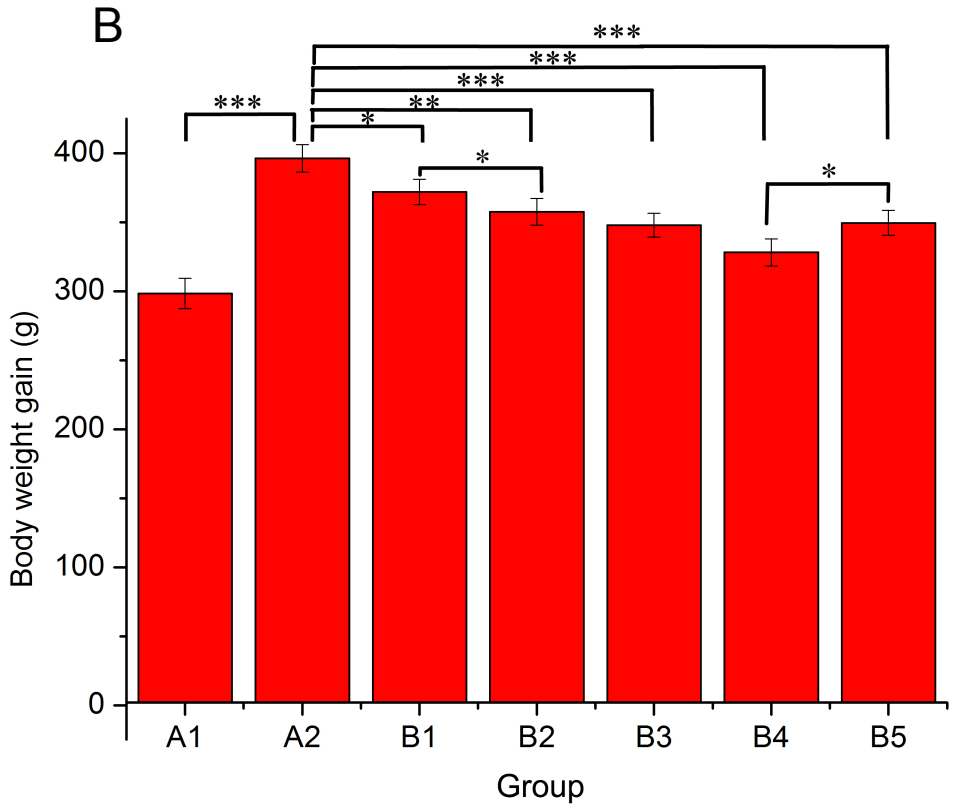
B
***
***
***
**
*
*
*
400
300
200
100
0
Body weight gain (g)
A1
A2
B1
B2
B3
B4
B5
Group

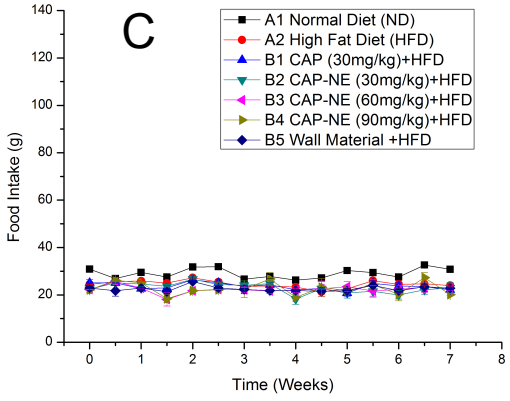
C
A1 Normal Diet (ND)
A2 High Fat Diet (HFD)
B1 CAP (30mg/kg)+HFD
B2 CAP-NE (30mg/kg)+HFD
B3 CAP-NE (60mg/kg)+HFD
B4 CAP-NE (90mg/kg)+HFD
B5 Wall Material +HFD
Food Intake (g)
Time (Weeks)

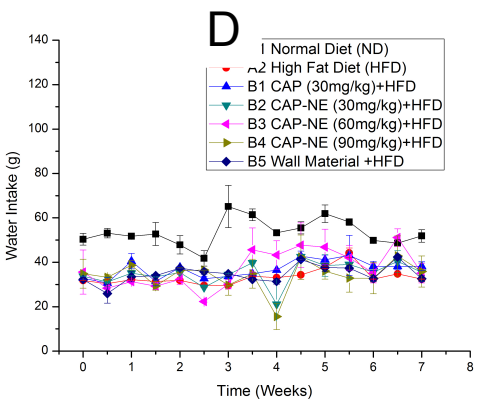
D
Normal Diet (ND)
High Fat Diet (HFD)
B1 CAP (30mg/kg)+HFD
B2 CAP-NE (30mg/kg)+HFD
B3 CAP-NE (60mg/kg)+HFD
B4 CAP-NE (90mg/kg)+HFD
B5 Wall Material +HFD
Water Intake (g)
Time (Weeks)

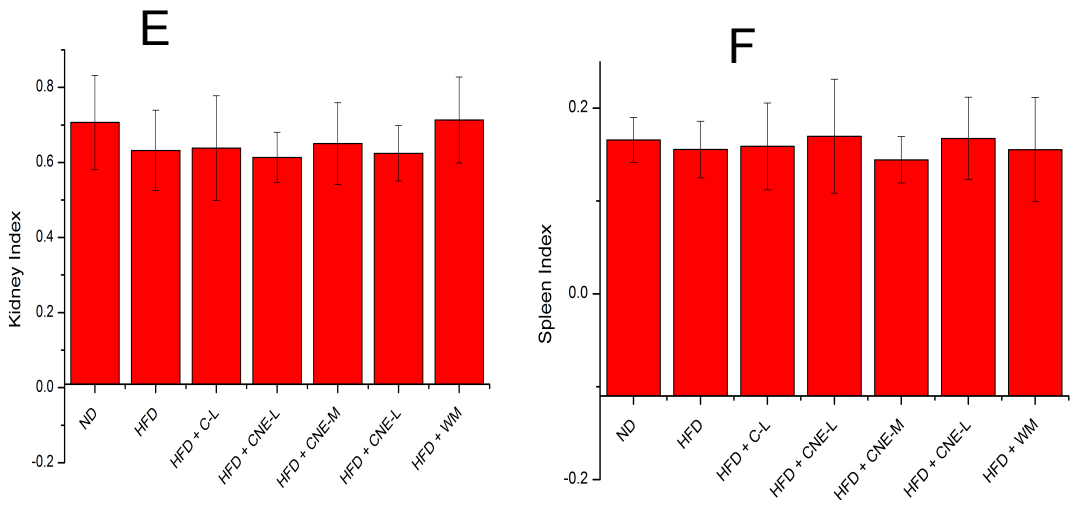


**Figure 24.** Chronic oral treatment of CAP and C-NE reduced HFD-induced body weight gain in male SD rats: (A) body weight growth curve of rats; (B) body weight gain in each group; (C) food intake of rats; (D) water intake of rats for 7 weeks; (E) Kidney Index (g/100g body weight); (F) Spleen Index (g/100g body weight). Data are presented as the mean value ± SE (n = 8): (∗) $P < 0.05$, (∗∗) $P < 0.01$, and (∗∗∗) $P < 0.001$ versus HFD; all error bars, SE.

*Effects of C-NE on serum biochemical values.*

Serum biochemical parameters were measured by an automatic biochemical analyzer, and results were presented in Table 14 and Fig. 25. Serum lipids, such as TC, TG and LDLC levels in groups treated with C-NE showed a decrease compared with HFD group, while HDLC levels were higher in former groups. Other groups, such as low doses of CAP water suspension and WM of C-NE also showed good control of TC levels (Fig. 3, TC). The serum cholesterol-suppressing effect of WM might be attributed to MCT's activity in decreasing cholesterol intake, which was reported by Han, *et al* (*176*). High

doses of C-NE was most effective in reducing the TC, TG and LDLC levels by 29.2%, 54.3% and 32.4%, respectively ($P < 0.001$) than other doses, in comparison with HFD group. These results indicated that C-NE had an anti-hyperlipidemic potential for rats fed by HFD. ALT is measured to see if the liver is damaged or diseased. Low levels of ALT are normally found in the blood. But when the liver is damaged or diseased, it releases ALT into the bloodstream, which makes ALT levels go up. Most increases in ALT levels are caused by liver damage. Besides, no apparent difference was observed for serum ALT activities in C-NE groups when compared to those of the normal diet group and HFD group, showing that C-NEs were well tolerated by the rats.

**Table 15.** Effects of C-NE on serum lipids, ALT activities.

| Plasma Biochemical Values | ND | HFD | HFD+C 30mg/kg (Low dose) | HFD+C-NE 30mg/kg (Low dose) | HFD+C-NE 60mg/kg (Medium dose) | HFD+C-NE 90mg/kg (High dose) | HFD+WM Equal to 90mg/kg |
|---|---|---|---|---|---|---|---|
| TC [a] (mmol/L) | 1.78±0.11 | 3.80±0.06 | 3.41±0.07 | 3.16±0.04 | 2.91±0.12 | 2.69±0.07 | 3.42±0.10 |
| TG [b] (mmol/L) | 0.81±0.01 | 1.27±0.24 | 1.05±0.21 | 0.86±0.16 | 0.7±0.18 | 0.58±0.12 | 0.65±0.06 |
| HDLC [c] (mmol/L) | 0.58±0.04 | 0.41±0.02 | 0.48±0.03 | 0.50±0.05 | 0.48±0.03 | 0.45±0.02 | 0.43±0.03 |
| LDLC [d] (mmol/L) | 0.30±0.02 | 0.74±0.08 | 0.69±0.09 | 0.81±0.09 | 0.65±0.09 | 0.50±0.12 | 0.57±0.05 |
| ALT [e] (U/L) | 26.25±2.13 | 26.78±2.97 | 25.50±2.49 | 24.12±2.44 | 23.43±2.44 | 24.43±1.46 | 24.13±1.29 |

**Notes:** Data are presented as mean ± standard error (n=8).

**Abbreviations:** a) TC, total cholesterol; b) TG, triglycerides; c) HDLC, high-density lipoprotein cholesterol; d) LDLC, low-density lipoprotein cholesterol; e) ALT, alanine aminotransferase.

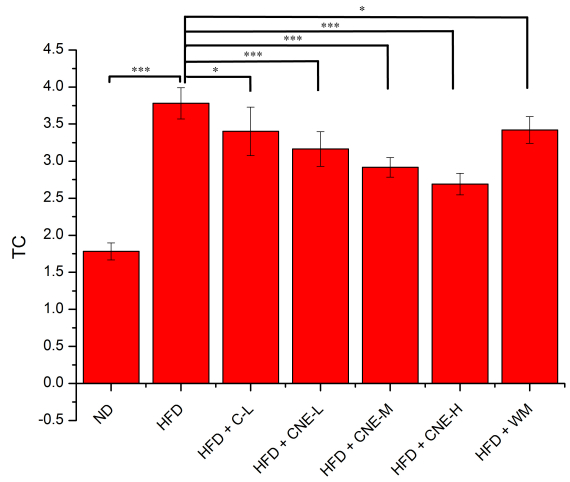
TC
4.5
4.0
3.5
3.0
2.5
2.0
1.5
1.0
0.5
0.0
-0.5
***
*
***
***
***
*
ND
HFD
HFD + C-L
HFD + CNE-L
HFD + CNE-M
HFD + CNE-H
HFD + WM

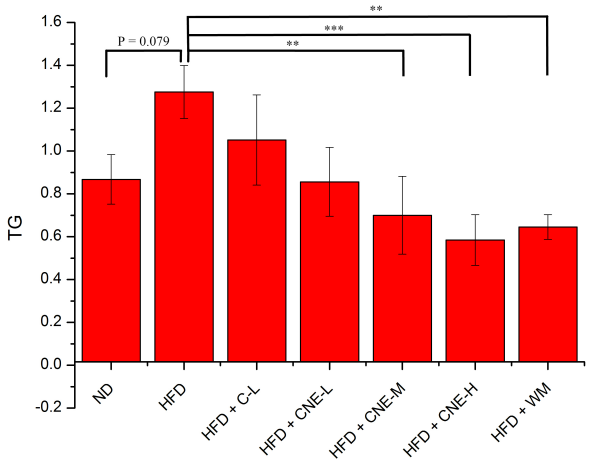
TG
1.6
1.4
1.2
1.0
0.8
0.6
0.4
0.2
0.0
-0.2
P = 0.079
**
***
**
ND
HFD
HFD + C-L
HFD + CNE-L
HFD + CNE-M
HFD + CNE-H
HFD + WM

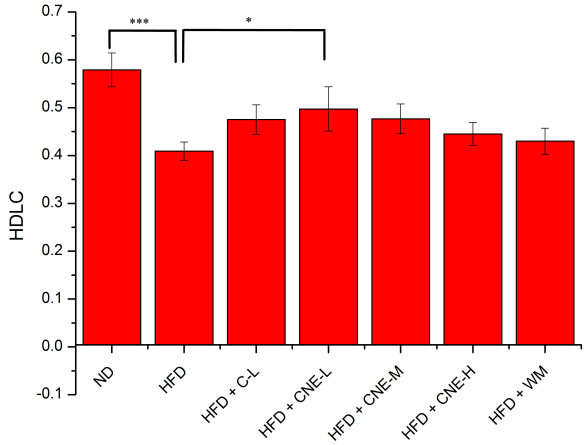
HDLC
0.7
0.6
0.5
0.4
0.3
0.2
0.1
0.0
-0.1
***
*
ND
HFD
HFD + C-L
HFD + CNE-L
HFD + CNE-M
HFD + CNE-H
HFD + WM

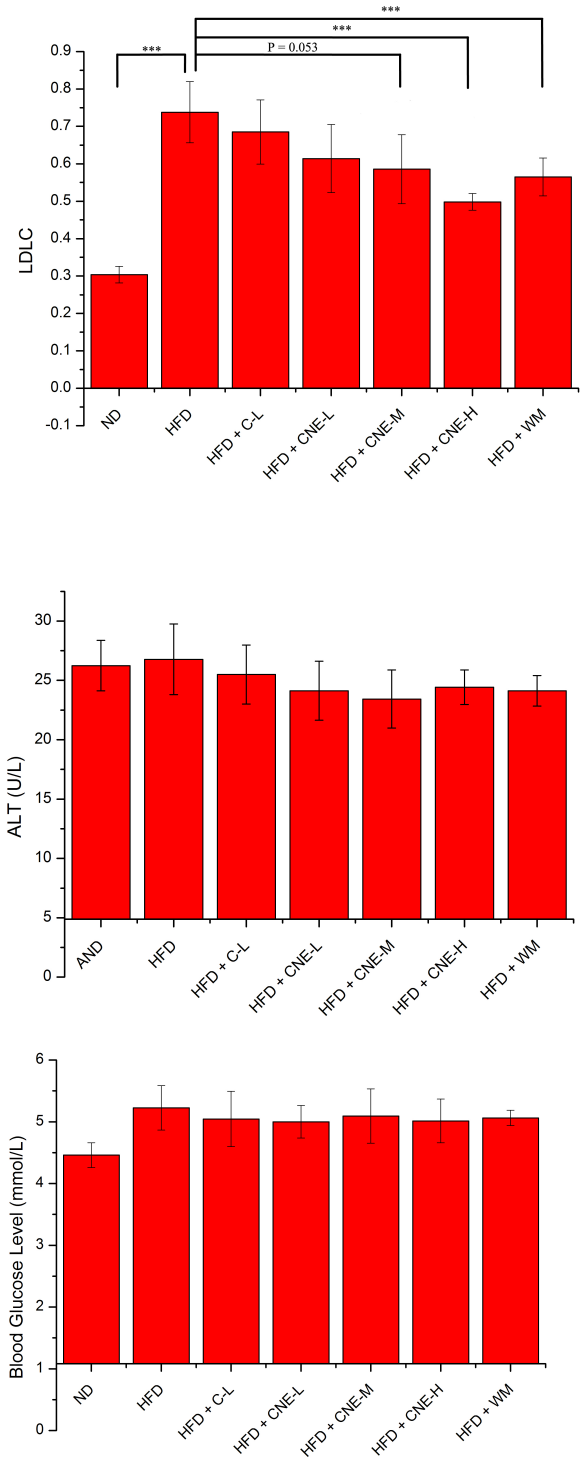


**Figure 25.** The serum lipid levels of TC, TG, LDLC, HDLC, ALT activity and blood glucose level in each group after 7-weeks treatment in male SD rats. Data are presented

as the mean value ± SE (n = 8): (∗) P < 0.05, (∗∗) P < 0.01, and (∗∗∗) P < 0.001 versus HFD; all error bars, SE.

*Inhibitory Effects of C-NE on Diet-Induced Hepatic Steatosis.*

The weight of rat liver tissue in each group was measured after the 7-week experiment. According to Fig. 26 A, rats treated with high energy diets had 39.9% increases in the liver weight than that of rats fed by normal diets. In comparison with HFD, medium doses (60 mg/kg) and high doses (90 mg/kg) of C-NE could reduce the liver weight by10.3% and 13.2% with significance. Additionally, we observed the appearance of rat liver in each group, among which the HFD, ND and HFD + high doses of C-NE groups were compared and presented in Fig. 26 B. Rats fed by HFD showed an enlarged liver size with pale color, while rats treated with high doses of C-NE showed a reduced liver size and light red color. Even though the appearances of rat livers in C-NE groups were not as healthy as those in normal diet group, the results above could indicate that high doses of C-NE had an inhibitory effects on diet-induced fatty liver, which were represented by decreased liver weight and size.

The histological sections of liver tissues in seven groups were also observed under microscope. As was shown in Fig. 26 C, cytoplasmic swelling and vacuolation of hepatocytes was most obvious in HFD group, followed by CAP group, which indicated an accumulation of intracellular lipid oil droplets. 30 mg/kg of C-NEs resulted in ameliorated vacoulation of hepatocytes compared with same dose of CAP water suspensions, confirming a better effect in suppressing intracellular lipid droplets of C-NE

than free CAP. As doses of C-NE increased, the amount of lipid droplets gradually reduced, suggesting that C-NE could alleviate diet-induced hepatic steatosis in a dose-dependent manner.

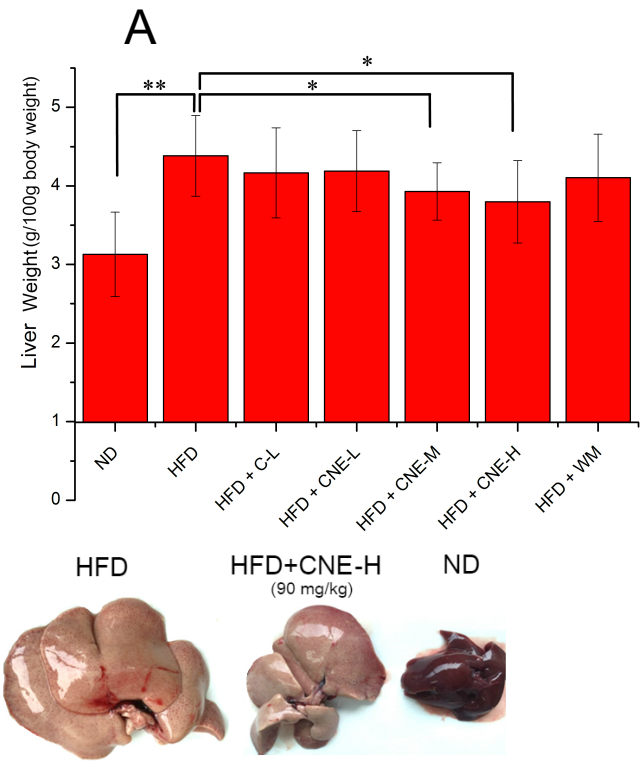


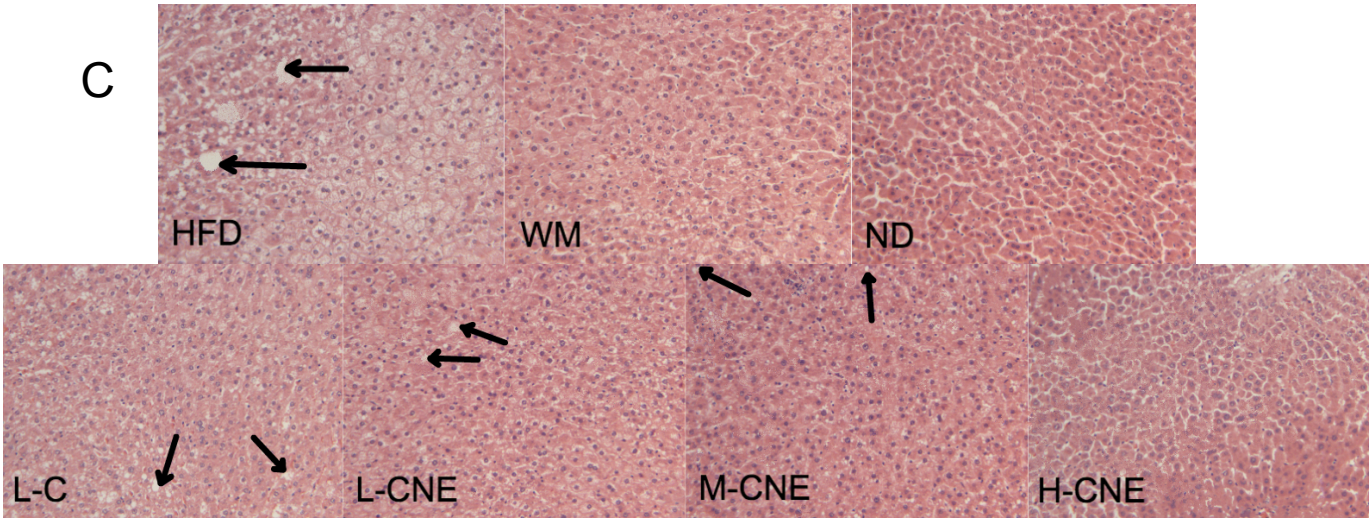

**Figure 26.** Chronic oral treatment of CAP and C-NE reduced HFD-induced hepatic steatosis in male SD rats: (A) liver weight of each group (g/100g body weight); (B) Liver samples of HFD group, high doses (90 mg/kg) C-NE group, and normal diet group; (C) liver tissues stained with hematoxylin and eosin (H&E) in each group after treatment for 7 weeks (white areas in hepatocytes are intracellular lipid droplets). Data are presented as the mean value ± SE (n = 8): (∗) $P < 0.05$, (∗∗) $P < 0.01$, and (∗∗∗) $P < 0.001$ versus HFD; all error bars, SE.

*C-NE Reduced Rats Adipose Tissue Mass and Adipocyte Size.*

Previous studies on anti-obesity effect of CAP had demonstrated its inhibitory effect on adipogenesis in 3T3-L1 preadipocytes and adipocytes (*180*). As shown in Figure 5A and B, the treatment of CAP and C-NE limited the HFD-induced weight gain in epididymal adipose tissues and retroperitoneal adipose tissues. Group fed with high doses of C-NE was most effective than other experimental groups in reducing the epididymal fat mass by 18.9% and retroperitoneal fat mass by 20.0%. Histological analysis of epididymal fat tissues indicated that both CAP and C-NE could reduce adipocyte size (Figure 5C). In addition, we measured the number of adipocytes by counting nuclei in microscopic fields selected at random in each group and found that the number of nuclei per field of C-NE groups at 30, 60 and 90 mg/kg doses were significantly more than that of HFD group (Figure 5D), revealing that C-NE played an important role in reducing HFD-induced adipocytes mass and size. The number of adipocytes became higher with the increase of C-NE doses, implying that C-NE exerted dose dependent effects in controlling HFD-induced adipocytes hypertrophy.

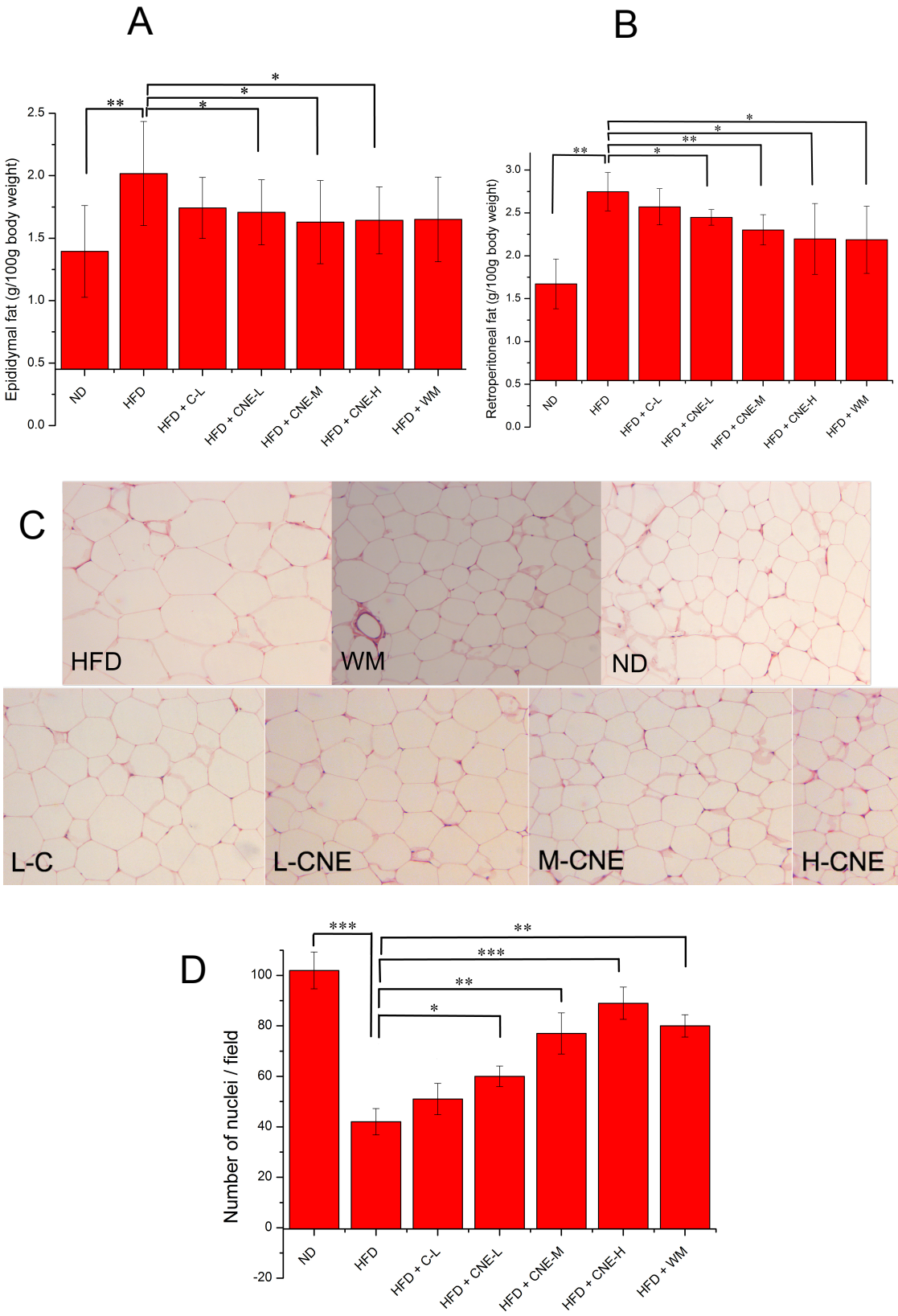
A
B
Epididymal fat (g/100g body weight)
Retroperitoneal fat (g/100g body weight)
ND
HFD
HFD + C-L
HFD + CNE-L
HFD + CNE-M
HFD + CNE-H
HFD + WM
C
HFD
WM
ND
L-C
L-CNE
M-CNE
H-CNE
D
Number of nuclei / field

**Figure 27.** Chronic oral treatment of CAP and C-NE decreased HFD-induced white adipose tissue mass (WAT) and adipocyte size in male SD rats: (A) Epididymal fat mass of each group (g/100g body weight); (B) Retroperitoneal fat mass of each group (g/100g body weight) (C) epididymal fat tissues stained with hematoxylin and eosin (H&E) in each group after treatment for 7 weeks. (D) The number of nuclei in microscopic fields selected at random from H&E stained sections in each group. Data are presented as the mean value ± SE (n = 8): (∗) $P < 0.05$, (∗∗) $P < 0.01$, and (∗∗∗) $P < 0.001$ versus HFD; all error bars, SE.

*C-NE Alleviated Gastric Mucosa Irritations Caused by CAP.*

The gastro-protective effect of C-NE was examined by histological analysis of gastric mucosa in each group after seven-week experiment. For rats fed with free CAP water suspension at dose of 30 mg/kg, the inflammatory cell infiltration was clearly observed in rat gastric mucosa, represented by accumulations of erythrocytes and leukocytes (Fig. 28, L-C (1)). Rupture of membranes can also be seen in Fig. 28, L-C (2). However, for other groups, which were given distilled water (HFD, ND groups), C-NE at different doses (30, 60, 90 mg/kg), and wall material of C-NE, respectively, neither infiltration of inflammatory cells nor folds of mucous membranes was seen in histological sections of gastric mucosa. Results above indicated that C-NE could alleviate the irritations in rat stomach tissues induced by CAP. Also, wall materials of C-NE would not cause irritations in stomach.

The ameliorated gastric mucosa irritations of C-NE could be explained by the fact that

CAP compound was encapsulated within the nanoemulsion system, thereby reducing the chances of CAP getting in direct contact with stomach tissues. Additionally, C-NE would be digested into micelles with decreased droplet sizes (≈13 nm, according to an *in-vitro* lipolysis experiment) after the lipid hydrolysis in the stomach by gastric lipase, limiting the mucosal inflammation caused by large CAP crystals. As C-NE passed through the gastrointestinal tract, the CAP-containing lipid droplets may attach to the surface of alimentary canal, preventing the sudden release of CAP compound with an extended retention time. Therefore, the gastro-protective effect of C-NE was confirmed.

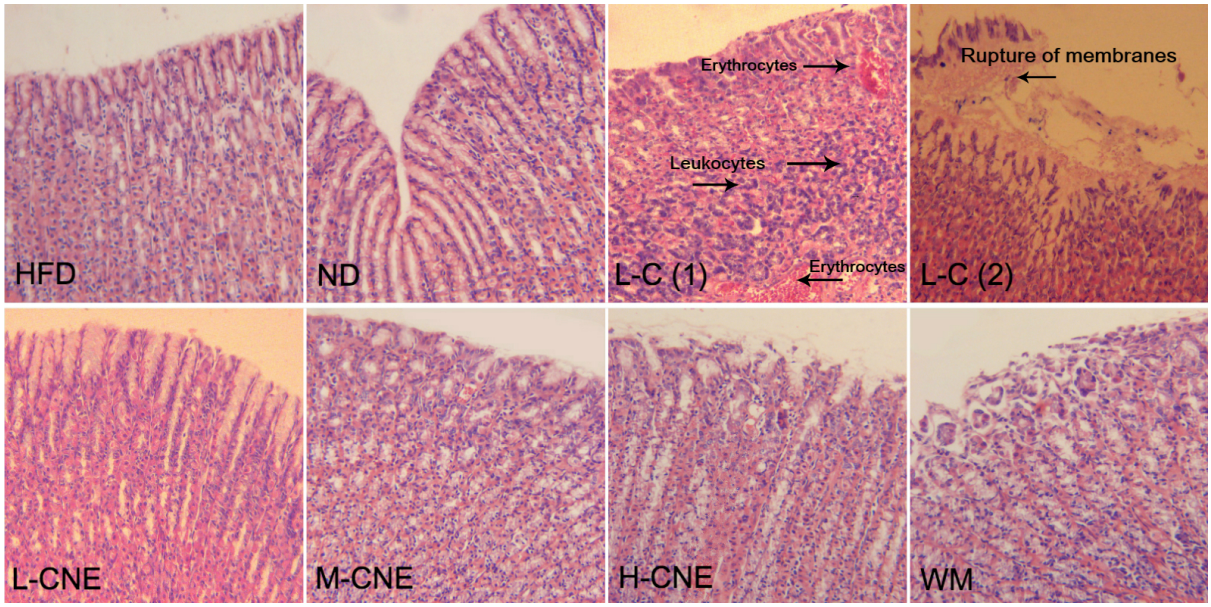


**Figure 28.** Histological tissues of gastric mucosa stained with hematoxylin and eosin (H&E) in each group.

## CONCLUSION

In this study, the anti-obesity effects of CAP-loaded nanoemulsion (C-NE) were analyzed in the aspect of body weight, serum lipid levels, and relative organ weight in male SD

rats. C-NE demonstrated an enhanced effect in controlling the HFD-induced weight gain compared to free unformulated CAP water suspensions. MCT, which was contained in the wall material of C-NE, might work synergistically with CAP as a weight-loss agent due to its ability to increase fat oxidation and energy expenditure. Serum biochemical evaluations showed that C-NE had an anti-hyperlipidemic potential with low toxicity for rats. Histological sections of liver and adipose tissues proved the inhibitory activity of C-NE on HFD-induced hepatic steatosis and adipocytes hypertrophy, which was effective in a dose-dependent manner. Gastric mucosa irritation test showed that C-NE alleviated the inflammations in rat stomach tissues caused by CAP.

# SUMMARY AND FUTURE WORK

Encapsulation and control-release of functional food or nutraceuticals has become a very important application of food nanotechnology. Many isolated compounds from food-grade natural products were proved to have beneficial functionalities for human health, including anti-obesity, anti-oxidation and anti-cancer activities. However, there exist various limiting factors, such as low water solubility and low bioavailability of bioactive compound, which hinder its absorption and bio-transformation *in vivo* and therefore, weakening the beneficial bioactivities of nutraceuticals. Through the use of novel processing methods (i.e. wet-milling technique, spray & freeze drying process) and application of nanoemulsion systems, the bioavailability of nutraceuticals is expected to be enhanced.

In this work, the novel processing method of wet-milling technique was used to reduce the particle sizes of quercetin crystals and increase its stability as well as dissolution rates. Through this process, we have learned some basic processing methods in the field of food nanotechnology and their effects in improving the physiochemical characteristics of active food ingredients. Also, an oil-in-water nanoemulsion system was developed and applied to enhance the dissolution and bioaccessibility of capsaicin. The capsaicin-loaded nanoemulsion had an increased loading percentage of capsaicin compared with previously-reported formulation systems, which was 80.4 mg/mL with mean droplet sizes of 167.9 ± 0.3 nm as determined by dynamic light scattering. Animal studies further proved that this CAP-loaded nanoemulsion had an enhanced anti-obesity effect for male SD rats fed with high energy diet. Histological evaluations proved its inhibitory activity

on HFD-induced hepatic steatosis and adipocytes hypertrophy in a dose-dependent manner. Furthermore, this emulsion can mitigate both the acute and chronic gastric mucosa irritation caused by capsaicin crystals, showing that CAP-loaded nanoemulsion has a potential to be further developed into multifunctional beverages with anti-obesity effects, though it may require thorough toxicity analysis before its broader applications in food industry.

This study helps us better understand the relationship between physiochemical properties of a compound (such as particle sizes and dissolution rates) and biological characteristics (such as bioaccessibility and bioavailability). In addition, we can gain knowledge about the digestion routes, metabolism and the underlying mechanisms of water-insoluble nutraceuticals through oral administrations. This work can also offer new horizons for food industry to develop multi-functional foods using novel delivery systems for nutraceuticals. In the meantime, there are still lots of research work needed to be done in the future. Firstly, we need to study the mechanisms underlying the enhanced anti-obesity of CAP-loaded nanoemulsions. After the absorption, distribution and metabolism process, it remains to be discovering how orally-administrated CAP-loaded nanoemulsion can interact with gut microbiota and how their metabolites influence the modulation of the gut microbiota composition. Additionally, we want to know if other beneficial biofunctions of capsaicin are enhanced in this developed nanoemulsion system, for example, anti-cancer activities and cardioprotevtive effects, etc. To expand our study, we could further apply this nanoemulsion system to other bioactive compounds with similar physiochemical properties and determine if the system would enhance their

bioavailability or if new limiting factors exist. In this way, we can develop a more effective and safe encapsulation system for oral delivery of nutraceuticals to better promote human health.

# REFERENCES


1. C., S., Prioritizing molecules based on physicochemical characteristics. *Am. Pharm. Rev.* **2006,** *9*, 60-67.
2. Kakran, M.; Shegokar, R.; Sahoo, N. G.; Shaal, L. A.; Li, L.; Muller, R. H., Fabrication of quercetin nanocrystals: comparison of different methods. *Eur. J. Pharm. Sci.* **2012,** *80*, 113-21.
3. Niwa, T.; Danjo, K., Design of self-dispersible dry nanosuspension through wet milling and spray freeze-drying for poorly water-soluble drugs. *Eur J Pharm Sci* **2013,** *50*, 272-81.
4. Functional Foods: Opportunities and Challenges. *Institute of Food Technologists* **2005**.
5. Daniells, S., US Functional food market up 31% since 2006, says new report. *Leatherhead Food Research* **2011**.
6. Definition and classification of Drug or Pharmaceutical Regulatory aspects of drug approval. *J. Pharm. Pharmacol* **2013**.
7. Chitindingu, K.; Benhura, M. A. N.; Muchuweti, M., In vitro bioaccessibility assessment of phenolic compounds from selected cereal grains: A prediction tool of nutritional efficiency. *Food sci. technol.* **2015,** *63*, 575-581.
8. CHM Versantvoort, E. v. d. K., CJM Rompelberg, Development and applicability of an in vitro digestion model in assessing the bioaccessibility of contaminants from food. *RIVM* **2004**, 87.
9. Christopher J.H. Porter, W. N. C., Intestinal lymphatic drug transport an update. *Adv. Drug Deliv. Rev.* **2001,** *50*, 61-80.
10. Ting, Y.; Jiang, Y.; Ho, C.-T.; Huang, Q., Common delivery systems for enhancing in vivo bioavailability and biological efficacy of nutraceuticals. *J Funct Foods.* **2014,** *7*, 112-128.
11. McClements, D. J., Emulsion design to improve the delivery of functional lipophilic components. *Annu Rev Food Sci Technol* **2010,** *1*, 241-69.
12. Anders Lindahl, A.-L. U., Lars Knutson, and Hans Lennernas, Characterization of fluids from the stomach and proximal jejunum in men and women. *Pharm Res*

**1997,** *14*, 497-502.

13. Dabak, T. K.; Sertkaya, O.; Acar, N.; Donmez, B. O.; Ustunel, I., The Effect of Phospholipids (Surfactant) on Adhesion and Biomechanical Properties of Tendon: A Rat Achilles Tendon Repair Model. *Biomed Res Int* **2015,** *2015*, 689314.
14. Maswadeh, H. M.; Aljarbou, A. N.; Alorainy, M. S.; Alsharidah, M. S.; Khan, M. A., Etoposide incorporated into camel milk phospholipids liposomes shows increased activity against fibrosarcoma in a mouse model. *Biomed Res Int* **2015,** *2015*, 743051.
15. Koynova, R.; Tenchov, B., Recent progress in liposome production, relevance to drug delivery and nanomedicine. *Recent Pat Nanotechnol* **2015,** *9*, 86-93.
16. Marczylo, T. H.; Verschoyle, R. D.; Cooke, D. N.; Morazzoni, P.; Steward, W. P.; Gescher, A. J., Comparison of systemic availability of curcumin with that of curcumin formulated with phosphatidylcholine. *Cancer Chemother Pharmacol* **2007,** *60*, 171-177.
17. Pietta, P.; Simonetti, P.; Gardana, C.; Brusamolino, A.; Morazzoni, P.; Bombardelli, E., Relationship between rate and extent of catechin absorption and plasma antioxidant status. *Biochem Mol Biol Int* **1998,** *46*, 895-903.
18. Choi, A. Y.; Kim, C. T.; Park, H. Y.; Kim, H. O.; Lee, N. R.; Lee, K. E.; Gwak, H. S., Pharmacokinetic Characteristics of Capsaicin-Loaded Nanoemulsions Fabricated with Alginate and Chitosan. *J. Agric. Food Chem.* **2013,** *61*, 2096-2102.
19. Bricarello, D. A.; Pan, Y.; Nitin, N., Interactions Between the Lipid Core and the Phospholipid Interface in Emulsions and Solid Lipid Nanoparticles. *Food Biophys* **2015**.
20. R.H. Muller , M. R., S.A. Wissing, Solid lipid nanoparticles (SLN) and nanostructured lipid carriers (NLC) in cosmetic and dermatological preparations. *Adv. Drug Deliv. Rev.* **2002,** *54*, 131-155.
21. Yu, H.; Huang, Q., Improving the oral bioavailability of curcumin using novel organogel-based nanoemulsions. *J. Agric. Food. Chem.* **2012,** *60*, 5373-5379.
22. Ma, N.; Lai, C.-S.; Chung, C.-H.; Yang, J.-M.; Hsu, K.-C.; Chen, C.-Y.; Chung, T.-S.; Li,

S.; Ho, C.-T.; Pan, M.-H., 5-Demethyltangeretin is more potent than tangeretin in inhibiting dimethylbenz(a)anthracene (DMBA)/12-O-tetradecanoylphorbol-13-acetate (TPA)-induced skin tumorigenesis. *J Funct Foods* **2014,** *11*, 528-537.

23. Chiou, Y. S.; Ma, N. J.; Sang, S.; Ho, C. T.; Wang, Y. J.; Pan, M. H., Peracetylated (-)-epigallocatechin-3-gallate (AcEGCG) potently suppresses dextran sulfate sodium-induced colitis and colon tumorigenesis in mice. *J Agric Food Chem* **2012,** *60*, 3441-51.
24. Janssens, S.; Anne, M.; Rombaut, P.; Van den Mooter, G., Spray drying from complex solvent systems broadens the applicability of Kollicoat IR as a carrier in the formulation of solid dispersions. *Eur J Pharm Sci* **2009,** *37*, 241-8.
25. Wang, Q.; Zhang, J.; Wang, A., Freeze-drying: A versatile method to overcome re-aggregation and improve dispersion stability of palygorskite for sustained release of ofloxacin. *Appl Clay Sci* **2014,** *87*, 7-13.
26. Jacobs, H.; Moalin, M.; van Gisbergen, M. W.; Bast, A.; van der Vijgh, W. J.; Haenen, G. R., An essential difference in the reactivity of the glutathione adducts of the structurally closely related flavonoids monoHER and quercetin. *Free Radic Biol Med* **2011,** *51*, 2118-23.
27. Azuma, K.; Ippoushi, K.; Terao, J., Evaluation of tolerable levels of dietary quercetin for exerting its antioxidative effect in high cholesterol-fed rats. *Food Chem Toxicol* **2010,** *48*, 1117-22.
28. Ramos, A. A.; Lima, C. F.; Pereira, M. L.; Fernandes-Ferreira, M.; Pereira-Wilson, C., Antigenotoxic effects of quercetin, rutin and ursolic acid on HepG2 cells: evaluation by the comet assay. *Toxicol Lett* **2008,** *177*, 66-73.
29. Jeyadevi, R.; Sivasudha, T.; Rameshkumar, A.; Ananth, D. A.; Aseervatham, G. S.; Kumaresan, K.; Kumar, L. D.; Jagadeeswari, S.; Renganathan, R., Enhancement of anti arthritic effect of quercetin using thioglycolic acid-capped cadmium telluride quantum dots as nanocarrier in adjuvant induced arthritic Wistar rats. *Colloids Surf B Biointerfaces* **2013,** *112*, 255-63.
30. Kleemann, R.; Verschuren, L.; Morrison, M.; Zadelaar, S.; van Erk, M. J.; Wielinga, P. Y.; Kooistra, T., Anti-inflammatory, anti-proliferative and anti-atherosclerotic

effects of quercetin in human in vitro and in vivo models. *Atherosclerosis* **2011,** *218*, 44-52.

31. Bagad, M.; Khan, Z. A., Poly(n-butylcyanoacrylate) nanoparticles for oral delivery of quercetin: preparation, characterization, and pharmacokinetics and biodistribution studies in Wistar rats. *Int J Nanomedicine* **2015,** *10*, 3921-35.
32. Asnin, L.; Park, S. W., Isolation and analysis of bioactive compounds in Capsicum peppers. *Crit. Rev. Food Sci. Nutr.* **2015,** *55*, 254-89.
33. Zewdie, Y.; Bosland, P. W., Capsaicinoid profiles are not good chemotaxonomic indicators for Capsicum species. *Biochem. Syst. Ecol.* **2001,** *29*, 161-169.
34. Barbero, G. F.; Liazid, A.; Azaroual, L.; Palma, M.; Barroso, C. G., Capsaicinoid Contents in Peppers and Pepper-Related Spicy Foods. *Int. J. Food Prop.* **2015,** *19*, 485-493.
35. Thiele, R.; Mueller-Seitz, E.; Petz, M., Chili Pepper Fruits: Presumed Precursors of Fatty Acids Characteristic for Capsaicinoids. *J. Agric. Food Chem.* **2008,** *56*, 4219-4224.
36. Rollyson, W. D.; Stover, C. A.; Brown, K. C.; Perry, H. E.; Stevenson, C. D.; McNees, C. A.; Ball, J. G.; Valentovic, M. A.; Dasgupta, P., Bioavailability of capsaicin and its implications for drug delivery. *J control release* **2014**.
37. Jang, J. J.; Kim, S. H.; Yun, T. K., Inhibitory effect of capsaicin on mouse lung tumor development. *In Vivo* **1989,** *3*, 49-54.
38. Mori, A.; Lehmann, S.; O'Kelly, J.; Kumagai, T.; Desmond, J. C.; Pervan, M.; McBride, W. H.; Kizaki, M.; Koeffler, H. P., Capsaicin, a component of red peppers, inhibits the growth of androgen-independent, p53 mutant prostate cancer cells. *Cancer Res.* **2006,** *66*, 3222-3229.
39. Kwang-Kyun Park, Y.-J. S., Effects of capsaicin on chemically-induced two-stage mouse skin carcinogenesis *Cancer Lett* **1997,** *114*, 183-184.
40. Tanaka, T.; Kohno, H.; Sakata, K.; Yamada, Y.; Hirose, Y.; Sugie, S.; Mori, H., Modifying effects of dietary capsaicin and rotenone on 4-nitroquinoline 1-oxide-induced rat tongue carcinogenesis. *Carcinogenesis* **2002,** *23*, 1361-1367.
41. Gilardini Montani, M. S.; D'Eliseo, D.; Cirone, M.; Di Renzo, L.; Faggioni, A.;

Santoni, A.; Velotti, F., Capsaicin-mediated apoptosis of human bladder cancer cells activates dendritic cells via CD91. *Nutrition* **2015,** *31*, 578-81.

42. F. Ziglioli, A. F., U. Maestroni, F. Dinale, et al., Vanilloid-mediated apoptosis in prostate cancer cells through a TRPV-1 dependent and a TRPV-1-independent mechanism. *Acta Biomedica* **2009,** *80*, 7.
43. Seonhoe Kim, A. M., Capsaicin-induced apoptosis of H-ras-transformed human breast epithelial cells is Rac-dependent via ROS generation. *Arch Pharm Res* **2004,** *27*, 845-849.
44. Oh, S. H.; Lim, S. C., Endoplasmic reticulum stress-mediated autophagy/apoptosis induced by capsaicin (8-methyl-N-vanillyl-6-nonenamide) and dihydrocapsaicin is regulated by the extent of c-Jun NH2-terminal kinase/extracellular signal-regulated kinase activation in WI38 lung epithelial fibroblast cells. *J Pharmacol Exp Ther* **2009,** *329*, 112-22.
45. Brown, K. C.; Witte, T. R.; Hardman, W. E.; Luo, H.; Chen, Y. C.; Carpenter, A. B.; Lau, J. K.; Dasgupta, P., Capsaicin displays anti-proliferative activity against human small cell lung cancer in cell culture and nude mice models via the E2F pathway. *PLoS One* **2010,** *5*, e10243.
46. Srinivasan, K.; Sambaiah, K.; Chandrasekhara, N., Spices as Beneficial Hypolipidemic Food Adjuncts: A Review. *Food Rev. Int.* **2004,** *20*, 187-220.
47. Amichand Dairam, R. F., Santy Daya, And Janice L. Limson, Antioxidant and Iron-Binding Properties of Curcumin, Capsaicin, and S-Allylcysteine Reduce Oxidative Stress in Rat Brain Homogenate. *J. Agric. Food Chem.* **2008,** *56*, 3350-3356.
48. Manjunatha, H.; Srinivasan, K., Hypolipidemic and antioxidant effects of curcumin and capsaicin in high-fat-fed rats. *Can J Physiol Pharmacol* **2007,** *85*, 588-96.
49. Kiran D. K. Ahuja, D. A. K., Madeleine J. Ball, And Dominic P. Geraghty, Effects of Capsaicin, Dihydrocapsaicin, and Curcumin on Copper-Induced Oxidation of Human Serum Lipids. *J Agric Food Chem* **2006,** *54*, 6436-6439.
50. Chen, K. S.; Chen, P. N.; Hsieh, Y. S.; Lin, C. Y.; Lee, Y. H.; Chu, S. C., Capsaicin protects endothelial cells and macrophage against oxidized low-density

lipoprotein-induced injury by direct antioxidant action. *Chem Biol Interact* **2015,** *228*, 35-45.

51. Lee, C. Y.; Kim, M.; Yoon, S. W.; Lee, C. H., Short-term control of capsaicin on blood and oxidative stress of rats in vivo. *Phytother Res* **2003,** *17*, 454-8.
52. Bencsik, P.; Kupai, K.; Giricz, Z.; Gorbe, A.; Huliak, I.; Furst, S.; Dux, L.; Csont, T.; Jancso, G.; Ferdinandy, P., Cardiac capsaicin-sensitive sensory nerves regulate myocardial relaxation via S-nitrosylation of SERCA: role of peroxynitrite. *Br J Pharmacol* **2008,** *153*, 488-96.
53. Hassan, M. H.; Edfawy, M.; Mansour, A.; Hamed, A. A., Antioxidant and antiapoptotic effects of capsaicin against carbon tetrachloride-induced hepatotoxicity in rats. *Toxicol Ind Health* **2012,** *28*, 428-38.
54. Lorna Mason, R. A. M., Sheena Derry, Jayne E Edwards, Henry J McQuay, Systematic review of topical capsaicin for the treatment of chronic pain. *BMJ* **2004,** *328*, 991-994.
55. Holzer, P., Capsaicin: Cellular Targets, Mechanisms of Action, and Selectivity for Thin Sensory Neurons. *Pharma Rev* **1991,** *43*, 143-201.
56. Baamonde, A.; Lastra, A.; Juarez, L.; Hidalgo, A.; Menendez, L., TRPV1 desensitisation and endogenous vanilloid involvement in the enhanced analgesia induced by capsaicin in inflamed tissues. *Brain Res Bull* **2005,** *67*, 476-81.
57. O'Neill, J.; Brock, C.; Olesen, A. E.; Andresen, T.; Nilsson, M.; Dickenson, A. H., Unravelling the mystery of capsaicin: a tool to understand and treat pain. *Pharma Rev* **2012,** *64*, 939-71.
58. Hayman, M.; Kam, P. C. A., Capsaicin: A review of its pharmacology and clinical applications. *Curr Anaesth Crit Care* **2008,** *19*, 338-343.
59. Olah, Z.; Szabo, T.; Karai, L.; Hough, C.; Fields, R. D.; Caudle, R. M.; Blumberg, P. M.; Iadarola, M. J., Ligand-induced dynamic membrane changes and cell deletion conferred by vanilloid receptor 1. *J Biol Chem* **2001,** *276*, 11021-30.
60. Jones, W. K.; Fan, G. C.; Liao, S.; Zhang, J. M.; Wang, Y.; Weintraub, N. L.; Kranias, E. G.; Schultz, J. E.; Lorenz, J.; Ren, X., Peripheral nociception associated with surgical incision elicits remote nonischemic cardioprotection via neurogenic

activation of protein kinase C signaling. *Circulation* **2009,** *120*, S1-9.

61. Tremarin Cda, S.; Casali, K. R.; Meurer, L.; Schaan, B. D., Capsaicin-induced metabolic and cardiovascular autonomic improvement in an animal model of the metabolic syndrome. *Br J Nutr* **2014,** *111*, 207-14.
62. Gross ER, H. A., Gross GJ, Mochly-Rosen D, Acute capsaicin treatment reduces myocardial infarct size in rats via the transient receptor potential vallinoid 1 channel. *Curr Anaesth Crit Care* **2010,** *25*.
63. Ma, L.; Zhong, J.; Zhao, Z.; Luo, Z.; Ma, S.; Sun, J.; He, H.; Zhu, T.; Liu, D.; Zhu, Z.; Tepel, M., Activation of TRPV1 reduces vascular lipid accumulation and attenuates atherosclerosis. *Cardiovasc Res* **2011,** *92*, 504-13.
64. Wahlqvist, M. L., Wattanapenpaiboon, N., Hot foods–unexpected help with energy balance? *Lancet* **2001,** *358*, 348–349.
65. Leung, F. W., Capsaicin-sensitive intestinal mucosal afferent mechanism and body fat distribution. *Life Sci.* **2008,** *83*, 1-5.
66. Luo, X. J.; Peng, J.; Li, Y. J., Recent advances in the study on capsaicinoids and capsinoids. *Eur. J. Pharmacol.* **2011,** *650*, 1-7.
67. Joo, J. I.; Kim, D. H.; Choi, J. W.; Yun, J. W., Proteomic Analysis for Antiobesity Potential of Capsaicin on White Adipose Tissue in Rats Fed with a High Fat Diet. *J. Proteome Res.* **2009,** *9*, 2977-2987.
68. Lu, M.; Cao, Y.; Ho, C. T.; Huang, Q., Development of Organogel-Derived Capsaicin Nanoemulsion with Improved Bioaccessibility and Reduced Gastric Mucosa Irritation. *J. Agric. Food Chem.* **2016,** *64*, 4735-4741.
69. 69. Tan, S.; Gao, B.; Tao, Y.; Guo, J.; Su, Z. Q., Antiobese effects of capsaicin-chitosan microsphere (CCMS) in obese rats induced by high fat diet. *J Agric Food Chem* **2014,** *62*, 1866-74.
70. Zhu, Y.; Zhang, J.; Zheng, Q.; Wang, M.; Deng, W.; Li, Q.; Firempong, C. K.; Wang, S.; Tong, S.; Xu, X.; Yu, J., In vitro and in vivo evaluation of capsaicin-loaded microemulsion for enhanced oral bioavailability. *J. Sci. Food Agric.* **2015,** *95*, 2678-2685.
71. Barbero, G. F.; Liazid, A.; Palma, M.; Barroso, C. G., Ultrasound-assisted extraction of capsaicinoids from peppers. *Talanta* **2008,** *75*, 1332-7.

72. Kirschbaum-Titze, P.; Hiepler, C.; Mueller-Seitz, E.; Petz, M., Pungency in Paprika (Capsicum annuum). 1. Decrease of Capsaicinoid Content Following Cellular Disruption. *J. Agric. Food Chem.* **2002,** *50*, 1260-1263.
73. Contreras-Padilla, M.; Yahia, E. M., Changes in Capsaicinoids during Development, Maturation, and Senescence of Chile Peppers and Relation with Peroxidase Activity. *J. Agric. Food Chem.* **1998,** *46*, 2075-2079.
74. Santamaria, R. I.; Reyes-Duarte, M. D.; Barzana, E.; Fernando, D.; Gama, F. M.; Mota, M.; Lopez-Munguıa, A., Selective Enzyme-Mediated Extraction of Capsaicinoids and Carotenoids from Chili Guajillo Puya (*Capsicum annuum* L.) Using Ethanol as Solvent. *J. Agric. Food Chem.* **2000,** *48*, 3063-3067.
75. Williams, O. J.; Viyaya-Raghavan, G. S.; Orsat, V.; Dai, J. M., Microwave-assisted extraction of capsaicinoids from capsicum fruit. *J. Food Biochem.* **2004,** *28*, 113-122.
76. Karnka, R.; Rayanakorn, M.; Watanesk, S.; Vaneesorn, Y., Optimization of high-performance liquid chromatographic parameters for the determination of capsaicinoid compounds using the simplex method. *Anal. Sci.* **2002,** *18*, 661-665.
77. Korel, F.; Bagdatlioglu, N.; Balaban, M. O.; Hisil, Y., Ground red peppers-Capsaicinoids content, scoville scores, and discrimination by an electronic nose. *J. Agric. Food Chem.* **2002,** *50*, 3257-3261.
78. Daood, H. G.; Illés, V.; Gnayfeed, M. H.; Mészáros, B.; Horváth, G.; Biacs, P. A., Extraction of pungent spice paprika by supercritical carbon dioxide and subcritical propane. *J. Supercrit. Fluids* **2002,** *23*, 143-152.
79. Chen, J. H.; Wang, F. M.; Liu, J.; Lee, F. S.-C.; Wang, X. R.; Yang, H. H., Analysis of alkaloids in Coptis chinensis Franch by accelerated solvent extraction combined with ultra performance liquid chromatographic analysis with photodiode array and tandem mass spectrometry detections. *Anal.Chim. Acta* **2008,** *613*, 184-195.
80. Domínguez, H.; Núñez, M. J.; Lema, J. M., Enzymatic pretreatment to enhance oil extraction from fruits and oilseeds: a review. *Food Chem.* **1994,** *49*, 271-286.
81. Desikacharya, S. S. R.; Naidu, M. M.; Sowbhagya, H. B.; Naik, J. P.; Krishnamurthy,

N., Process of extracting chili (Capsicum) oleoresin. *U.S. Patent Application 20040191364 A1* **2004**.

82. Salgado-Roman, M.; Botello-Alvarez, E.; Rico-Martinez, R.; Jimenez-Islas, H.; Cardenas-Manriquez, M.; Navarrete-Bolanos, J. L., Enzymatic Treatment To Improve Extraction of Capsaicinoids and Carotenoids from Chili (Capsicum annuum) Fruits. *J. Agric. Food Chem.* **2008,** *56*, 10012-10018.
83. Boonkird, S.; Phisalaphong, C.; Phisalaphong, M., Ultrasound-assisted extraction of capsaicinoids from Capsicum frutescens on a lab- and pilot-plant scale. *Ultrason. Sonochem.* **2008,** *15*, 1075-1079.
84. Bajer, T.; Bajerová, P.; Kremr, D.; Eisner, A.; Ventura, K., Central composite design of pressurised hot water extraction process for extracting capsaicinoids from chili peppers. *J. Food Compost. Anal.* **2015,** *40*, 32-38.
85. Liu, A.; Han, C.; Zhou, X.; Zhu, Z.; Huang, F.; Shen, Y., Determination of three capsaicinoids in Capsicum annuum by pressurized liquid extraction combined with LC-MS/MS. *J. Sep. Sci.* **2013,** *36*, 857-862.
86. Sharif, K. M.; Rahman, M. M.; Azmir, J.; Mohamed, A.; Jahurul, M. H. A.; Sahena, F.; Zaidul, I. S. M., Experimental design of supercritical fluid extraction – A review. *J. Food Eng.* **2014,** *124*, 105-116.
87. Dias, A. L. B.; Arroio Sergio, C. S.; Santos, P.; Barbero, G. F.; Rezende, C. A.; Martínez, J., Effect of ultrasound on the supercritical CO2 extraction of bioactive compounds from dedo de moça pepper (Capsicum baccatum L. var. pendulum). *Ultrason. Sonochem.* **2016,** *31*, 284-294.
88. Brunner, G., Supercritical fluids: technology and application to food processing. *J. Food Eng.* **2005,** *67*, 21-33.
89. de Aguiar, A. C.; dos Santos, P.; Coutinho, J. P.; Barbero, G. F.; Godoy, H. T.; Martínez, J., Supercritical fluid extraction and low pressure extraction of Biquinho pepper (Capsicum chinense). *LWT-Food Sci. Technol.* **2014,** *59*, 1239-1246.
90. Santos, P.; Aguiar, A. C.; Barbero, G. F.; Rezende, C. A.; Martinez, J., Supercritical carbon dioxide extraction of capsaicinoids from malagueta pepper (Capsicum frutescens L.) assisted by ultrasound. *Ultrason. Sonochem.* **2015,** *22*, 78-88.

91. Kantiani, L.; Farre, M.; Grases i Freixiedas, J. M.; Barcelo, D., Development and validation of a pressurised liquid extraction liquid chromatography-electrospray-tandem mass spectrometry method for beta-lactams and sulfonamides in animal feed. *J Chromatogr A* **2010,** *1217*, 4247-4254.
92. Barbero, G. F.; Palma, M.; Barroso, C. G., Pressurized liquid extraction of capsaicinoids from pepper. *J. Agric. Food Chem.* **2006,** *54*, 3231-3236.
93. Barbero, G. F.; Palma, M.; Barroso, C. G., Determination of capsaicinoids in peppers by microwave-assisted extraction-high-performance liquid chromatography with fluorescence detection. *Anal. Chim. Acta* **2006,** *578*, 227-233.
94. Chuichulcherm, S.; Prommakort, S.; Srinophakun, P.; Thanapimmetha, A., Optimization of capsaicin purification from Capsicum frutescens Linn. with column chromatography using Taguchi design. *Ind. Crop Prod.* **2013,** *44*, 473-479.
95. Donnerer, J.; Amann, R.; Schuligoi, R.; Lembeck, F., Absorption and metabolism of capsaicinoids following intragastric administration in rats. *Naunyn Schmiedebergs Arch. Pharmacol.* **1990**, 357-361.
96. Kuzma, M.; Fodor, K.; Maasz, G.; Avar, P.; Mozsik, G.; Past, T.; Fischer, E.; Perjesi, P., A validated HPLC-FLD method for analysis of intestinal absorption and metabolism of capsaicin and dihydrocapsaicin in the rat. *J Pharm Biomed Anal* **2014,** *103C*, 59-66.
97. Halme, M.; Pesonen, M.; Salo, H.; Soderstrom, M.; Pasanen, M.; Vahakangas, K.; Vanninen, P., Comparison of in vitro metabolism and cytotoxicity of capsaicin and dihydrocapsaicin. *J. Chromatogr. B Analyt. Technol. Biomed. Life Sci.* **2016,** *1009-1010*, 17-24.
98. Suresh, D.; Srinivasan, K., Distribution and elimination of capsaicin, piperine & curcumin following oral intake in rats. *Indian J. Med. Res.* **2010,** *131*, 682-691.
99. Kawada, T.; Suzuki, T.; Takahashia, M.; Iwai, K., Gastrointestinal absorption and metabolism of capsaicin and dihydrocapsaicin in rats. *Toxicol. Appl. Pharmacol.* **1984,** *72*.

100. Chanda, S.; Bashir, M.; Babbar, S.; Koganti, A.; Bley, K., In vitro hepatic and skin metabolism of capsaicin. *Drug Metab. Dispos.* **2008,** *36*, 670-675.
101. Reilly, C. A.; Ehlhardt, W. J.; Jackson, D. A.; Kulanthaivel, P.; Mutlib, A. E.; Espina, R. J.; Moody, D. E.; Crouch, D. J.; Yost, G. S., Metabolism of Capsaicin by Cytochrome P450 Produces Novel Dehydrogenated Metabolites and Decreases Cytotoxicity to Lung and Liver Cells. *Chem. Res. Toxicol.* **2003,** *16*, 336-349.
102. Reilly, C. A.; Henion, F.; Bugni, T. S.; Ethirajan, M.; Stockmann, C.; Pramanik, K. C.; Srivastava, S. K.; Yost, G. S., Reactive intermediates produced from the metabolism of the vanilloid ring of capsaicinoids by p450 enzymes. *Chem. Res. Toxicol.* **2013,** *26*, 55-66.
103. Chaiyasit, K.; Khovidhunkit, W.; Wittayalertpanya, S., Pharmacokinetic and the effect of capsaicin in capsicum frutescens on decreasing plasma glucose level. *J Med Assoc Thai* **2009,** *92*, 108-113.
104. Viktor Nedovica, A. K., Verica Manojlovicb, Steva Levica, Branko Bugarskib, An overview of encapsulation technologies for food applications. *Procedia Food Sci* **2011,** *1*, 9.
105. Wang, J. C.; Chen, S. H.; Xu, Z. C., Synthesis and Properties Research on the Nanocapsulated Capsaicin by Simple Coacervation Method. *J Dispers Sci Technol* **2008,** *29*, 687-695.
106. Paudel, K. S.; Milewski, M.; Swadley, C. L.; Brogden, N. K.; Ghosh, P.; Stinchcomb, A. L., Challenges and opportunities in dermal/transdermal delivery. *Ther Deliv.* **2010,** *1*, 109-131.
*107.* Witting, M.; Obst, K.; Friess, W.; Hedtrich, S., Recent advances in topical delivery of proteins and peptides mediated by soft matter nanocarriers. *Biotechnol. Adv.*
108. Shakeel, F.; Shafiq, S.; Haq, N.; Alanazi, F. K.; Alsarra, I. A., Nanoemulsions as potential vehicles for transdermal and dermal delivery of hydrophobic compounds: an overview. *Expert Opin. Drug Deliv* **2012,** *9*, 953-974.
109. Peng, X.; Wen, X.; Pan, X.; Wang, R.; Chen, B.; Wu, C., Design and in vitro evaluation of capsaicin transdermal controlled release cubic phase gels. *AAPS Pharm Sci Tech* **2010,** *11*, 1405-10.
110. Kim, S. W.; Bae, Y. H.; Okano, T., Hydrogels: swelling, drug loading, and release.

*Pharma Res* **1992,** *9*, 283-290.

111. Ying-Yue Wang, C.-T. H., Wen-Ta Chiu, Jia-You Fang, In vitro and in vivo evaluations of topically applied capsaicin and nonivamide from hydrogels. *Int J Pharm* **2001,** *224*, 15.
112. Contri, R. V.; Katzer, T.; Ourique, A. F.; Da Silva, A. L. M.; Beck, R. C. R.; Pohlmann, A. R.; Guterres, S. S., Combined effect of polymeric nanocapsules and chitosan hydrogel on the increase of capsaicinoids adhesion to the skin surface. *J. Biomed. Nanotechnol.* **2014,** *10*, 820-830.
113. Brodsky, M.; Cho, J.; Fang, J.; Kim, E.; Cho, Y.; Song, M., P02.02. Efficacy of a topical 0.1% Capsaicin hydrogel patch to treat chronic neck pain: a double-blind randomized clinical trial. *BMC Complement Altern Med* **2012,** *12*, 58.
114. Kulkantrakorn, K.; Lorsuwansiri, C.; Meesawatsom, P., 0.025% capsaicin gel for the treatment of painful diabetic neuropathy: a randomized, double-blind, crossover, placebo-controlled trial. *Pain Pract* **2013,** *13*, 497-503.
115. Allen Jr, L. V., Capsaicin 0.05% and Ketamine HCl 2% in Pluronic lecithin organogel. *U.S. Pharm.* **2011,** *36*.
116. Raza, K.; Singh, B.; Mahajan, A.; Negi, P.; Bhatia, A.; Katare, O. P., Design and evaluation of flexible membrane vesicles (FMVs) for enhanced topical delivery of capsaicin. *J Drug Target* **2011,** *19*, 293-302.
117. Ning, M. G., Z.; Pan, H.; Yu, H.; Xiao, K.. , Preparation and in vitro evaluation of liposomal:niosomal delivery systems for antifungal drug clotrimazole. *Indian J Exp Biol* **2005,** *43*, 7.
118. Tavano, L.; Alfano, P.; Muzzalupo, R.; de Cindio, B., Niosomes vs microemulsions: new carriers for topical delivery of Capsaicin. *Colloids Surf B Biointerfaces* **2011,** *87*, 333-9.
119. Desai, P. R.; Marepally, S.; Patel, A. R.; Voshavar, C.; Chaudhuri, A.; Singh, M., Topical delivery of anti-TNFalpha siRNA and capsaicin via novel lipid-polymer hybrid nanoparticles efficiently inhibits skin inflammation in vivo. *J Control Release* **2013,** *170*, 51-63.
120. Raza, K.; Shareef, M. A.; Singal, P.; Sharma, G.; Negi, P.; Katare, O. P., Lipid-based

capsaicin-loaded nano-colloidal biocompatible topical carriers with enhanced analgesic potential and decreased dermal irritation. *J. Liposome Res* **2014**.

121. Popescu, M.; Chiutu, L.; Mircioiu, C.; Dima, Ş., Capsaicin microemulsions: Preparation, characterization and in vitro release study. *Farmacia* **2013,** *62*, 58-68.
122. Prow, T. W.; Grice, J. E.; Lin, L. L.; Faye, R.; Butler, M.; Becker, W.; Wurm, E. M. T.; Yoong, C.; Robertson, T. A.; Soyer, H. P.; Roberts, M. S., Nanoparticles and microparticles for skin drug delivery. *Adv Drug Deliv Rev* **2011,** *63*, 470-491.
123. Kim, J. H.; Ko, J. A.; Kim, J. T.; Cha, D. S.; Cho, J. H.; Park, H. J.; Shin, G. H., Preparation of a Capsaicin-Loaded Nanoemulsion for Improving Skin Penetration. *J Agric Food Chem* **2014**.
124. Wang, J.; Zheng, X.; Chen, S., Preparation and Properties of Nanocapsulated Capsaicin by Complex Coacervation Method. *Chem Eng Commun* **2010,** *197*, 919-933.
125. Zhu, Y.; Wang, M.; Zhang, J.; Peng, W.; Firempong, C. K.; Deng, W.; Wang, Q.; Wang, S.; Shi, F.; Yu, J.; Xu, X.; Zhang, W., Improved oral bioavailability of capsaicin via liposomal nanoformulation: preparation, in vitro drug release and pharmacokinetics in rats. *Arch Pharm Res* **2014**.
126. Zhu, Y.; Peng, W.; Zhang, J.; Wang, M.; Firempong, C. K.; Feng, C.; Liu, H.; Xu, X.; Yu, J., Enhanced oral bioavailability of capsaicin in mixed polymeric micelles: Preparation, in vitro and in vivo evaluation. *J Funct Foods* **2014,** *8*, 358-366.
127. Goycoolea, F. M.; Valle-Gallego, A.; Stefani, R.; Menchicchi, B.; David, L.; Rochas, C.; Santander-Ortega, M. J.; Alonso, M. J., Chitosan-based nanocapsules: physical characterization, stability in biological media and capsaicin encapsulation. *Colloid Polym. Sci* **2012,** *290*, 1423-1434.
128. Zhu, Y.; Zhang, J.; Zheng, Q.; Wang, M.; Deng, W.; Li, Q.; Firempong, C. K.; Wang, S.; Tong, S.; Xu, X.; Yu, J., In vitro and in vivo evaluation of capsaicin-loaded microemulsion for enhanced oral bioavailability. *J. Sci. Food Agric.* **2014**.
129. Weiss, J.; Takhistov, P.; McClements, D. J., Functional Materials in Food Nanotechnology. *J Food Sci* **2006,** *71*, R107-R116.
130. Choi, A.-J.; Kim, C.-J.; Cho, Y.-J.; Hwang, J.-K.; Kim, C.-T., Characterization of

Capsaicin-Loaded Nanoemulsions Stabilized with Alginate and Chitosan by Self-assembly. *Food Bioprocess Tech* **2011,** *4*, 1119-1126.

131. Peng, W.; Jiang, X. Y.; Zhu, Y.; Omari-Siaw, E.; Deng, W. W.; Yu, J. N.; Xu, X. M.; Zhang, W. M., Oral delivery of capsaicin using MPEG-PCL nanoparticles. *Acta Pharmacol Sin* **2015,** *36*, 139-148.
132. Shaikh, J.; Bhosale, R.; Singhal, R., Microencapsulation of black pepper oleoresin. *Food Chemistry* **2006,** *94*, 105-110.
133. Sansone, F.; Picerno, P.; Mencherini, T.; Villecco, F.; D'Ursi, A. M.; Aquino, R. P.; Lauro, M. R., Flavonoid microparticles by spray-drying: Influence of enhancers of the dissolution rate on properties and stability. *J Food Eng* **2011,** *103*, 188-196.
134. Pralhad, T.; Rajendrakumar, K., Study of freeze-dried quercetin–cyclodextrin binary systems by DSC, FT-IR, X-ray diffraction and SEM analysis. *J Pharm Biomed Anal* **2004,** *34*, 333-339.
135. Gagos, M., Molecular organization of 2-(2,4-dihydroxylphenyl)-5,6-dichlor 1,3-benzothiazole in monomolecular layers formed with diphytanoylphosphatidylcholine: a linear dichroism-FTIR study. *Biochimica et biophysica acta* **2008,** *1778*, 2520-5.
136. Hao, S.; Wang, Y.; Wang, B.; Deng, J.; Liu, X.; Liu, J., Rapid preparation of pH-sensitive polymeric nanoparticle with high loading capacity using electrospray for oral drug delivery. *Mater Sci Eng C Mater Biol Appl.* **2013,** *33*, 4562-7.
137. Wang, S.; Gao, W.; Chen, H.; Xiao, P., Studies on the morphological, thermal and crystalline properties of starches separated from medicinal plants. *J. Food Eng* **2006,** *76*, 420-426.
138. Ribnicky, D. M.; Roopchand, D. E.; Oren, A.; Grace, M.; Poulev, A.; Lila, M. A.; Havenaar, R.; Raskin, I., Effects of a high fat meal matrix and protein complexation on the bioaccessibility of blueberry anthocyanins using the TNO gastrointestinal model (TIM-1). *Food Chem* **2014,** *142*, 349-57.
139. Havenaar, R.; Anneveld, B.; Hanff, L. M.; de Wildt, S. N.; de Koning, B. A.; Mooij, M. G.; Lelieveld, J. P.; Minekus, M., In vitro gastrointestinal model (TIM) with

predictive power, even for infants and children? Int. J. Pharm. **2013,** *457*, 327-32.

140. Pongpeerapat, A.; Wanawongthai, C.; Tozuka, Y.; Moribe, K.; Yamamoto, K., Formation mechanism of colloidal nanoparticles obtained from probucol/PVP/SDS ternary ground mixture. *Int. J. Pharm.* **2008,** *352*, 309-16.

*141.* Lu, X.; Ross, C. F.; Powers, J. R.; Rasco, B. A., Determination of quercetins in onion (Allium cepa) using infrared spectroscopy. *J. Agric. Food Chem.* **2011,** *59*, 6376-82.

142. Sun-Waterhouse, D.; Wadhwa, S. S.; Waterhouse, G. I. N., Spray-Drying Microencapsulation of Polyphenol Bioactives: A Comparative Study Using Different Natural Fibre Polymers as Encapsulants. *Food Bioprocess Tech* **2012,** *6*, 2376-2388.

143. Srinivas, K.; King, J. W.; Howard, L. R.; Monrad, J. K., Solubility and solution thermodynamic properties of quercetin and quercetin dihydrate in subcritical water. *J Food Eng.* **2010,** *100*, 208-218.

144. Prabhu, Y. T.; Rao, K. V.; Kumar, V. S. S.; Kumari, B. S., X-Ray Analysis by Williamson-Hall and Size-Strain Plot Methods of ZnO Nanoparticles with Fuel Variation. *WJNSE* **2014,** *04*, 21-28.

145. Maniammal, K.; Madhu, G.; Biju, V., X-ray diffraction line profile analysis of nanostructured nickel oxide: Shape factor and convolution of crystallite size and microstrain contributions. *Physica E Low Dimens Syst Nanostruct* **2017,** *85*, 214-222.

146. Hayman, M.; Kam, P. C. A., Capsaicin: A review of its pharmacology and clinical applications. *Curr. Anaesth. Crit. Care* **2008,** *19*, 338-343.

147. Reyes-Escogido, M. D.; Gonzalez-Mondragon, E. G.; Vazquez-Tzompantzi, E., Chemical and pharmacological aspects of capsaicin. *Molecules* **2011,** *16*, 1253-1270.

148. Lee, E. J.; Jeon, M. S.; Kim, B. D.; Kim, J. H.; Kwon, Y. G.; Lee, H.; Lee, Y. S.; Yang, J. H.; Kim, T. Y., Capsiate inhibits ultraviolet B-induced skin inflammation by inhibiting Src family kinases and epidermal growth factor receptor signaling. *Free Radic. Biol. Med.* **2010,** *48*, 1133-1143.

149. Lu, H. F.; Chen, Y. L.; Yang, J. S.; Yang, Y. Y.; Liu, J. Y.; Hsu, S. C.; Lai, K. C.; Chung, J. G., Antitumor activity of capsaicin on human colon cancer cells in vitro and colo 205 tumor xenografts in vivo. *J. Agric. Food Chem.* **2010,** *58*, 12999-13005.

150. Ziglioli, F.; Frattini, A.; Maestroni, U.; Dinale, F.; Ciuffreda, M.; Cortellini, P., Vanilloid-mediated apoptosis in prostate cancer cells through a TRPV-1 dependent and a TRPV-1-independent mechanism. *Acta Biomed.* **2009,** *80*, 13-20.

151. Thoennissen, N. H.; O'Kelly, J.; Lu, D.; Iwanski, G. B.; La, D. T.; Abbassi, S.; Leiter, A.; Karlan, B.; Mehta, R.; Koeffler, H. P., Capsaicin causes cell-cycle arrest and apoptosis in ER-positive and -negative breast cancer cells by modulating the EGFR/HER-2 pathway. *Oncogene* **2010,** *29*, 285-296.

152. Huh, H. C.; Lee, S. Y.; Lee, S. K.; Park, N. H.; Han, I. S., Capsaicin induces apoptosis of cisplatin-resistant stomach cancer cells by causing degradation of cisplatin-inducible Aurora-A protein. *Nutr. Cancer* **2011,** *63*, 1095-1103.

153. O'Neill, J.; Brock, C.; Olesen, A. E.; Andresen, T.; Nilsson, M.; Dickenson, A. H., Unravelling the mystery of capsaicin: a tool to understand and treat pain. *Pharmacol . Rev .* **2012,** *64*, 939-971.

154. Chen, L.; Kang, Y. H., Anti-inflammatory and antioxidant activities of red pepper (Capsicum annuum L.) stalk extracts: Comparison of pericarp and placenta extracts. *J. Funct. Foods* **2013,** *5*, 1724-1731.

155. Yoshioka, M.; Imanaga, M.; Ueyama, H.; Yamane, M.; Kubo, Y.; Boivin, A.; St-Amand, J.; Tanaka, H.; Kiyonaga, A., Maximum tolerable dose of red pepper decreases fat intake independently of spicy sensation in the mouth. *Br. J. Nutr.* **2004,** *91*, 991-995.

156. Rollyson, W. D.; Stover, C. A.; Brown, K. C.; Perry, H. E.; Stevenson, C. D.; McNees, C. A.; Ball, J. G.; Valentovic, M. A.; Dasgupta, P., Bioavailability of capsaicin and its implications for drug delivery. *J. Control. Release.* **2014,** *196*, 96-105.

157. Zi, P.; Yang, X.; Kuang, H.; Yang, Y.; Yu, L., Effect of HPbetaCD on solubility and transdermal delivery of capsaicin through rat skin. *Int. J. Pharm.* **2008,** *358*, 151-158.

158. Choi, Y. J.; Kim, J. Y.; Yoo, S. B.; Lee, J. H.; Jahng, J. W., Repeated oral

administration of capsaicin increases anxiety-like behaviours with prolonged stress-response in rats. *J. Biosci.* **2013,** *38*, 561-571.

159. Zhu, Y.; Wang, M.; Zhang, J.; Peng, W.; Firempong, C. K.; Deng, W.; Wang, Q.; Wang, S.; Shi, F.; Yu, J.; Xu, X.; Zhang, W., Improved oral bioavailability of capsaicin via liposomal nanoformulation: preparation, in vitro drug release and pharmacokinetics in rats. *Arch. Pharm. Res.* **2015,** *38*, 512-521.
160. Zhu, Y.; Peng, W.; Zhang, J.; Wang, M.; Firempong, C. K.; Feng, C.; Liu, H.; Xu, X.; Yu, J., Enhanced oral bioavailability of capsaicin in mixed polymeric micelles: Preparation, in vitro and in vivo evaluation. *J. Funct. Foods* **2014,** *8*, 358-366.
161. Goycoolea, F. M.; Valle-Gallego, A.; Stefani, R.; Menchicchi, B.; David, L.; Rochas, C.; Santander-Ortega, M. J.; Alonso, M. J., Chitosan-based nanocapsules: physical characterization, stability in biological media and capsaicin encapsulation. *Colloid. Polym. Sci* **2012,** *290*, 1423-1434.
162. Allen Jr, L. V., Capsaicin 0.05% and Ketamine HCl 2% in Pluronic lecithin organogel. *U.S. Pharm.* **2011,** *36*, 39-40.
163. Yu, H. L.; Shi, K.; Liu, D.; Huang, Q. R., Development of a food-grade organogel with high bioaccessibility and loading of curcuminoids. *Food Chem.* **2012,** *131*, 48-54.
164. Dahan, A.; Hoffman, A., Rationalizing the selection of oral lipid based drug delivery systems by an in vitro dynamic lipolysis model for improved oral bioavailability of poorly water soluble drugs. *J. Control. Release.* **2008,** *129*, 1-10.
165. Arik Dahan, A. H., Rationalizing the selection of oral lipid based drug delivery systems by an in vitro dynamic lipolysis model for improved oral bioavailability of poorly water soluble drugs. *J Control Release* **2008,** *129*, 1-10.
166. Takeuchi, H.; Sekine, S.; Kojima, K.; Aoyama, T., The application of medium-chain fatty acids: edible oil with a suppressing effect on body fat accumulation. *Asia Pac. J. Clin. Nutr.* **2008,** *17*, 320-323.
167. Yoza, K.; Amanokura, N.; Ono, Y.; Shinkai, S.; Akao, T.; Shinmori, H.; Takeuchi, M.; Reinhoudt, D. N., Sugar-integrated gelators of organic solvents - Their remarkable diversity in gelation ability and aggregate structure. *Chem. Eur. J.*

**1999,** *5*, 2722-2729.

168. Skilling, K. J.; Citossi, F.; Bradshaw, T. D.; Ashford, M.; Kellam, B.; Marlow, M., Insights into low molecular mass organic gelators: a focus on drug delivery and tissue engineering applications. *Soft matter* **2014,** *10*, 237-56.
169. Gilbert, R. G.; Hess, M.; Jenkins, A. D.; Jones, R. G.; Stepto, R. F. T.; Kratochvíl, P., Dispersity in polymer science (IUPAC Recommendations 2009). *Pure Appl. Chem.* **2009,** *81*, 351-353.
170. Wang, L. J.; Dong, J. F.; Chen, J.; Eastoe, J.; Li, X. F., Design and optimization of a new self-nanoemulsifying drug delivery system. *J. Colloid Interface Sci.* **2009,** *330*, 443-448.
171. Zahi, M. R.; Wan, P. Y.; Liang, H.; Yuan, Q. P., Formation and stability of D-limonene organogel-based nanoemulsion prepared by a high-pressure homogenizer. *J. Agric. Food Chem.* **2014,** *62*, 12563-12569.
172. Guo, J.; Tao, H.; Cao, Y.; Ho, C. T.; Jin, S.; Huang, Q., Prevention of Obesity and Type 2 Diabetes with Aged Citrus Peel (Chenpi) Extract. *J. Agric. Food Chem.* **2016,** *64*, 2053-2061.
173. Mielgo-Ayuso, J.; Barrenechea, L.; Alcorta, P.; Larrarte, E.; Margareto, J.; Labayen, I., Effects of dietary supplementation with epigallocatechin-3-gallate on weight loss, energy homeostasis, cardiometabolic risk factors and liver function in obese women: randomised, double-blind, placebo-controlled clinical trial. *Br. J. Nutr.* **2014,** *111*, 1263-1271.
174. Reinbach, H. C.; Smeets, A.; Martinussen, T.; Moller, P.; Westerterp-Plantenga, M. S., Effects of capsaicin, green tea and CH-19 sweet pepper on appetite and energy intake in humans in negative and positive energy balance. *Clin. Nutr.* **2009,** *28*, 260-265.
175. Saito, A.; Yamamoto, M., Acute oral toxicity of capsaicin in mice and rats. *J. Toxicol. Sci.* **1996,** *21*, 195-200.
176. Han, J. R.; Deng, B.; Sun, J.; Chen, C. G.; Corkey, B. E.; Kirkland, J. L.; Ma, J.; Guo, W., Effects of dietary medium-chain triglyceride on weight loss and insulin sensitivity in a group of moderately overweight free-living type 2 diabetic Chinese subjects. *Metabolism* **2007,** *56*, 985-991.

177. Clegg, M. E., Medium-chain triglycerides are advantageous in promoting weight loss although not beneficial to exercise performance. *Int. J. Food Sci. Nutr.* **2010,** *61*, 653-679.

178. St-Onge, M. P.; Ross, R.; Parsons, W. D.; Jones, P. I. H., Medium-Chain Triglycerides Increase Energy Expenditure and Decrease Adiposity in Overweight Men. *Obes. Res.* **2003,** *11*, 395-402.

179. Mumme, K.; Stonehouse, W., Effects of medium-chain triglycerides on weight loss and body composition: a meta-analysis of randomized controlled trials. *J. Acad. Nutr. Diet* **2015,** *115*, 249-263.

180. Hsu, C. L.; Yen, G. C., Effects of Capsaicin on Induction of Apoptosis and Inhibition of Adipogenesis in 3T3-L1 Cells. *J. Agric. Food Chem.* **2007,** *55*, 1730-1736.